CANCER IMMUNOTHERAPY: TARGETED CELLULAR VEHICLE-MEDIATED IMMUNOGENE THERAPY AND DENDRITIC CELL-BASED VACCINE

YOVITA IDA PURWANTI

NATIONAL UNIVERSITY OF SINGAPORE

2013

CANCER IMMUNOTHERAPY: TARGETED CELLULAR VEHICLE-MEDIATED IMMUNOGENE THERAPY AND DENDRITIC CELL-BASED VACCINE

YOVITA IDA PURWANTI

(B.Sc.Hons., National University of Singapore)

A THESIS SUBMITTED

FOR THE DEGREE OF DOCTOR OF PHILOSOPHY

DEPARTMENT OF BIOLOGICAL SCIENCES

NATIONAL UNIVERSITY OF SINGAPORE

&

INSTITUTE OF BIOENGINEERING AND NANOTECHNOLOGY (A*STAR)

2013

DECLARATION

I hereby declare that the thesis is my original work and it has been written by me in its entirety. I have duly acknowledged all the sources of information which have been used in the thesis.

This thesis has also not been submitted for any degree in any university previously.

Yovita Ida Purwanti

20 Aug 2013

Acknowledgements

I would like to express my gratitude to my supervisor A/P Wang Shu for providing me the opportunity to work on this project. Thank you for your support and guidance which have allowed me to learn and make tremendous progress in my research and thinking abilities throughout my candidature.

I would like to thank my past and present lab mates in IBN and DBS, NUS. I deeply appreciate all the help and advices I have received for my project. Special thanks to Tim and Lam for the fun, laughter and friendships that have made my lab life fruitful and memorable.

I am grateful for my loving parents and sisters. Thank you for supporting my decision to embark on this journey and for the care and reliance that I can always turn to.

I would also like to thank Alvin, Meirita, Elis, Budi, Sin Man, Yunika and all other good friends of mine whom I cannot possibly name one by one. I am grateful for all the encouragements which have motivated me a great deal throughout this PhD journey.

Lastly, I would like to acknowledge the National University of Singapore and the Institute of Bioengineering and Nanotechnology for the opportunity and support granted to me to do a PhD.

"Bless the Lord, O my soul, and do not forget all His benefits"

– Psalm 103:2

Table of Contents

Summary

Cancer immunotherapies have treated many cancer patients and improved their quality of life. In spite of their clinical effects, the available treatments using cytokines and antibodies are still hindered by their toxic effects, half-life and efficacies. In this project, we are interested in the developments of immunotherapies using the stem cell vehicles to deliver immunogene products and the dendritic cell (DC)-based vaccination approach.

Targeted immuno-gene therapy approach using the stem cell delivery vehicle is based on the inherent tumor tropism of stem cells. Endothelial progenitor cells (EPCs) is particularly attractive, not only due to their intrinsic tumor tropism but also their involvement in cancer angiogenesis. However, collecting a sufficient amount of EPCs is one of the challenging issues critical to achieving effective clinical translation of this new approach. In this study, we sought to explore whether human induced pluripotent stem (iPS) cells could be used as a reliable and accessible cell source to generate uniform human EPCs with cancer gene therapy potential. We showed that by using an embryoid body formation method, $CD133^{+}CD34^{+}$ EPCs could be efficiently derived from human iPS cells. The generated EPCs expressed endothelial markers such as CD31, Flk1 and VE-cadherin but not the CD45 hematopoietic marker. Subsequently, we showed that intravenously injected iPS cell-derived EPCs migrated towards orthotopic and lung metastatic tumors in the mouse 4T1 breast cancer model, and that injection of the EPCs alone did not escalate tumor growth and metastatic progression. Most importantly, the systemic injection of EPCs transduced with baculovirus encoding the potent DC co-

stimulatory molecule CD40 ligand could impede tumor growth, leading to prolonged survival of the tumor-bearing mice. Therefore, our findings suggest that human iPS cell-derived EPCs could potentially serve as tumor-targeted cellular vehicles for anticancer gene immunotherapy.

Despite their proven effectiveness in reducing the tumor burden, most of the available cancer treatments, including chemotherapy and radiation therapy, fail in eradicating cancer stem cells (CSCs). With their capability for self-renewal and differentiation, CSCs are capable of re-establishing the tumor mass, resulting in the relapse of tumors in patients. By utilizing baculovirus-zinc-finger technology, we have reprogrammed human glioma and colorectal cancer cell lines into CSC-like cells. We generated whole tumor lysates from these enriched CSCs using freeze-thaw-cycles and used them to pulse PBMC-derived DCs. We showed that we could obtain sufficient functional DCs that were capable of stimulating naïve T cells into cytotoxic T lymphocytes (CTLs). The stimulated CTLs were capable of producing IFNγ cytokine in a CSC-like antigen-specific manner. Our findings suggest that DC-based immunotherapy approach can be used to target CSC-like cell population.

List of Tables

List of Figures

List of Abbreviations

2-D	2-Dimension
4F-BV-ZFN	4 Factors – Baculovirus – Zinc Finger Nuclease
5-FU	5-fluorouracil
AAVS1	Adeno-Associated Virus Integration Site 1
Ac-LDL	Acetylated-Low Density Lipoprotein
ADCC	Antibody-Dependent Cell Mediated Cytotoxicity
AdCD40L	Adenoviral-CD40Ligand
AIDS	Acquired Immunodeficiency Syndrome
AML	Acute Myeloid Leukemia
ANOVA	Analysis Of Variance
anti-HER	anti-herceptin
APCs	Antigen Presenting Cells
bFGF	basic Fibroblast Growth Factor
BHQ1	Black Hole Quencher
BM	Bone Marrow
BSA	Bovine Serum Albumin
BV	Baculovirus
CAF	Carcinoma-Associated Fibroblasts
CAR	Chimeric Antigen Receptor
CCD camera	Charge-Coupled Devices camera
CCL	C-C Chemokine Ligand
CCR	C-C Chemokine Receptor
CD	Cluster of Differentiation
CD/5-FC	Cytosine Deaminase/5-Fluoro Cytosine
CLL	Chronic Lymphocytic Leukemia
CML	Chronic Myelogenous Leukemia
CMV	Cytomegalovirus
Cre-RMCE	Cre-Recombinase-Mediated Cassette Exchange
CSCs	Cancer Stem Cells
CTL	Cytotoxic T Lymphocytes
CTLA-4	Cytotoxic T Lymphocyte Antigen-4
CXCL	Chemokine (C-X-C motif) Ligand
CXCR	Chemokine (C-X-C motif) Receptor
DCs	Dendritic Cells
DMEM	Dulbecco's Modified Eagle Medium
DPBS	Dulbecco’s Phosphate-Buffered Saline
EBs	Embryoid Bodies
ECs	Endothelial Cells
EDTA	Ethylenediaminetetraacetic Acid
eGFP	enhanced Green Fluorescent Protein
EGM-2	Endothelial cell Growth Medium-2
ELCs	Endothelial Lineage Cells
EpCAM	Epithelial Cell Adhesion Molecule
EPCs	Endothelial Progenitor Cells

FBS	Fetal Bovine Serum
FDA	Food and Drug Administration
GCV	Ganciclovir
GFP	Green Fluorescent Protein
GITR	Glucocorticoid-induced TNF-related Receptor
GM-CSF	Granulocyte-macrophage colony-stimulating factor
GVHD	Graft Versus Host Disease
HCC	Hepatocellular Carcinoma
HER2	Human Epidermal growth factor Receptor 2
hESC	Human Embryonic Stem cells
HLA	Human Leukocyte Antigen
HPSCs	Human Pluripotent Stem Cells
HPV	Human Papillomavirus
HSCs	Hematopoietic Stem Cells
HSV-tk	Herpes Simplex Virus-thymidine kinase
HSV-ttk	Herpes Simplex Virus-truncated thymidine kinase
HUVEC	Human Umbilical Vein Endothelial Cells
i.p	intraperitoneal
i.v	intravenous
IFN	Interferon
IL	Interleukin
IMDM	Iscove's Modified Dulbecco's Media
iPS cells	induced Pluripotent Stem cells
iPS-EPCs	induced Pluripotent Stem cell – derived Endothelial Progenitor Cells
iPS-NSCs	induced Pluripotent Stem cell – derived Neural Stem Cells
ISM	Isthmin
IVIS	*In Vivo* Imaging System
LPS	Lipopolysaccharide
Luc	Luciferase
mAbs	monoclonal Antibodies
MACS	Magnetic-activated cell *sorting*
MART-1	Melanoma Antigen Recognized by T cells-1
M-CSF	Macrophage-Colony Stimulating Factor (M-CSF)
MHC	Major Histocompatibility Complex
MMPs	Matrix Metalloproteinases
MOI	Multiplicity Of Infection
mRNA	messenger Ribonucleic Acid
MSCs	Mesenchymal Stem Cells
MSCs	Mesenchymal Stem Cells
MTG	Monothioglycerol
NK	Natural Killer
NKT	Natural Killer T
NSCs	Neural Stem Cells
NSG	NOD scid gamma
P/S	Penicillin/Streptomycin
P-/UP-DCs	Pulsed-/Unpulsed-Dendritic Cells
PBMCs	Peripheral Blood Mononuclear Cells

PD	Programmed cell Death
PDL	Programmed cell Death Ligand
PRRs	Patter Recognition Receptors
qPCR	quantitative Polymerase Chain Reaction
RCC	Renal Cell Carcinoma
RPMI-1640	Roswell Park Memorial Institute-1640
s.d/ SD	Standard Deviation
SCID	Severe Combined Immunodeficiency
SDF-1	Stromal-derived Factor-1
Sf-9	Spodoptera frugiperda-9
SFM	Serum-Free Media
TAP	Transporter associated with antigen processing
TCR	T cell receptor
TGF	Transforming Growth Factor
T_H1	T Helper 1
T_H2	T Helper 2
TILs	Tumor Infiltrating Lymphocytes
TRAIL	TNF-related apoptosis-inducing ligand
Treg	T regulatory
VE-cadherin	Vascular Endothelial-cadherin
VEGF	Vascular Endothelial Growth Factor
VEGFR	Vascular Endothelial Growth Factor Receptor
VSVG	Vesicular Stomatitis Virus-G
vWF	von Willebrand Factor
WPRE	Woodchuck hepatitis virus Post-transcriptional Regulatory Elements
WT	Wild Type
ZFN	Zinc Finger Nucleases

List of Publications

1. Purwanti YI, Chen C, Lam DH, Wu CX, Wang S. Antitumor Effects of CD40 Ligand-expressing Endothelial Progenitor Cells Derived from Human iPS Cells in a Metastatic Breast Cancer Model. (Submitted).

2. Zhu D, Lam DH, Purwanti YI, Goh SL, Wu C, Zeng J, Fan W, Wang S. Systemic Delivery of Fusogenic Membrane Glycoprotein-expressing Neural Stem Cells to Selectively Kill Tumor Cells. Mol Ther. (2013); doi:10.1038/mt.2013.123.

3. Chen C, Wang Y, Goh SS, Yang J, Lam DH, Choudhury Y, Tay FC, Du S, Tan WK, Purwanti YI, Fan W, Wang S. Inhibition of neuronal nitric oxide synthase activity promotes migration of human-induced pluripotent stem cell-derived neural stem cells toward cancer cells. J Neurochem. 2013 Aug;126(3):318-30.

4. Shahbazi M, Kwang TW, Purwanti YI, Fan W, Wang S. Inhibitory effects of neural stem cells derived from human embryonic stem cells on differentiation and function of monocyte-derived dendritic cells. J Neurol Sci. 2013 Jul 15;330(1-2):85-93

CHAPTER I: INTRODUCTION

1.1 Cancer immunology

Cancer is a pathological condition affecting people regardless of their age and gender, and is one of the leading causes of death worldwide[1]. While vast amounts of research have been conducted to treat and improve the health and life expectancy of cancer patients, an ideal cure has not yet been found. Though cancer seems formidable, our own body's immune system is built with the capability to recognize and destroy malignantly transformed autologous cells. Dendritic cells (DCs), the body's designated professional antigen presenting cells (APCs), play a critical role in recognizing tumor cells and activating arrays of immune effectors to eliminate them. One such effector that has a central role in eradicating tumor cells is cytotoxic T lymphocytes (CTLs). The intricate mechanisms which control how our immune system recognizes and kills the cancerous cells, as well as the evolving mechanisms of the tumor to evade this system, will be discussed briefly below.

1.1.1 Tumor antigen recognition and presentation by dendritic cells

1.1.1.1 Dendritic cells as professional antigen presenting cells

Macrophages and dendritic cells in the innate immune system possess phagocytic capability and antigen recognition ability. These cells use innate non-clonal receptors, such as Toll-like receptors, lectins, scavenger receptors, FC receptors and other pattern recognition receptors (PRRs) to perceive and recognize different types of antigens[2, 3]. However, unlike macrophages which have antimicrobial and scavenging functions, DCs are inefficient in destroying the antigen-expressing cells[2, 3]. The phagocytic activities of DCs are designed to facilitate antigen processing and presentation to the T cells for the initiation

of antigen-specific adaptive immune response. As professional APCs, DCs exist in two functional states: the immature and mature states[4]. Immature DCs are adept at acquiring the antigens whereas the mature DCs are responsible for stimulating T cells by presenting the acquired antigens.

Tumor cells express proteins or peptides which are considered foreign by the immune system of the body. Tumor development is associated with the chaotic proliferation of viable tumor cells as well as disordered tumor cell deaths in the form of apoptosis and necrosis. Moreover, tumor cells are known to secrete soluble proteins and exosomes which carry antigens[5]. The immature DCs in the periphery are actively engulfing antigens (both self and foreign) via endocytic processes including phagocytosis, pinocytosis and clathrin-mediated endocytosis[4]. Thus, tumor antigens may be transferred into the dendritic cells via phagocytosis of apoptotic or necrotic tumor cells, pinocytosis of soluble antigens or capture of exosomes.

Upon tumor antigen encounter, DCs undergo maturation, upregulate chemokine receptors to facilitate migration into the lymph nodes via the blood or lymph and increase their expression of co-stimulatory molecules for engaging T cells[2, 3, 6]. In the lymph nodes, their job is to properly present these tumor antigens to the adaptive immune effectors in the context of MHC (Major Histocompatibility Complex) to their cell surface.

1.1.1.2 Tumor antigen presentation

Antigen presentation is the process by which protein fragments are complexed with MHC products and posted to the surface of dendritic cells, resulting in the orchestration of immune responses repertoire. MHC molecules are

encoded by a large gene family that is located on chromosome 6 in humans[7]. MHC class I and II regions encode for genes which are involved in antigen presentation to T cells and hence control immune reactions against antigens such as, grafts acceptance/rejection and anti-tumor responses[7, 8].

In MHC I antigen presentation pathways, tumor antigens are acquired and presented in a process known as cross-presentation[3, 5]. The acquired tumor antigens will be targeted for destruction and proteolysis processes resulting in smaller peptides in the cytosol. Subsequently, these processed peptides are delivered and bound to the MHC class I molecules in the endoplasmic reticulum with the help of TAP (Transporter associated with Antigen Processing) proteins[9, 10]. Subsequently, these MHC-peptide complexes are transported to the cell membrane of the DCs and presented to the $CD8^+$ T cells.

MHC II molecules (HLA-DR, -DQ and -DP), unlike MHC I molecules that are expressed by all nucleated cells, are only found on APCs. Tumor antigen presentation by MHC II molecules expressed on the DCs triggers the activation of T helper cells (T_H) via interaction with the CD4 receptor. The stimulation of T_H cells results in the secretion of cytokines to boost the CTL responses and the production of antibodies by B cells[8, 11]. Upon tumor antigen recognition, which can be in the form of foreign nucleic acid, glycolipid, peptide or carbohydrate, the antigen-specific B cell will undergo clonal expansion, producing high affinity antibodies[12]. Thus, the presentation of tumor antigen-MHC complexes by APCs directs the activation of adaptive immune arsenals, both T and B cells, to kill the tumor cells.

1.1.1.3 Dendritic cells bridge the innate and adaptive immunities

The components of innate immunity, which include APCs, natural killer (NK) cells and complement system, are quick in responding to danger signals given by the tumors. Although fast in its response, innate immunity is not powerful enough to eradicate the tumor cells. Activation, production and clonal expansion of tumor specific T cells and B cell antibodies are required to kill the tumor cells more effectively. The DCs play a central role in the cross-talks between adaptive and innate immunities.

As the DCs uptake, process and present tumor antigens to activate the adaptive immune effectors, NK cells act as the first line of defense against the tumors[13]. The NK cells recognize neoplastic cells due to the down-regulation of MHC I expression ('missing-self' signal) and expression of NKG2d ('induced-self' signal) on these target cells[13-15]. Once activated, NK cells exert cytolytic effect on the target cells via perforin and granzymes production[14]. NK cells also secrete various cytokines such as IFNγ to help DC maturation[16]. Moreover, the killing of target cells by NK cells can enhance presentation of antigens from the apoptotic cells by DCs[17]. Consequently, the mature DCs will activate T cells via antigen presentation. In turn, the activated T cells produce cytokines such as IL2, which can enhance and stabilize the NK cell activities further[18].

Aside from presenting antigens, DCs also produce various cytokines that are important in regulating both innate and adaptive immune responses against tumors. One such cytokine is IL12, which has been shown to be an essential regulator for skewing toward T_H1 responses. IL12 is also important

in further enhancing cytolytic activities of NK cells[14, 17, 19]. Thus, through the presentation of antigens, cell-cell interaction and cytokine production, DCs communicate with both arms of the immune system to ensure proper responses against cancer.

1.1.2 Cytotoxic T Lymphocytes: professional killers of immune system

1.1.2.1 Activation of cytotoxic T lymphocytes

The adaptive immune cells, both B and T cells, are produced in the bone marrow. However, as the name implies, T cells undergo maturation in the thymus. T cells are segregated into different subtypes including $CD8^+$ naïve T cells which can differentiate into CTLs and memory cells as well as $CD4^+$ T_H cells[20, 21]. These different T cell populations play different roles in the immune system. Memory T cells provide long-term immunity against previously encountered antigens. T_H cells, mainly categorized into T_H1 and T_H2, provide signals in the form of direct cellular contact and cytokines to enhance both B and T cell responses[22]. T_H1 cells produce cytokines such as IFNs and IL2 cytokines to promote the CTL-mediated immune response[11, 22]. T_H2 cells produce cytokines such as IL4 to enhance antibody production[11, 22]. However, the mechanism of tumor cell elimination relies largely on $CD8^+$ CTLs.

CTL activation is initiated when the $CD8^+$ T cell receptor (TCR) recognizes the antigen peptide-MHC I complex on an APC which leads to T cell differentiation and extensive proliferation into CTLs[22, 23]. However, antigen recognition alone is insufficient to fully activate CTL. Interaction of co-stimulatory signals between APCs and T cells is needed to promote T cell survival, proliferation and migration towards the tumor microenvironment[24].

For example, CD28 interaction with CD80 and CD86 on APCs is needed to stimulate T cell activation via amplification of the signals from TCR[11, 25]. The development of optimal CTL activation also requires survival signals provided by cytokines that are produced by mature DCs (such as IL6, IL12 and IFNs) and T_H1 cells[25].

1.1.2.2 Antitumor effects of cytotoxic T lymphocytes

If DCs are the professional APCs, CTLs are the professional killers which can specifically target and eliminate malignant cells. CTLs inspect MHC I molecules that are found in all nucleated cells through the binding of CD8 receptor[11]. MHC I gene products, which are designated as HLA (Human Leukocyte Antigen) -A, -B and -C, are encoded by different loci whereby each locus possesses extensive allelic variations[7]. The recognition of tumor antigens by CTLs is HLA restricted, in that CTLs and tumor cells must have the same HLA type for appropriate recognition[11].

When the cells expressing the antigen that has been reported by the DCs have been found, they will be targeted by CTLs for destruction. CTLs kill the target cells in a contact-dependent manner[22]. Upon target cell recognition, CTL granules are mobilized towards the target cells, followed by fusion of the granule membranes with the plasma membrane of the target cells. Exocytosis of the granule contents, which are the granzymes and perforin, into the target cells triggers cell lysis[22]. Apoptotic pathways can also be activated through the expression of the Fas ligand on the CTLs which engages the Fas (CD95) receptor on the target cell membrane[22]. CTLs also exert their antitumor effects via the production of cytokines such as IFNγ and TNFα that can arrest

malignant cell proliferation[24]. Effective antigen-specific cytolysis which spares normal cells is the inherent characteristic of CTLs and has become the ultimate goal of cancer immunotherapies. Unfortunately, the current available treatments still evoke some degree of off-target toxic effects.

Tumor tissues are often infiltrated with activated adaptive immune cells, indicating the presence of vigorous responses against cancer[26, 27]. Although adaptive immune effectors provide powerful antitumor effects, their activation requires time. Eventually, the interplay of innate and adaptive immune responses is important for fully-mounted immunity against cancer. When all the parts are serving their purposes well, tumor eradication will ensue. Unfortunately, in cancer patients, this is not the case.

1.1.3 Tumor evasions of dendritic cells surveillance and cytotoxic T lymphocytes killing mechanisms

Although the immune system is capable of recognizing and eliminating tumor cells, the inherent genetic instability of the latter frequently interferes with the development and function of immune responses[1, 24]. Progressive tumors often exhibit strategies that promote evasion from immune recognition and/or killing. These mechanisms include developing poor immunogenic properties to avoid proper presentation by DCs and to evade CTLs targeting, producing immunosuppressive cytokines and mediators, as well as piggybacking the pro-inflammatory immune cells to render DCs and T cells tolerant.

One mechanism to evade immune surveillance is to down-regulate the expressions of MHC I molecule so as to avoid CTLs inspection. Likewise, the NK cell activating ligands on the tumor cells are usually down-regulated too.

As such, they could avoid being targeted by the T cells as well as escaping NK cells attacks[24, 28, 29].

Another scenario by which tumor cells reduce immune stimulation is the induction of tolerogenic DCs. Indeed, a number of studies have reported that DCs are dysfunctional in cancer patients[30, 31]. The accumulation of tolerogenic DCs is attributed to the secretion of SDF-1 (Stromal-derived Factor-1) and IL6 by tumor cells[28, 32]. These DCs are defective in antigen presentation and further induce T and NK cells tolerance through the production of IL10 or TGFβ[28, 33].

Aside from SDF-1, IL10 and TGFβ, other immunosuppressive mediators which are abundant in tumor microenvironment include adenosine, prostaglandin E2 and Vascular Endothelial Growth Factor A (VEGF-A)[34]. These mediators promote angiogenesis via attraction of endothelial cells and favor stromal development by recruiting pro-inflammatory immune effectors (such as macrophages and complement components)[28, 35]. In addition, they promote the development of the $CD4^+CD25^+$ T cell subpopulation known as Tregs, which suppress CTL responses[28, 36]. Increased accumulation of Treg cells in many human malignancies, such as lung, head and neck, ovarian, stomach and skin cancer, is associated with poor prognosis for patients[28, 36]. Depletion of Tregs through the administration of anti-CTLA-4 antibody showed marked therapeutic effects in murine models and clinical trials[24, 36]. Undeniably, the understanding of immunosuppressive strategies mediated by tumor cells leads to development of more promising anti-cancer treatments.

1.2 Cancer immunotherapy

Cancer immunotherapy aims to strengthen the cancer patient's immune system[37]. Initial studies on cancer immunotherapy dated back to the late 1800s when Dr. William Coley concocted a mixture of killed *Streptococcus pyogens* and *Serratia marcescens*. The administration of Coley's toxins was shown to eliminate carcinomas[11]. Currently, various clinical trials employing immunotherapy approaches are being conducted. A search on clinicaltrials.gov using the search terms "cancer immunotherapy" revealed 903 search results encompassing a wide range of cancer diseases (as of July 2013). Some of the major approaches in immunotherapy will be discussed below.

1.2.1 Stem cells as cellular delivery vehicle for cancer gene immunotherapy

1.2.1.1 Stem cell candidates for immunotherapy

Stem cells are a population of cells that demonstrate self-renewal capacity and differentiation capability. With recent advances in the study of stem cells, different types of stem cells/progenitors such as mesenchymal stem cells (MSCs), neural stem cells (NSCs), hematopoietic stem cells (HSCs) or endothelial progenitor cells (EPCs) are believed to be ideal candidates as vehicles for anti-cancer gene delivery. Tumor microenvironments are abundant with various chemotactic cytokines and inflammatory signals that attract these progenitor cells. The migration of the cells toward tumor sites is mediated by chemokine receptors such as CXCR4 or CXCL12 on the stem cells[38]. Due to their tumoritropic properties, the principal advantage of stem

cell-based delivery of anticancer therapeutics is in its potential to achieve tumor-specificity, thus enhancing therapeutic effectiveness.

Mesenchymal Stem Cells (MSCs) have been widely proven to be ideal vehicles for the targeted delivery of anticancer agents. This is attributed to their easy isolation from bone marrow or adipose tissues and enormous expansion potential in culture on top of their tumor-tropic capacities[38]. MSCs play an important role in maintaining tissue homeostasis by repairing injured tissues. A tumor microenvironment mimics that of a wound, thus attracting MSCs which can then be exploited to promote the growth of tumor stroma. Based on this, MSCs can be employed as cellular vehicles to send immune-inducing agents to the tumor sites with the aim of killing the tumor cells via immune responses.

Malignant brain tumors such as glioblastoma multiforme remain lethal and incurable[39]. Infiltrating immune cells are found in brain tumors, but their functions can be curbed by tumor-derived immunosuppressors as mentioned above. Recent studies have shown that intracranially or intravenously injected NSCs migrate toward brain tumors[40, 41]. Therefore, the NSCs-mediated immuno-stimulatory gene delivery system has the potential to significantly improve clinical outcomes for brain cancer patients.

Another promising candidate for cellular delivery-based therapies is EPCs due to their involvement in tumor angiogenesis. In order to grow, tumors actively construct new vessels, and in the course of this neovascularization, circulating EPCs are actively incorporated into the tumor sites. Therefore, these cells can also be utilized as a ‘Trojan horse’ equipped

with immunostimulatory genes to kill the tumor cells. As Hamanishe et al. demonstrated, the systemic delivery of EPCs that express a lymphocyte migrating C-C chemokine ligand (CCL)-19 led to tumor repression in a murine ovarian cancer model. The use of EPCs is especially useful for targeting remote metastases as angiogenesis is a crucial factor in tumor metastatic progression.

1.2.1.2 Stem cell delivery of cytokine for cancer immunotherapy

Cytokines are biologic immune modulators produced by and acting on cells[11]. As mentioned above, cytokines play important roles in the regulation of immune responses and tolerance. Immunological manipulation using cytokines for cancer therapy has been prevalently attempted. For instance, IL2 and IFNα have been used for the treatment of various cancers in the clinic such as renal cell carcinoma (RCC), AIDS related Kaposi's sarcoma, melanoma, renal cancers and chronic myelogenous leukemia (CML)[11, 24, 42, 43].These cytokines act mainly by skewing the immune responses towards T_H1 axis, which in turn promotes CTL anti-tumor activities[11]. Although their efficacies have been proven under clinical conditions, the systemic administration of cytokines requires relatively high doses to obtain clinical effects. The non-specific and broad activation of the immune system by these cytokines can lead to life-threatening toxicities such as liver failure in human recipients[24]. The combination of the cytokine-mediated activation of immune responses and tumor suppression together with tumor-targeted delivery of transgene by stem cells is expected to provide therapeutic effects with minimal off-target toxic effects.

MSCs have been widely used as a cellular vehicle to deliver immune-stimulatory genes to tumors and tumor microenvironments to enhance antitumor immune responses. It has been shown that MSCs stably transduced with a retroviral vector expressing IL12 strongly reduced formation of lung metastases and retarded the growth of pre-established melanoma mouse model[44]. In another example, intra-tumor injection of primary mouse NSCs transduced with a retroviral vector encoding IL4 resulted in the extended survival of glioma-bearing mice[39, 45]. Likewise, intracranial injection of NSCs expressing IL12 into glioma mouse model resulted in the prolonged survival of the animals[46]. Moreover, human NSCs expressing IFNβ by adenoviral transduction reduced metastatic neuroblastoma upon injection[47]. These preclinical studies have spurred the idea of using stem cells as an excellent platform for tumor-specific cytokine-mediated cancer immunotherapies.

1.2.1.3 Immunotherapy via *in situ* antibodies delivery by stem cells

The current top-selling cancer drugs are monoclonal antibodies (mAbs) such as trastuzumab, rituximab and bevacizumab[27]. The anticancer effects of mAbs are based on multiple immunologic mechanisms, including complement-mediated cytotoxicity, antibody dependent cytotoxicity and enhancement of adaptive immune response[27]. Trastuzumab (also known as Herceptin), is a human epidermal growth factor receptor 2- (HER2-) targeted antibody which has been shown to significantly improve outcomes for HER2-positive breast cancer patients[48].

Despite the promise shown by antibody-based therapies, the size, half-life and toxic effects of these antibodies pose problems in clinical

circumstances. The large molecular size and short half-life of antibodies limit their ability to efficiently penetrate large solid tumors or tumor in obscure places, e.g. brain tumors whereby the antibodies are inefficient in crossing the blood brain barrier to exert their therapeutic effects. Moreover, toxic side effects due to interactions with unintended targets need to be resolved. A delivery vehicle system using stem cells can be harnessed to overcome these problems. The inherent tumor tropism of stem cells could be useful to deliver therapeutic genes to solid tumors and across blood brain barrier.

Studies have shown that NSCs could deliver the tumor-specific anti-HER2 antibody (functionally equivalent to commercially available Trastuzumab) *in vivo*[49, 50]. The anti-HER2 immunoglobulin-secreting NSCs exhibit preferential tropism to tumor cells *in vivo* and are capable of delivering tumor-specific antibodies to human breast cancer xenografts in mice[50].

Although promising, there are several critical challenges that require attention before stem cell-based gene immunotherapy is applied for clinical use. The first challenge is the choice and source of stem cells used for different types of cancer. It has been shown that NSCs perform better than MSCs in delivering an oncolytic adenovirus in a rodent orthotopic glioma model. Thus, NSCs may be a better candidate to deliver immunotherapeutic gene for brain tumors treatment. Another challenge is that this approach has to be able to produce the therapeutic agents of effective concentration at the tumor site. In addition to this, finding balance between therapeutic effects and tumor promoting effects as well as fine-tuning the gene expression and safety

of genetic engineering in the stem cells are important for this approach to be fully optimized in the clinics.

1.2.2 Dendritic cell-based vaccinations

Vaccines are one application of immunology that has successfully eradicated diseases such as polio and smallpox. Vaccines work by inducing protective immunity against the disease. The same principle applies to cancer vaccines in which the vaccines aim to stimulate tumor-specific immune responses for prophylactic (preventive) and therapeutic purposes. Two types of prophylactic vaccines have been approved by FDA, the vaccine against hepatitis B virus to prevent liver cancer and the vaccine against human papillomavirus (HPV) to prevent cervical cancer (Gardasil® and Cervarix®)[34]. In contrast, the development of therapeutic vaccines is more challenging. Recently, Provenge, a DC-based cancer vaccine for prostate cancer treatment, has been approved by FDA, inciting more studies for the development of next-generation DC-based cancer vaccines.

1.2.2.1 Dendritic cells as an excellent candidate for developing therapeutic vaccines against cancer

There are several different approaches in cancer vaccines, including viral-, peptide-, vector-, tumor cell- and DC-based, each offering unique advantages and disadvantages[11]. DC-based vaccines aside, all these approaches are based on the presumption that they can stimulate DCs and generate immune responses *in vivo.* Unfortunately, these vaccines are likely to have poor pharmacokinetic properties and may be cleared rapidly before being loaded onto the DCs due to their short half-lives[34]. Moreover, as mentioned above,

the DCs in cancer patients may be functionally defective and induced to become tolerogenic DCs. Dendritic-cell-activating adjuvants such as GM-CSF and IL2 cytokines have been used together with these vaccines to boost their therapeutic efficacies. This underscores the importance of dendritic cells in regulating immune responses. Therefore, dendritic cells themselves become the obvious target and adjuvant tool-base for cancer vaccination.

The approach of DC-based vaccines involves the isolation of DCs from the patients, followed by loading of antigens *ex vivo*, activation and conditioning to induce DC maturation, and finally re-infusion of the DCs back into the patient. The closest approach to DC-based vaccine by definition is Provenge, the only therapeutic vaccine to have been approved by the FDA to date. This vaccine, which comprises a mixture of the patient's own PBMCs (Peripheral Blood Mononuclear Cells), prostate antigen PAP (Prostatic Acid Phosphatase) and GM-CSF supplement (DC growth and differentiation factor), is used for prostate cancer treatment[34].

1.2.2.2 Loading dendritic cells with tumor-specific antigens

The development of DC-based vaccines requires the introduction of antigens into the DCs which in turn will present them to T cells. The antigens used can be in various forms and there are several methods to load them to DCs. To date, studies have used antigens in the form of DNA, peptides/proteins, RNA (mRNA/total RNA), exosomes and whole tumor cells (alive/killed). These antigens can be loaded into the DCs via viral vector-mediated gene transfer, electroporation, transfection as well as co-culture/mixing.

The advantage of using DNA to load antigens to DCs is that the tumor antigens will be expressed by the DCs and presented via MHC I complex in a way that mimics endogenous protein presentation[51]. Some studies have shown its efficacy in mounting cytotoxic effect against tumors[52-54]. However, since usually viral vector-mediated loading is adopted, this method raises safety concerns regarding the use of the virus and its effect on the transduced DCs.

Antigen loading using peptides has the advantage of being specific, hence reducing the unwanted toxicities from non-specific immune responses[6, 51]. Yet, this specificity is a double-edged sword, as it also limits the target cells. Moreover, as mentioned previously, the application of peptide-based vaccine is MHC restricted. However, the efficacy of using peptide-pulsed DCs for cancer immunotherapies has been proven in several studies and even in clinics[55-57].

Targeting a broader spectrum of tumor antigens without the restriction of MHC typing is sometimes preferred although such approaches are usually limited by the minute quantity of cancer antigenic molecules present. The use of proteins, total RNA, exosomes and whole cell-based antigens can achieve this. However, greater technical demands are required to prepare antigens from proteins, RNA and exosomes especially in large-scale productions and it is costlier too. Despite this, their efficacies in preclinical and clinical studies have been proven[58, 59]. Loading DCs with whole tumor cell antigens can be achieved with tumor lysate prepared by repeated freeze-thaw cycles or apoptotic cells generated by irradiation. This approach is simple yet well-

established in DC-based vaccine immunotherapies and its therapeutic effects have been reported by many studies[60-64].

More research needs to be done since even the success story of Provenge can only deliver a meager 4-month advantage in overall survival[27, 34]. A better understanding of DCs generation and differentiation, of immune tolerance and of tumor antigen choices, formulation and incorporation into the DCs will allow us to design a better cancer vaccine.

1.2.3 Other approaches

1.2.3.1 Adoptive T cells for cancer therapy

Growing cancers contain tumor infiltrating lymphocytes (TILs), indicating the presence of T cell immune response against cancer. It has been shown that the prognosis of hepatocellular carcinoma (HCC) cancer patients with marked TILs is better than that of patients without TILs. Unfortunately, TILs very often succumb to the immunosuppressive and tolerogenic tumor microenvironment. This is why the idea of providing improved anti-tumor reactive T cells via adoptive T cell therapy becomes very promising.

The feasibility of adoptive immunity was discovered after a study in mice revealed that specific immunity to tumors could be transferred to normal mice using lymphocytes from the spleen or peritoneal cavity of immunized donors[43]. The donation of T cells can be allogeneic or autologous. Though it has been performed with marked therapeutic effects in clinical condition, allogeneic donation may lead to graft-vs-host disease (GVHD). Thus, isolation, expansion and reinfusion of autologous tumor reactive T cells into the patient are more preferred.

T cells can be isolated from peripheral blood, tumor effusions or from draining the lymph nodes of the patient/donor[21]. Once obtained, the T cells are stimulated and expanded *in vitro* via priming with DCs which present the tumor antigens or using CD28/CD3 antibodies[11, 21, 24]. Regardless of the methods to isolate and expand the T cells, the challenge is to maintain the survival and properties of the cells after being re-injected into the patient[11, 24].

1.2.3.2 Genetic engineering of T cells

Genetic engineering to confer T cells with a stronger and more specific tumor-killing power has also been adopted. This can be achieved through tumor antigen-specific TCR gene transfer or introduction of chimeric antigen receptor (CAR)[1]. TCR gene transfer has been used in clinical trial for melanoma using melanoma tumor antigen melanin A (MART-1)[1]. Adoptive T cell transfer with an HLA-A2 restricted T cell receptor (TCR) specific for NY-ESO-1, a cancer-testis antigen expressed by human cancers and testis but no other normal adult tissues, resulted in tumor regression in 5 out of 11 patients with melanoma and 4 of 6 patients with synovial cell sarcoma[27]. One drawback of this therapeutic regime is its limitation due to the MHC-restriction.

CARs, single-chain constructs composed of an Ig variable domain fused to a TCR constant domain, were developed to overcome this[21]. When introduced into the T cells, they combine the antigen recognition properties of antibodies with T cell lytic functions. Thus, this method broadens the spectrum of tumor antigen recognition and is not MHC-restricted. The first generation of CAR consists of a single signaling domain, CD3ζ. Although the

resulted redirected T cells are functional, they fail to persist in the long term. In the second generation of CAR, the CD28 signaling domain was added to confer resistance to the T cells. The newer generations include more co-stimulatory molecules such as 4-1BB (CD137) domains to enhance T cell survival and function even further[1]. Encouraging early clinical results have been obtained in patients with lymphoma[65]. However, the toxicities as well as the search for the optimal configuration for CAR are the challenges faced by this immunotherapy[1].

1.2.4 Challenges in cancer immunotherapy

Despite surmounting evidence and convincing data in preclinical studies, cancer immunotherapies in clinical trials have failed to deliver promising results. Clearly, some roadblocks need to be cleared in order to attain success in clinical applications. One such hindrance is the limitations of preclinical animal models. The existing models, be it the syngeneic or xenograft models, have provided us with tools to understand the mechanisms of cancer immunology and immunotherapy. Yet, they are still far from recapitulating the complex and progressive pathophysiological of cancer in patients[66]. Improvements in animal models will result in better prediction of therapeutic efficacies in humans. Naturally occurring cancers have been observed in companion animals (pet dogs and cats)[67-70]. Understanding the biology and treatment of cancer in these animals may bridge the gap between preclinical and clinical studies closer.

Another major roadblock hampering the success of cancer immunotherapy is the lack of understanding of the overall immune status of

patients. Mechanisms that suppress the immune system provide a fundamental reason why immunotherapy fails to induce consistently robust immune responses in patients[71]. Prescreening of patients for immune status will help identifying patients who are more likely to respond to certain therapies. Eventually, this knowledge will be useful in designing cancer therapy that will work for certain groups of patients with the same immune parameters. Development of biomarkers and assays that can test arrays of markers efficiently would be very valuable. Recently, a new generation of flow cytometry based on mass spectrometry readout of heavy metal ion-labeled probes has been developed[72-75]. This technology allows testing of 40 biomarkers samples at once, which is beyond the ability of traditional multicolor flow cytometry[73].

While the heterogeneity of cancer is considered a critical hurdle, appreciating this complexity and designing therapeutic combinations holds great potential in clinics. There is a substantial evidence to suggest that some combinations of chemo- or radiotherapy and vaccine treatment are synergistic[66, 76, 77]. Other emerging therapeutic strategies that can be used in combination with current available therapies are antibodies targeting the immune checkpoint blockade (e.g CTLA-4) or antibodies targeting PD-1, which will lead to depletion of Tregs population. However, more preclinical data and trials are required to demonstrate the effectiveness of these combination therapies[71, 78].

1.3 Purposes and motivations

The idea that our own immune systems could recognize and kill cancer cells have been supported by a large amount of evidence. Studies on cancer immune responses and immune tolerance have led to the emergence of various potential cancer immunotherapeutic modalities. Yet, only a few could eventually develop into clinical applications despite all the effort, time and funding invested in myriad clinical research studies and trials.

One critical hurdle is breaking the immune tolerance barriers created by the tumor microenvironment. To achieve this, we need to equip immune effectors with the appropriate signals which not only activate but also maintain the anti-tumor immune responses long enough to eradicate the tumor cells. Another crucial challenge is to fine-tune the balance between the specificity and the efficacy of the cancer therapy. We need to design treatments which can abrogate the tumor heterogeneous cell population while minimizing the off-target toxicities against the healthy normal cells. Treatments that can overcome these obstacles will be very valuable in the clinics.

Targeted immuno-gene therapy using the stem cell delivery vehicle is an attractive approach to create such a treatment. The inherent tumor tropism of the stem cells combined with the immune-stimulating gene can become a powerful cancer treatment modality. Endothelial progenitor cells (EPCs) is particularly an excellent choice of cellular vehicle, not only due to their tumor tropism but also their involvement in cancer angiogenesis. However, deriving sufficient amount of EPCs for effective clinical translation is one of the critical challenges. In this study, we sought to explore whether human induced

pluripotent stem (iPS) cells could be used as a reliable and accessible cell source to generate uniform human EPCs with cancer gene therapy potential (Chapter 2).

The presence of TILs indicates that immune cells also possess natural tumor homing capability. Moreover, DCs, the immune cells which bridge the innate and adaptive immune arms, are capable of stimulating adaptive immune responses by presenting tumor antigen to the T cells. Thus, we turn our focus utilizing and stimulating these cells to overcome the immune tolerance barriers created by the tumor microenvironment.

Another immense obstacle in finding a cure for cancer is the presence of cancer stem cells (CSCs). Most of the available cancer treatments including chemotherapy and radiation therapy, while proven as effective in reducing the tumor burden, cannot eliminate the chance of tumor recurrence in patients. This is because these treatments failed to target the cancer stem cells (CSCs) population. The surviving CSCs, with their self-renewal and differentiation capability, are capable of reestablishing the tumor mass. Thus, we aim to develop a targeted DC-based immunotherapy approach against this subpopulation of cancer (Chapter 3).

CHAPTER II: ANTITUMOR EFFECTS OF CD40 LIGAND-EXPRESSING ENDOTHELIAL PROGENITOR CELLS DERIVED FROM HUMAN IPS CELLS IN A METASTATIC BREAST CANCER MODEL

2.1 Introduction

2.1.1 EPCs

2.1.1.1 Definition, Sources and characterization

Endothelial progenitor cells (EPCs) are a population of $CD34^+/Flk1^+/CD133^+$ stem cells that can differentiate into endothelial cells (ECs), the cells that make up the lining of blood vessels[79-82]. EPCs are also identified by a set of markers, including the von Willebrand Factor (vWF), CD31 and vascular endothelial (VE)-cadherin[80, 83]. EPCs play significant roles in vasculogenesis (formation of blood vessels by in situ differentiation of EPCs), angiogenesis (development of pre-existing blood vessels) and the growth of solid tumors. Over the past decade, the observation that circulating EPCs from the bone marrow can be recruited into tumor neovessels has promoted many studies using various sources of endogenous and exogenous EPCs for therapeutic targeting to inhibit tumor neovasculaturization[81, 83, 84]. The systemic delivery of therapeutic gene-loaded EPCs can potentially enable efficient therapy for metastatic cancer by targeting multiple metastases in different sites through circulation, and this is probably the most attractive feature of EPC cellular vehicles in cancer treatment[85, 86].

In vitro, EPCs can be isolated from various sources, such as peripheral blood, bone marrow, adipose tissue and umbilical cord blood[87, 88]. However, the relatively low yield and difficult expansion of these cells pose a challenge for clinical usage. With the increasing potential to use EPCs as cancer therapeutics, it is desirable to have a reliable and stable supply of human EPCs. Pluripotent stem cells, such as embryonic stem (ES) cells, can be

expanded indefinitely in culture and have the potential to generate different types of cells, including endothelial lineage cells[87, 89-92], *in vitro* in virtually unlimited numbers. Interestingly, mouse embryonic EPCs have been shown to be able to target lung metastases in an allogenetic setting in mice[83, 85, 93]. Most recently, Su and colleagues presented that human ES cell-derived $CD34^+/CD133^+$ endothelial cells armed with herpes simplex virus truncated thymidine kinase (HSV-ttk) could inhibit MDA-MB-231 breast cancer growth[94].

Induced pluripotent stem (iPS) cells are another type of commonly used pluripotent stem cells. Human iPS cells appear more attractive for clinical applications since these cells can be generated relatively easily through reprogramming differentiated somatic cells with transcription factors, a procedure that circumvents the bioethical controversies associated with the derivation of human ES cells from human embryos[95-98]. Utilizing iPS cells to generate EPCs therefore holds great potential for clinical applications.

2.1.1.2 EPCs gene therapy strategies

2.1.1.2.1 Suicide gene therapy

The major challenges of cancer therapy using cytotoxic drugs are the short drug half-life, insufficient delivery of the drug to tumor and their suboptimal specificity to malignant tissue. Tumor-targeted suicide gene delivery by stem cells will alleviate these issues. This therapy involves the stem cell-delivery of an enzyme which converts an inactive non-toxic pro-drug into a cytotoxic agent. Subsequently, the toxic drugs kill the cancer cells via bystander effects through diffusion or formation of gap junctions.

The first study to show that embryonic EPCs can be used as cellular vehicles to systemically deliver a suicide gene for cancer therapy was done by Wei et al[99]. In this study, cytosine deaminase/5-fluorocytosine (CD/5-FC) was used to treat mice with metastatic lung cancer. This CD/5-FC enzyme/prodrug system utilizes the conversion of an inactive non-toxic prodrug into a cytotoxic drug metabolite through the enzyme, cytosine deaminase. The 5-FC prodrug, an antifungal agent, will be converted to a diffusible and highly cytotoxic DNA synthesis inhibitor compound, 5-fluorouracil (5-FU), upon injection. Another suicide gene which has been extensively studied is the herpes simplex virus thymidine kinase/ganciclovir (HSVtk/GCV) system. In this system, HSVtk mediates GCV conversion to GCV 5'-triphosphate, which inhibits cell DNA polymerase[100]. HSVtk delivered by EPCs has been used to treat mice models of human ovarian cancer[83].

Although suicide gene therapy has been widely used and studied, it has limitations too. The bystander killing effect of the suicide gene requires time. Hence, it may not be able to compete with fast progressing tumor cells, or tumor cells in large amounts. Furthermore, the suicide gene vehicle has an inherent disadvantage, since it destroys itself, thus limiting the therapeutic window time[99].

2.1.1.2.2 Antiangiogenic therapy

The growth and progression of solid tumors are dependent on newly formed blood vessels for cancer cells to get nutrients, as well as for a route via which the tumor cells can form metastases[79, 101]. Antiangiogenic therapy follows a rationale in which tumor vessels are disrupted, thus starving the tumor[102]. The

prolonged administration of high doses of angiogenic inhibitors such as endostatin, thrombospondin or angiostatin *in vivo* is commonly required to produce antitumor effects due to its short half-life in circulation[83, 101]. Thus, EPC cellular delivery-based antiangiogenic gene therapy, which facilitates gene-encoding such proteins directly into the tumor, may solve this problem[101].

2.1.1.2.3 Immunotherapy

Several studies have demonstrated the use of EPCs to deliver immuno-therapeutic genes for cancer therapy. One such studiy was done by Ojeifo et al., in which the administration of 3 sequential i.v (intravenous) injections of 10^5 ECs expressing the human IL2 transgene abrogated the tumor metastases and prolonged the survival of C57Bl/6 mice harboring lung metastases from melanoma[83, 103]. In another study, using mouse embryonic EPCs (eEPCs) which were retrovirally transduced with the mouse CC chemokine ligand-19 (CCL19) gene, Hamanishi et al. showed the suppression of growth and metastasis of murine ovarian cancer in animal models. CCL19 elicits chemotactic activity for T cells, B cells and mature DCs, which supports the homing of naïve T cells and DCs into T cell areas of secondary organs. The tumor repression was accompanied by increased numbers of tumor infiltrating $CD8^+$ lymphocytes. In contrast, no tumor repression was observed when the same experiment was done in immunodeficient (SCID) mice, suggesting that the crucial role of T cell function in this system[104].

The use of immune modulators for cancer therapy has been discussed in the previous chapter. However, the systemic administration of such immune

modulators can evoke toxic effects to the body due to their broad range of immune effects. Delivering their genes to the tumor sites via stem cells may lead to a more targeted approach to killing tumor cells, thereby attenuating the toxic effects.

2.1.2 CD40 ligand

CD40 ligand (CD40L) is a 33kDA type II membrane protein, a member of the TNF gene family. These ligands interact with CD40 receptors, which are expressed by a wide range of cells including antigen presenting cells (APCs), B cells, epithelial cells, endothelial cells (ECs) and malignant cells[105]. Since it was shown to have an antitumor effect in 1997 by Grossmann et al., many have studied the potential of CD40L as a cancer therapeutic agent. Binding of CD40L with CD40 receptors on APCs, such as dendritic cells, will result in the maturation of APCs. This, in turn, activates antitumoral T cell responses against cancer cells[106, 107]. Interestingly, studies using CD40L in immunodeficient mice showed delayed tumor progression, which may indicate other mechanisms than the T cell responses. In B cells, cross-linking CD40 drives differentiation, proliferation and immunoglobulin class switching while preventing B cell apoptosis[107]. Meanwhile, Gomez et al. showed that tumor cells treated with AdCD40L had decreased viability due to apoptosis induction by CD40L[106, 108]. Currently, there are several ongoing clinical investigations utilizing adenoviral-CD40L, involving diseases such as CLL (chronic lymphocytic leukemia), acute leukemia, urinary bladder cancer and malignant melanoma [106]. Moreover, humanized anti-CD40 monoclonal antibody SGN-40 has been used in a clinical phase I trial for multiple myeloma in the US[105].

2.1.3 Induced pluripotent stem cells

The iPS cells have provided us with a tool to generate EPCs perpetually. However this groundbreaking technology would not come about if not supported by abundant prior studies and knowledge on stem cells. One such impactful study is the work on somatic cells nuclear transfer (SCNT)[109]. This technique allow the generation of fully-functioned organisms, although usually with severe genetic abnormalities, from differentiated cells as nuclear donor and cytoplasm of an oocyte. Studies have also shown that various cell types have the capacity to functionally influence or reprogram one another following cell fusion[110]. Interestingly, pluripotent cells (ESCs or embryonic carcinoma cells) have the superiority to reprogram the differentiated cells[111, 112]. Both methods take advantage of cellular materials, either the nuclear factors present in the cytoplasm of the enucleated oocyte or in the hESCs fused to the adult cells, to establish pluripotency in somatic cells[113, 114].

Yamanaka and colleagues ingeniously compiled 24 'candidate factors': genes that were known to be highly associated with pluripotency. After removing the factors one by one, the final Yamanaka reprogramming factors, Oct4, Sox2, Klf4, and C-Myc, were deduced to be crucial to reprogram adult cells back into pluripotent state[110]. These genes encode for transcription factors which activate the expression of genes in the pluripotency network and suppress those that promote differentiation via chromatin remodeling[114]. Oct4 has been shown to be indispensable factor in the reprogramming cocktails. It forms heterodimers with Sox2 to attain a more stable and efficient DNA binding[115, 116]. Klf4 or Kruppel like factor 4 is a zinc finger transcription factor that regulates cell proliferation and differentiation[116]. Although dispensable,

C-Myc has been known to induce changes in histone methylation patterns, thus providing easier access to the reprogramming factors and enhancing the efficiency of the reprogramming process[116].

Although iPS cells hold great promise in cancer and regenerative medicine, it has to pass critical safety concerns prior entering the clinics. One concern is the use of viral systems that result in integration of the reprogramming factors into the host cell genome and subsequently may lead to mutagenesis and tumorigenesis[117]. Non-integrating approaches using vectors that do not integrate into host cell genome or that could subsequently be removed from the genome are preferred[112]. Another concern is the oncogenic nature of all the reprogramming factors. Thus, transient expression of these factors is favored[117]. One potential clinical application of iPS cells is the establishment of HLA-matched banks of lines. The use of hESCs for this purpose hits a major ethical block as it requires embryos to derive the cell lines. Furthermore, limited availability of hESCs derived from surplus embryos donated following IVF treatment is unlikely to provide sufficient numbers to populate a highly selected cell bank[118]. Collection of adult cells that can be used to derive iPS cells banks would be more feasible and less controversial.

2.1.4 Objective and Aim of Study

The overall aim of our study is to investigate the anti-tumor effect of CD40L while utilizing EPCs as the cellular delivery vehicle. Most studies utilized CD40L expression in DC or tumor cells in order to activate T cell responses[105, 106, 108, 119, 120]. However, in this study, we used EPC as a cellular

vehicle to deliver the CD40L systemically and tested its therapeutic effect on 4T1 metastatic breast cancer model in mice. It has been shown that CD40L can bind to the receptors located on ECs, which results in the localization of leukocytes to the tumor endothelium via cytokines and chemokines production[121], thus justifying our selection of EPCs as cellular vehicles for CD40L as cancer therapy.

The criteria for an excellent cellular delivery vehicle include simple production and expansion, capability for tumor tropism, feasibility of gene transfer, and ability to exert therapeutic effects. We will investigate whether our produced EPCs possess these traits in this project. In the first part of the study, we investigated the derivation and characterization of EPCs from hPSCs, both the hESCs and the iPS cells.

We continued by observing the tumor tropisms of EPCs toward cancer cells. We employed a dual-color imaging system, making use of luminescent-based luciferase and fluorescent-based near-infrared DiR systems. Using this method, we tracked both the growth of tumor cells expressing luciferase and the distribution of DiR-labeled cells after injection into the mice non-invasively over time. The tumor tropisms of EPCs in different mouse tumor models were investigated: the 4T1-luc mammary pad model, 4T1-luc lung metastatic model and orthotopic glioma model.

Though attractive, the tumor tropic properties can be a double edged sword. Mesenchymal stem cells (MSCs) are also favored as cellular vehicles due to their tumor tropism. Yet, it has been noted that MSCs may contribute to tumor growth by promoting angiogenesis, modulating the immune response

against cancer cells and promoting metastasis[122-124]. Hence, the therapeutic effects exerted by the transgene expressed via these cellular vehicles must be able to overcome the ability of these cells to sustain cancer cells. We investigated the capability of iPS-EPCs in tumor growth and immunomodulation alongside iPS-NSCs, another well-known cellular vehicle.

We went on to test the feasibility of gene transfer in hPSCs-derived EPCs. We focused on the use of baculovirus to facilitate the gene transfer to EPCs. Baculoviral vectors, which are derived from an insect virus *Autographa californica multiple nucleopolyhedrovirus*, emerged as a potentially safe class of gene delivery vectors due to its inability to replicate or cause toxicity in mammalian cells[125].

Finally, we investigated the cancer immunotherapeutic efficacy of CD40L delivered by EPCs in a mouse tumor model. We also examined the therapeutic effects of the HSVtk gene, the golden standard of the suicide gene therapy. Recently, a novel angiogenesis inhibitor, Isthmin (ISM), has been reported. Originally identified in *Xenopus* brains, this 60kDa protein could suppress mouse melanoma tumor growth when overexpressed[126, 127]. Whether ISM could inhibit tumor growth in pre-established tumors in mice when delivered systemically, will be investigated in this study.

2.2 Material and Methods

2.2.1 Cell culture

H1 or H9 hESC lines (WiCell, WI, Madison, USA) were cultured in mTeSR^{TM}1 medium (Stemcell Technologies Inc, Vancouver, Canada) on hESC-qualified matrigel (BD Biosciences, San Jose, California, USA). Human

iPS cells were generated by utilizing a Cre-excisable polycistronic lentiviral vector containing Oct4, Klf4, Sox2 and c-Myc genes (Millipore, Bedford, MA) as stated in our previous study[128]. The generated iPS cells were also cultured on hESC-qualified matrigel using mTeSR™1 medium. For passaging, confluent H1 or iPS cells were washed twice with 1× Dulbecco's phosphate-buffered saline (DPBS) without calcium and magnesium (Gibco, Invitrogen, Carlsbad, CA). Then 1 ml dipase (1 mg/ml; Gibco, Invitrogen) was added to dissociate the cells in a 37^{o}C incubator for 5 min. The cell colonies were gently scraped off with a 20 µl pipette tip and seeded onto a new matrigel-coated 6-well-plate (Nunc, Penfield, New York, USA). A medium change was performed every day until the next passaging at day 7.

Mouse 4T1-luc is a breast cancer cell line that stably expresses the luciferase gene (Caliper Life Sciences, Hopkinton, MA, USA). These cells were passaged every 4 days at a split ratio of 1:5 and maintained in a RPMI-1640 medium (Gibco, Invitrogen) supplemented with 10% FBS (fetal bovine serum, Hyclone, Waltham, Massachusetts, USA) and 1% penicillin/streptomycin (P/S; Gibco, Invitrogen). M2-10B4 mouse bone marrow stroma cells (ATCC, Manassas, Virginia, USA) were also maintained in this medium, but passaged in 1:10 ratio every 4 days. OP9 cells (ATCC) were maintained in α-MEM (Gibco, Invitrogen) supplemented with 20% FBS. OP9 cells were passaged every 4 days at a split ratio of 1:8. T-75 cm^2 flasks (Nunc) were coated overnight with 6 ml of 0.1% gelatin A (Sigma-Aldrich, St. Louis, Missouri, USA) prior to OP9 cell seeding. HUVEC (Lonza, Basel, Switzerland) were maintained in EGM-2 (Endothelial cell Growth Medium-2, Lonza).

To subculture the cells, the confluent cells were washed twice with 1× DPBS and treated with 1× trypsin-EDTA (Gibco, Invitrogen) for 5 min in an 37^{o}C incubator. The trypsinized cells were then collected and rinsed with the cell culture medium to neutralize the trypsin. The cells were centrifuged at 200-300g for 5 min. Then, the cells were re-suspended in the cell culture medium and seeded onto a new flask according to the appropriate split ratio. All the cells were maintained in a 5% CO_2 humidified incubator at 37^{o}C.

2.2.2 Stromal-based EPC derivation method

2.2.2.1 OP9 co-culture

To prepare for hematopoietic differentiation of hPSCs, OP9 cells were cultured in T-175 cm^2 flasks (instead of T-75 cm^2) for normal culture maintenance. When they became confluent on day 4, half of the medium was changed, and the culture dishes were maintained for an additional 4 days. On day 8, the super-confluent OP9 medium was replaced with 20 ml of hematopoietic differentiation medium, the α-MEM supplemented with 10% FBS and 100 μM monothioglycerol (MTG; Sigma Aldrich). Three wells of a 6-well-plate of confluent hPSCs were harvested and added to each dish of overgrown OP9 cells. The flask was tapped and swirled gently to ensure that the hPSCs colonies were well distributed throughout the co-culture before putting it into the 37^{o}C incubator. The differentiation medium was fully replaced at day 1, and from day 4 of the co-culture, half of the medium was changed every 2 days.

The cell co-cultures were harvested at day 8 using collagenase IV treatment for 10 min, followed by trypsin for 10 min. The cell suspension was

then filtered through a 70 μM nylon cell strainer (BD Labware, Bedford, MA, USA). The harvested cells were then magnetically sorted using CD34 microbeads (Miltenyi Biotec, Cologne, Germany). The sorted EPCs were seeded on fibronectin-coated plates in EGM-2 medium. Fibronectin was used as the extracellular matrix as it has been shown to improve endothelial cell adhesion and seeding efficiency[129].

2.2.2.2 M2-10B4 co-culture

To prepare M2-10B4 as stromal cells, the confluent cells were treated with mitomycin C (10ug/ml; Roche, Basel, Switzerland) for not more than 3 h. The cells were then collected, seeded onto a T-175 cm^2 flask (4.5e6 cells/flask) and were allowed to settle overnight in a 37^oC incubator with 5% CO_2. The next day, the hPSC colonies were seeded onto the M2-10B4 stroma as explained above. The co-culture medium used was RPMI-1640 supplemented with 15% FBS, 1 mM NEAA (Non-Essential Amino Acids; Invitrogen) and 0.1 mM β-mercaptoethanol (Gibco, Invitrogen). The medium change was performed every 2-3 days. The co-cultures were harvested after 13 days using the same method as above.

2.2.3 Non-stromal-based EPC derivation method

2.2.3.1 2-D culture

For 2-D monolayer differentiation, the method was drawn from a published article[130], with some modifications. Undifferentiated hPSCs were cultured at a higher density on matrigel for 7 days. At the start of the differentiation phase, the culture medium was changed to a 2-D differentiation medium, IMDM supplemented with 15% defined-FBS (Hyclone), 450 μM MTG, 2 mM L-

glutamine (Gibco, Invitrogen), 1× P/S and 0.1 mM NEAA. The medium was changed every 2-3 days for 10 days. After differentiation, the single-cell suspensions were prepared by treatment with 2 mg/ml collagenase B (Roche) for 10 min at 37^{o}C. CD34^{+} cells were then isolated as mentioned above.

2.2.3.2 Embryoid bodies method

The confluent hPSC cultures were treated with 1 mg/ml dispase for 5 min. After dispase was removed, the cells were washed twice with PBS. The colonies were then detached by scraping the colonies with a pipette tip. The scraped colonies were transferred in a low attachment dish in STEMdiff^{TM} APEL^{TM} medium (Stemcell Technologies Inc) to form embryoid bodies (EBs) for 4 days. This animal product-free medium has been shown to result in superior reproducibility of EB formation and high efficiency of differentiation[131]. Afterwards, the formed EBs were plated onto a matrigel coated 10-cm culture dish and cultured for another 10 days. Cytokines (Peprotech, Rocky Hill, New Jersey, USA) were added to supplement the medium as follows: 20 ng/ml BMP4 (day 0-7), 10 ng/ml Activin A (day 1-4), 8 ng/ml FGF2 (day 2 onwards), and 25 ng/ml VEGF (day 4 onwards). In addition, a TGF-β inhibitor, 10 μM SB431542 (Tocris Bioscience, Bristol, UK) was added from day 7 onwards[132]. On day 14, the cells were harvested by treatment with collagenase IV (Gibco, Invitrogen) for 10 min, followed by trypsinisation (trypLE, Invitrogen) for another 10 min. The harvested cells were then magnetically sorted using CD34 microbeads. The sorted EPCs were seeded on fibronectin plates in Endothelial Growth Medium-2 (EGM-2

medium, Lonza) supplemented with 10 μM SB431542. The cells from passages 2 and 3 were used for characterization and animal experiments.

2.2.4 Characterization of EPCs

2.2.4.1 Flow cytometry

Generated iPS-EPCs were characterized by flow cytometric analysis using anti-CD34, CD31, Flk1, CD144, CD45 antibodies (BD Biosciences) and anti-CD133/1 antibody (Miltenyi Biotec). Quantitative analyses were performed using FACSCalibur flow cytometer (BD Biosciences).

2.2.4.2 Immunostaining

Immunofluorescent staining was prepared using primary anti-von Willebrand factor (vWF; Abcam, Cambridge, UK) and secondary fluorescent Alexa488 conjugated anti-rabbit antibodies (Invitrogen). Antibodies were diluted at 1:200 in 1% BSA/PBS. Hoechst (Invitrogen) was used to stain the nucleus of cells. Immunofluorescence was visualized and images were captured using an Olympus image analysis system (Olympus, Tokyo, Japan).

2.2.4.3 Tubulogenesis assay

For tubulogenesis assay, a 48-well-plate was coated with matrigel (150 μl/well) and incubated at 37^{o}C for 1 h. EPCs were then seeded on the matrigel coated plates, 2×10^{4} cells/well, in 250 μl EGM-2 medium and incubated at 37^{o}C overnight. The tube-like structures were photographed under a phase-contrast microscope.

2.2.4.4 DiI-Ac-LDL assay

To test the ability of our iPS-EPCs to uptake acetylated-LDL (Ac-LDL), the cells were incubated with 1,1'-dioctadecyl 3,3,3',3'-tetramethylindo carbocyanine perchlorate (DiI-Ac-LDL; Invitrogen) at a concentration of 10 μg/ml in EGM-2 for 4 h at 37^{o}C. After washing, the cells uptaking Ac-LDL were observed by their fluorescent signal under the microscope and photographed.

2.2.5 Baculoviral vector preparation

Recombinant baculoviral vectors expressing eGFP, mouse Isthmin, HSVtk or CD40L were constructed using the BAC-to-BAC baculovirus expression system according to the manufacturer's manual (Invitrogen). These genes were under the control of a CMV promoter with the R segment and part of the U5 sequence of long terminal repeat from the human T-cell leukemia virus type 1 at 5' UTR and the woodchuck hepatitis virus posttranscriptional regulatory element (WPRE) at 3' UTR. The constructs were produced by homologous recombination after co-transfection of Sf9 insect cells with pBacPAK9 transfer vector containing the expression cassette and linearized AcMNPV viral DNA (Clonetech, Mountain View, CA, USA). The recombinant baculoviruses were propagated in Sf9 insect cells (Invitrogen) at an MOI of 0.1 in Sf-900 II SFM (Invitrogen) and maintained at 27^{o}C. The virus-containing supernatant was collected 3 days after virus infection. The budded viruses in the insect cell-culture medium were centrifuged at 1000 g for 10min to remove cell debris, and concentrated by a second round of centrifugation at 28,000 g for 1 h.

Virus pellets were re-suspended in 1× PBS and virus titers were determined by real time PCR for Gp64 expression. Viral DNA was isolated using a Viral DNA purification kit (Roche). For real time PCR, the forward and reverse primers used were gp64-F1337-S23: 5'-AAAGCAACCTCATAACCACCATG, and gp64-R1429-A20: 5'-CCAATTCGCCTTCAGCCATG. The Taqman probe gp64-P1395-A21 was labeled with FAM (6-carboxy-fluorescein) at the 5'-end and a non-fluorescent dark quencher, BHQ1(Black Hole Quencher), at the 3'-end, 6-FAM-5'-CAGACTGGTGCCGACGCCGCC-BHQ1. The PCR sample mix was as followed: 100 nM primers and Taqman probes, 2X iQ Supermix (Bio-Rad, Hercules, California, USA), 2 μl template viral DNA or water as the non-template control to a final volume of 25 μL. The thermal cycling included an initial denaturation step of 3 min at 95°C, followed by 40 cycles of 95°C for 15 sec, and 60°C for 1 min with fluorescence detection. For all real-time amplifications, triplicates of five 10-fold dilutions of the plasmid DNA standards, viral DNA samples and non-template water controls were simultaneously subjected to analysis.

For baculoviral transduction, cells were transduced in at a multiplicity of infection (MOI) of 100 plaque forming units (pfu) per cell overnight. A full change of medium was done the next day to remove the viral particles and stop the transduction. GFP expression was detected under a fluorescence microscope and by flow cytometric analysis. To confirm CD40L gene expression, flow cytometry was performed using anti-CD40L antibody (BD biosciences).

2.2.6 Animal studies

2.2.6.1 Animals

Pathogen-free, 6 to 8 week-old immunocompetent BALB/c mice, immunocompromised athymic nude (nu/nu) BALB/c mice or NSG mice (NOD.Cg-*Prkdc*^{scid} *Il2rg*^{tm1Wjl}/SzJ mice from Jackson Laboratory, USA) were used in this study. All handling and care of animals were carried out according to the Guidelines on the Care and Use of Animals for Scientific Purposes issued by the National Advisory Committee for Laboratory Animal Research, Singapore.

2.2.6.2 Dual *in vivo* imaging system

Mouse 4T1-luc was utilized to facilitate *in vivo* bioluminescent imaging. To generate an orthotopic breast cancer model, the cells were injected subcutaneously onto the mammary fat pad (1×10^5 cells in 50 µl PBS). To generate a breast cancer lung metastasis model, 4T1-luc cells were injected intravenously via the tail vein of the mice (1×10^4 cells in 200 µl PBS). To monitor the bioluminescent signals of 4T1-luc in the mice, isoflurane gas-anesthetized animals were injected intraperitoneally with D-luciferin (Promega, Madison, Wisconsin, USA) at 100 mg/kg in PBS.

To observe the biodistribution of iPS-EPCs in the mice non-invasively over time, a lipophilic, near-infrared fluorescent dye 1,1'-dioctadecyl-3,3,3',3'-tetramethyl indotricarbocyanine iodide (DiR; Caliper Life Sciences) was used to label the cells. Cells were labelled with 50 µg/ml DiR for 30 min in a 37^{o}C incubator. After labelling, the cells were washed three times with 1× PBS. Labelled or non-labelled iPS-EPCs cells were injected into mice through the

tail vein (5×10^5 in 200μl PBS) or via an intratumor injection (5×10^5 in 100μl PBS).

After injections, whole animal imagings were performed at day 1, 3, 7 and 14 to track the migration of the iPS-EPCs and observe the tumor growth. Briefly, the mice were placed on a warmed stage inside the camera box of the IVIS imaging system coupled with cool CCD camera (Xenogen, Alameda, CA, USA). Images and measurements of luminescent signals were acquired and analyzed with the Xenogen living imaging software v2.5 and quantified as photons per second.

2.2.6.3 Biodistribution of EPCs in intracranial 2M1 tumor model

Invasive human glioma cell line 2M1 previously established in our lab was used to test the biodistribution of EPCs in the mouse glioma model[133, 134]. To investigate iPS-EPCs distribution in the tumor, 5×10^5 2M1 cells were labeled with green fluorescent dye CM-DiO (Invitrogen) and inoculated into the right side of the nude mouse striatum. One week later, 1×10^6 iPS-EPCs, which were labeled with CM-DiI dye (Invitrogen), were injected at the same site of the tumor injection. Brain tissues were collected one week after the EPCs injection for sectioning and examination.

2.2.6.4 Therapeutic studies of EPCs

To investigate therapeutic effects of iPS-EPC-mediated gene delivery, the breast cancer lung metastasis model in nude (nu/nu) BALB/c mice described above was used. At day 3 post-tail vein injection, mice were randomly divided into different groups (n = 10 per group). For the CD40L experiment, the

groupings were as follows: PBS, iPS-EPC, iPS-EPC-Bacpak and iPS-EPC-CD40L. For the HSVtk experiment, the groupings were: PBS, iPS-EPC, iPS-EPC-HSVtk and iPS-EPC-HSVtk+GCV. Lastly, for the isthmin experiment, the groupings were: PBS, iPS-EPC, iPS-EPC-Bacpak and iPS-EPC-misthmin.

The iPS-EPCs were transduced with the respective recombinant baculovirus at an MOI of 100 pfu per cell. Three days after tumor inoculation, baculovirus-transduced iPS-EPCs (1×10^6 in 200 μl PBS per animal) were injected into the mice through the tail vein. Tumor growth was monitored using whole-animal imaging as described above and animal survival rates were recorded.

2.2.7 Histology

The collected organs from mice were submerged in 4% paraformaldehyde for 24 h. The organs were then transferred into a 30% sucrose solution and were immersed in 30% sucrose for another 24 h. Subsequently, the tissues were embedded in Jung tissue freezing medium (Leica Microsystems, Gmbh, Nussloch, Germany). Organs were then frozen and placed in a -80^{o}C freezer for storage. Sections 12μm thick were taken with a Leica CM3050S cryostat (Leica Microsystems, Wetzlar, Germany). They were then observed with a confocal microscope.

2.2.8 Statistical analyses

All data are represented as mean ±SD. The statistical significance of differences was determined by one-way ANOVA. The statistical analysis of survival data was performed using the Gehan-Breslow log rank test followed

by the Holm-Sidak method for pairwise multiple comparison tests. A p value of <0.05 was considered to be statistically significant.

2.3 Results

2.3.1 Generation of EPCs from Human Pluripotent Stem Cells

2.3.1.1 OP9 co-culture method

We first derived EPCs from hESC line H1 via co-culture with OP9 mouse stromal cells according to a previously published protocol by Vodyanik and Slukvin (**Fig. 2.1A**)[135]. The super-confluent OP9 cells ready for co-culture is shown in **Figure 2.1B,** whereas **Figure 2.1C** shows an example of a healthy undifferentiated H1 colony. The H1 colony was nicely seeded and attached on top of the OP9 stroma forming a button-like structure (**Fig. 2.1D left**). On day 4 of the co-culture (**Fig. 2.1D middle**), the H1 cells differentiated by forming organized root-like structures that penetrated the OP9 portion of the co-culture and spread away from the button-like structure. The root-like structures grew thicker over time, as seen in the image of the co-culture on day 6 (**Fig. 2.1D right**). After 8 days of co-culture, the cells were harvested and the $CD34^+$ cells were then sorted by two rounds of selection using the Magnetic Assorted Cell Sorting (MACS) method. From one T-175 cm^2 flask, in which three wells of a 6-well-plate H1 culture were seeded, we could obtain 5×10^5 to 1×10^6 $CD34^+$ cells after two rounds of MACS. The cells showed typical cobblestone EPC morphology, after they were reseeded on a fibronectin-coated plate (**Fig. 2.1E**).

We observed the percentage of $CD34^+$ cells by using flow cytometry (**Fig. 2.1F**). Before sorting, the percentage of $CD34^+$ cells varied from 5-10%.

After two rounds of sorting via MACS, the purity of the $CD34^+$ cells can reach up to 80-99%. Most of the sorted $CD34^+$ cells also co-expressed the CD31 marker (82.84%) as well as Flk1 (75.92%). On the contrary, the CD45 marker was expressed at a very low level (3.28%). Furthermore, these cells can maintain the CD34 and CD31 markers for up to four passages (**Fig. 2.1G**). The sorted EPCs formed tube-like formations upon seeding on matrigel (**Fig. 2.1H**), another *in vitro* characteristic of EPCs.

EPCs can also be generated from iPS cells (**Fig. 2.2A**) via the OP9 co-culture method. The co-culture of iPS colonies and OP9 cells at day 8 also displayed outward root-like expansion, similar to that of H1-OP9 co-culture (**Fig. 2.2B**). The resulting EPCs after sorting had similar morphology (**Fig. 2.2C**) and expression of endothelial markers shown by flow cytometry (**Fig. 2.2D**) as that of H1-EPCs. Furthermore, these cells also had the capability of tubulogenesis upon seeding on matrigel (**Fig. 2.2E**).

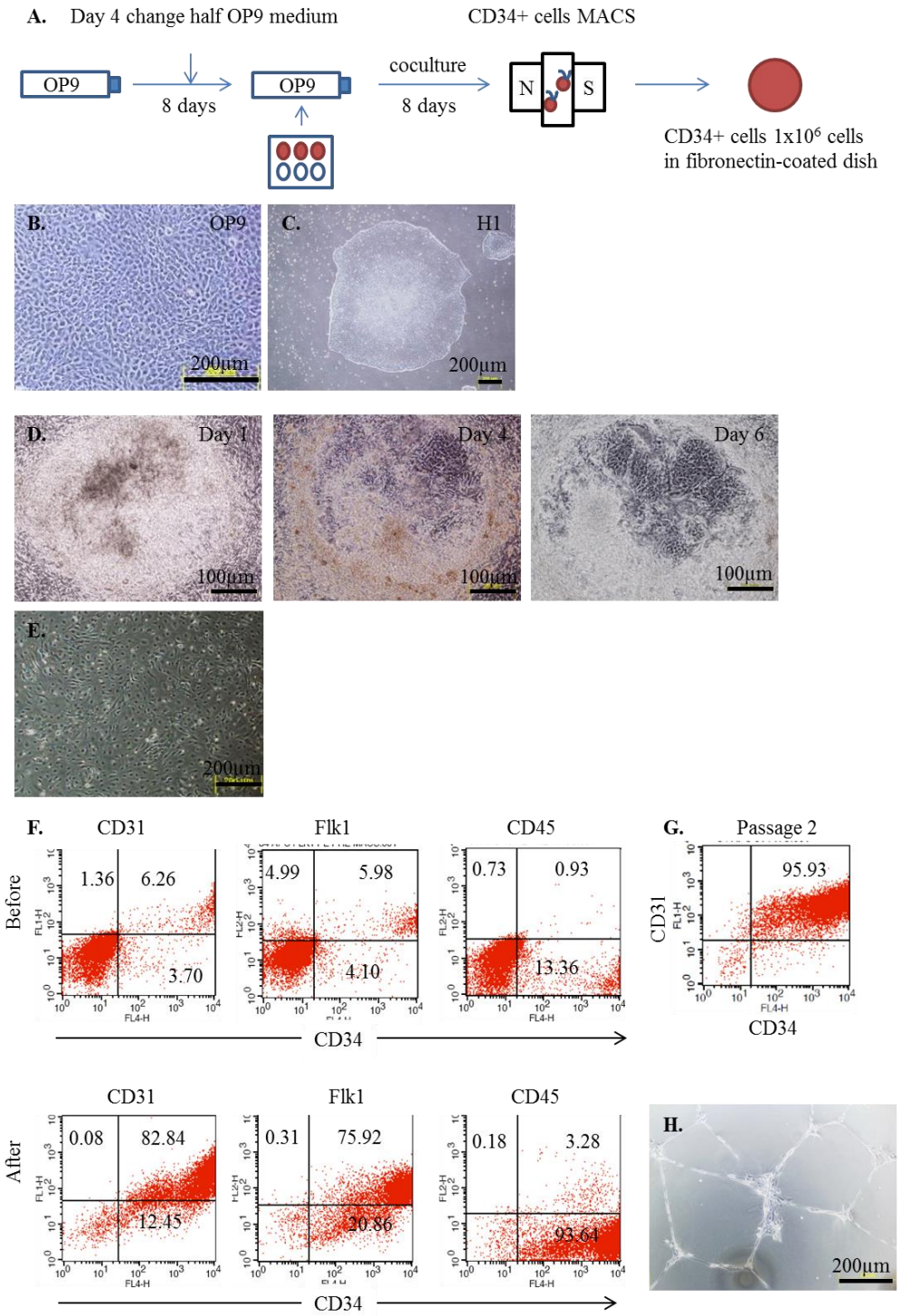

Figure 2.1. Derivation of hESC-derived EPCs via mouse stromal OP9 co-culture. A. Schematic diagram on the OP9 co-culture protocol. H1 colonies were co-cultured with overgrown OP9 culture for 8 days. $CD34^+$ cells were then collected using magnetic cell sorting. **B.** Super-confluent OP9 at day 8 ready for co-culture. **C.** H1, hESC cell line colony. **D.** Co-culture of H1 and OP9 at different time points (Left to right: day 1, 4 and 6). **E.** EPCs at day 5 after $CD34^+$ magnetic sorting on fibronectin-coated dish. **F.** Expression of EPCs surface markers: $CD34^+$, $CD31^+$, $Flk1^+$ before and after sorting process via flow cytometry. EPCs expressed very low CD45 markers, hematopoietic lineage markers. **G.** Expression of CD34 and CD31 after 2nd passage of EPCs. Most of the cells still co-expressed these markers (95.93%). **H.** EPCs form tubule-like formation when seeded onto a matrigel-coated dish.

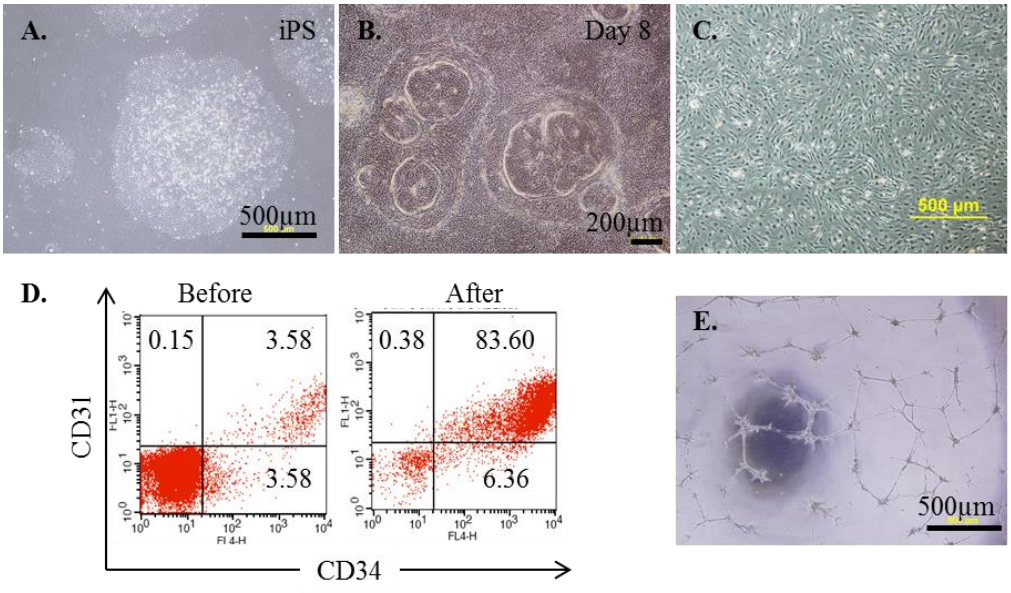

Figure 2.2. iPS-derived EPCs produced via mouse stromal OP9 co-culture. A. Colonies of iPS cells. **B.** iPS co-cultured on OP9 stromal cells after 8 days. **C.** iPS-EPCs after sorting by MACS seeded onto fibronectin coated dish. **D.** Flow cytometry showing the percentage of CD34 and CD31 markers in the cells before and after sorting via MACS. **E.** iPS – EPCs form tubule-like formation when seeded onto a matrigel-coated dish.

2.3.1.2 M2-10B4 co-culture method

M2-10B4 is a mouse bone marrow stroma cell that can support hematoendothelial differentiation[136, 137]. Thus, we also used this cell line alongside OP9 cells to generate EPCs from hPSCs (**Fig. 2.3A**). After reaching confluency (**Fig. 2.3B**), M2-10B4 cells will be treated with mitomycin C in order to prepare mitotically inactive feeder cells for the co-culture. The cells were then washed extensively with PBS before being reseeded onto a T-175 cm^2 flask and allowed to settle in a 37^oC incubator overnight. The next day, colonies of H1 or iPS cells were seeded onto the M2-10B4 feeder cells (**Fig. 2.3C**). The M2-10B4 co-culture process took a longer time of 13 days, compared to OP9 co-culture, which only took 8 days. After two rounds of MACS, we also obtained around 5×10^5 to 1×10^6 $CD34^+$ cells (**Fig. 2.3D**).

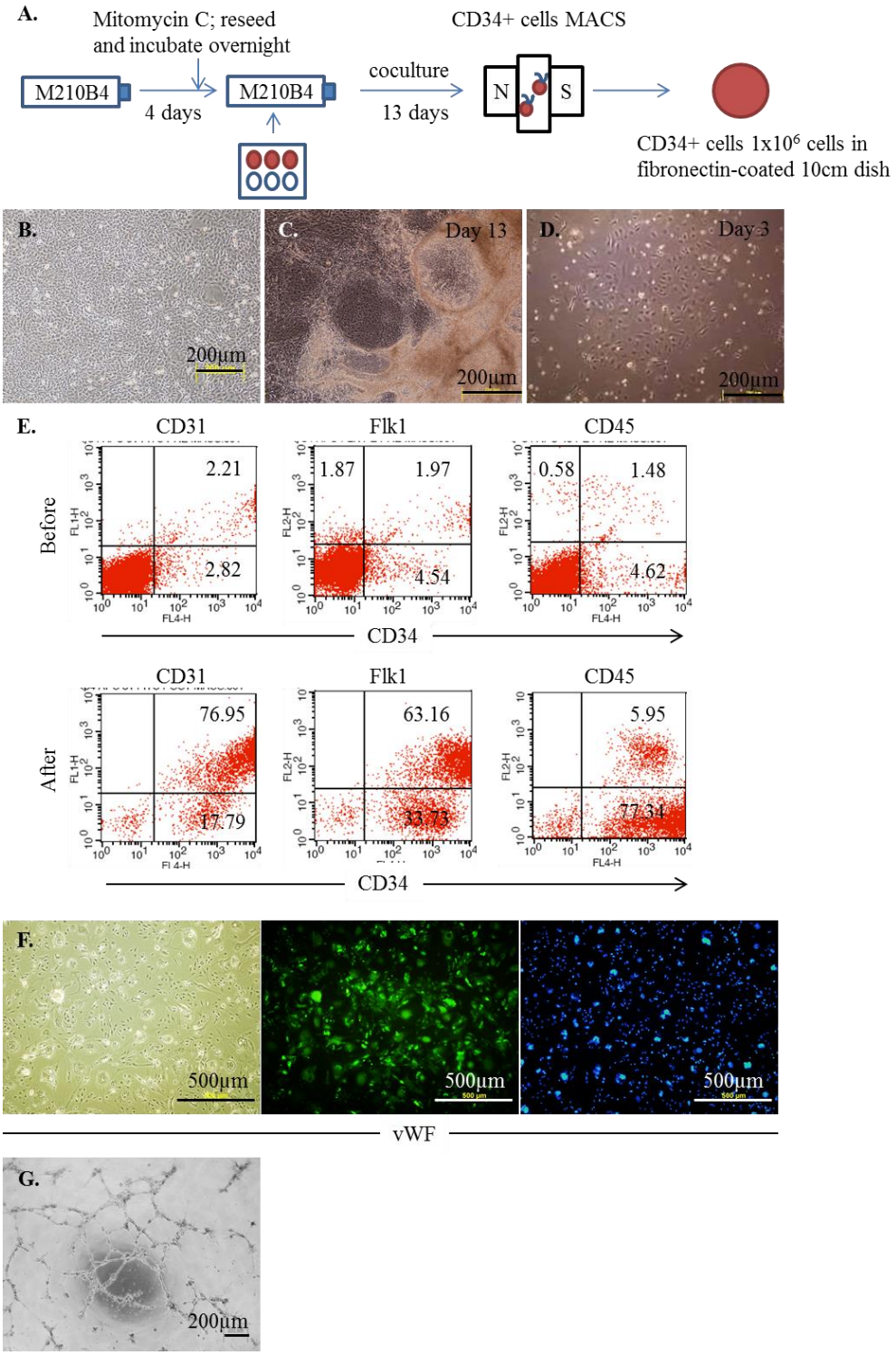

Figure 2.3. Derivation of hESC-derived EPCs via mouse stromal M2-10B4 co-culture. A. Scheme diagram on the M2-10B4 co-culture protocol. H1 colonies were co-cultured with mitomycin-C treated M2-10B4 cell culture for 13 days. Magnetic sorting was then performed to obtain $CD34^+$ cells. **B.** M2-10B4 culture at day 4. **C.** Co-culture of H1 and M2-10B4 at day 13. **D.** EPCs at day 3 after $CD34^+$ magnetic sorting on fibronectin-coated dish. **E.** H1 derived EPCs via M2-10B4 co-culture expressed endothelial lineage surface markers: $CD34^+$, $CD31^+$, $Flk1^+$ before and after sorting process via flow cytometry. EPC derived from H1 co-cultured with M2-10B4 cells express CD45 markers albeit at low level, which is a marker for hematopoietic lineage. **F.** Expression of von Willebrand Factor as shown by immunostaining (Left to right: phase-contrast, GFP expression, hoechst nucleus staining). **G.** hESC-EPCs form tubule-like formation when seeded onto a matrigel-coated dish.

The expression of EPCs markers were tested via flow cytometry (**Fig. 2.3E**). We observed that the percentage of $CD34^+$ cells varied from 5-20% prior to sorting. We also noticed that the co-expressions of the CD34 marker and other EPC markers such as CD31 and Flk1 were lower compared to OP9 co-culture derived EPCs. Furthermore, we noted that the sorted $CD34^+$ cells had a higher expression of the CD45 marker, compared to the OP9 co-culture derived EPCs.

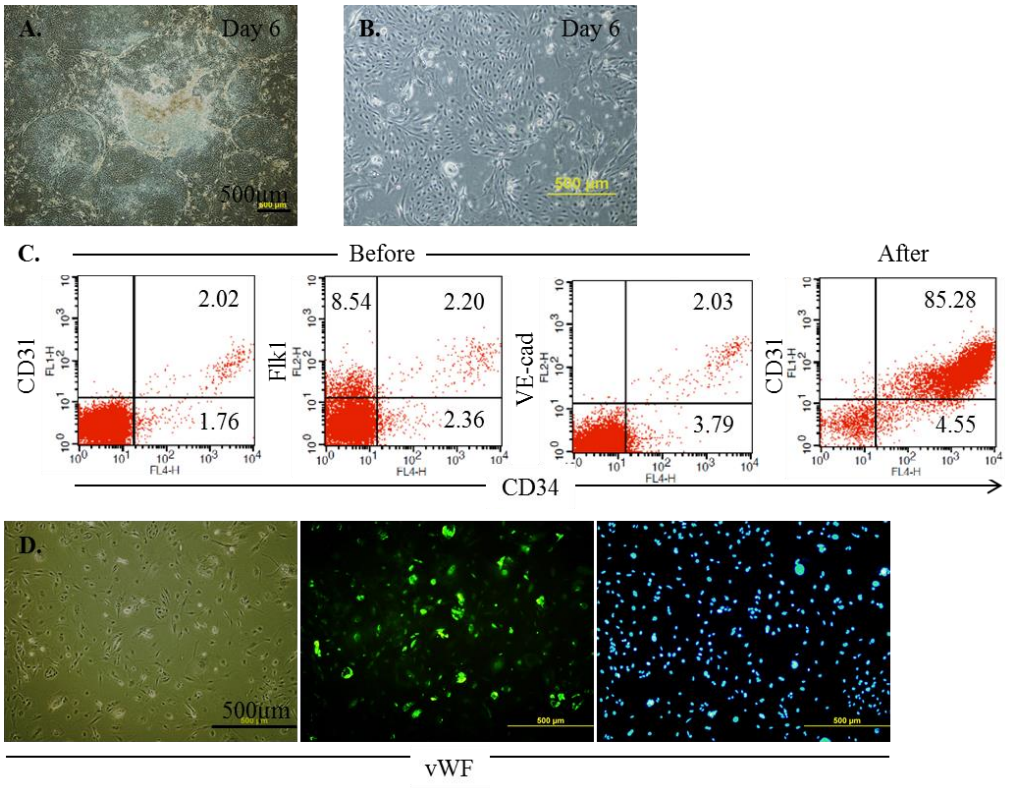

Figure 2.4. H9 hESC line-derived EPCs via mouse stromal M2-10B4 co-culture. **A.** Co-culture of H9 and M2-10B4 at day 6. **B.** EPCs at day 6 after $CD34^+$ magnetic sorting on fibronectin-coated dish. **C.** Flow cytometry showing expression of CD34 together with other EPCs markers: CD31, Flk1 and CD144 before and after MACS. **D.** Expression of von Willebrand Factor as shown by immunostaining (Left to right: phase-contrast, GFP expression, hoechst staining).

We further tested the expression of von Willebrand Factor (vWF), a glycoprotein constitutively produced in the endothelium, in the sorted $CD34^+$ cells via immunostaining, and the results were positive (**Fig. 2.3F**). These cells could also form tube-like formations when seeded onto matrigel (**Fig. 2.3G**). However, by observing the matrigel tubulogenesis results qualitatively, we noticed that tubulogenesis was more efficient for the cells that were produced via OP9 co-culture, compared to the M2-10B4 co-culture method. We also tested this method using H9 and iPS cells, and we obtained EPCs with similar characteristics (**Fig. 2.4 – 2.5**).

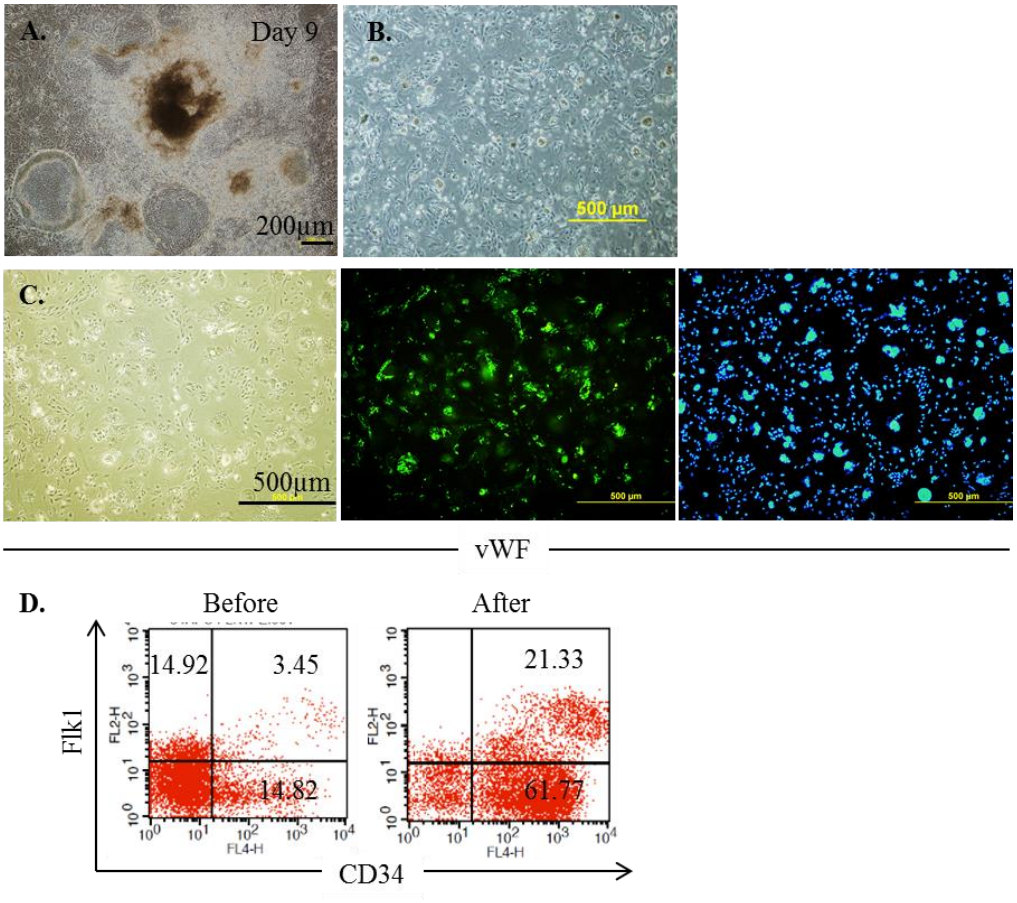

Figure 2.5. iPS cells-derived EPCs via mouse stromal M2-10B4 co-culture. A. Co-culture of iPS colonies and M2-10B4 at day 9. **B.** EPCs at day 6 after $CD34^+$ magnetic sorting on fibronectin-coated dish. **C.** Expression of von Willebrand Factor as shown by immunostaining (Left to right: phase-contrast, GFP expression, hoechst staining). **D.** Flow cytometry showing co-expression of CD34 and Flk1 before and after MACS.

2.3.1.3 Non-stromal 2-D differentiation method

The above co-culture method can recreate native stem cell niches, thus providing an inductive environment for the differentiation of hESCs. However, contamination of animal cells is one concern which needs to be tackled before this method can be used in clinical settings. Thus, we opted for a non-stromal 2-D differentiation method (**Fig. 2.6A**) described by Wang et al[130]. After changing the medium from mTeSR to the differentiation medium, the H1 cells started to spread out, leaving the colonies and filling the entire culture dish. Interestingly, they also formed root-like structures like those found in the co-culture (**Fig. 2.6B**). From one 10-cm dish of H1 culture, we obtained around 5×10^5 to 1×10^6 $CD34^+$ cells after 2 rounds of MACS (**Fig. 2.6C**). The EPCs generated via the 2-D differentiation method had a similar expression of surface markers as those produced by the OP9 co-culture method. After sorting, most of the $CD34^+$ cells also co-expressed CD31, Flk1 and VE-Cadherin, but not CD45 (**Fig. 2.6D**).

By using the same method, we can also generate iPS cell-derived EPCs (**Fig. 2.7A-B**). The flow cytometry results reveal some differences between the hESC and iPS cell-derived EPCs (**Fig. 2.7C**). For H1-derived EPCs, the purity of $CD34^+$ cells after 2 rounds of MACS was higher (>90%). Besides, most of the $CD34^+$ cells were also $CD31^+$, $Flk1^+$ and VE-$cadherin^+$ (approximately 90%). However, in the case of iPS cell-derived EPCs, approximately 50-55% of the cells co-expressed these markers. Yet, these cells were negative for CD45 expression, similar to those derived from H1.

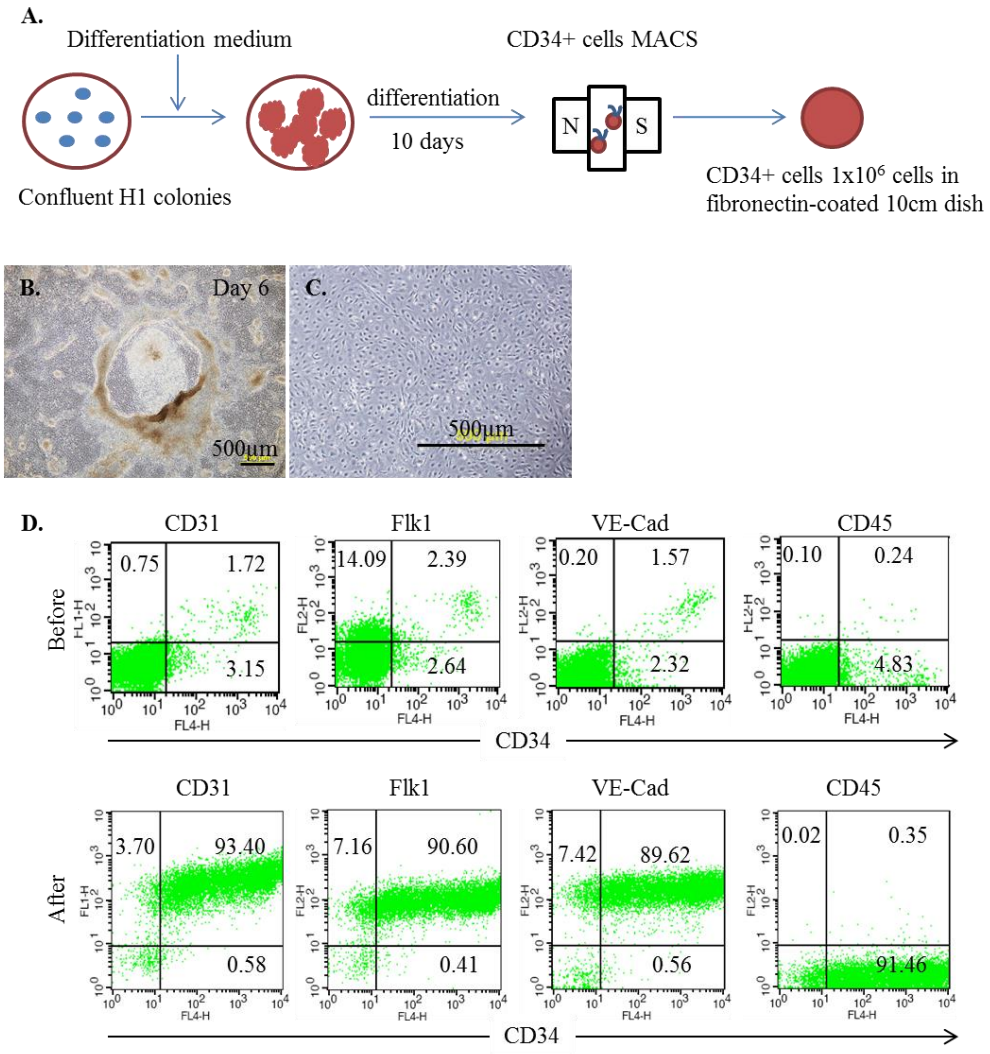

Figure 2.6. H1 hESC-derived EPCs via 2-D differentiation method. A. Protocol for 2-D differentiation method. H1 medium was changed to differentiation medium when H1 culture reached confluency. After 10 days, MACS was performed to obtain $CD34^+$ cells. **B.** H1 differentiation at day 6. **C.** Sorted CD34 on fibronectin-coated dish. **D.** Flow cytometry of the cells before and after sorting via MACS of the different EPCs markers. Most of the $CD34^+$ cells co-expressed CD31, Flk1, and VE-cadherin, but 0.35% expressed CD45 marker after sorting.

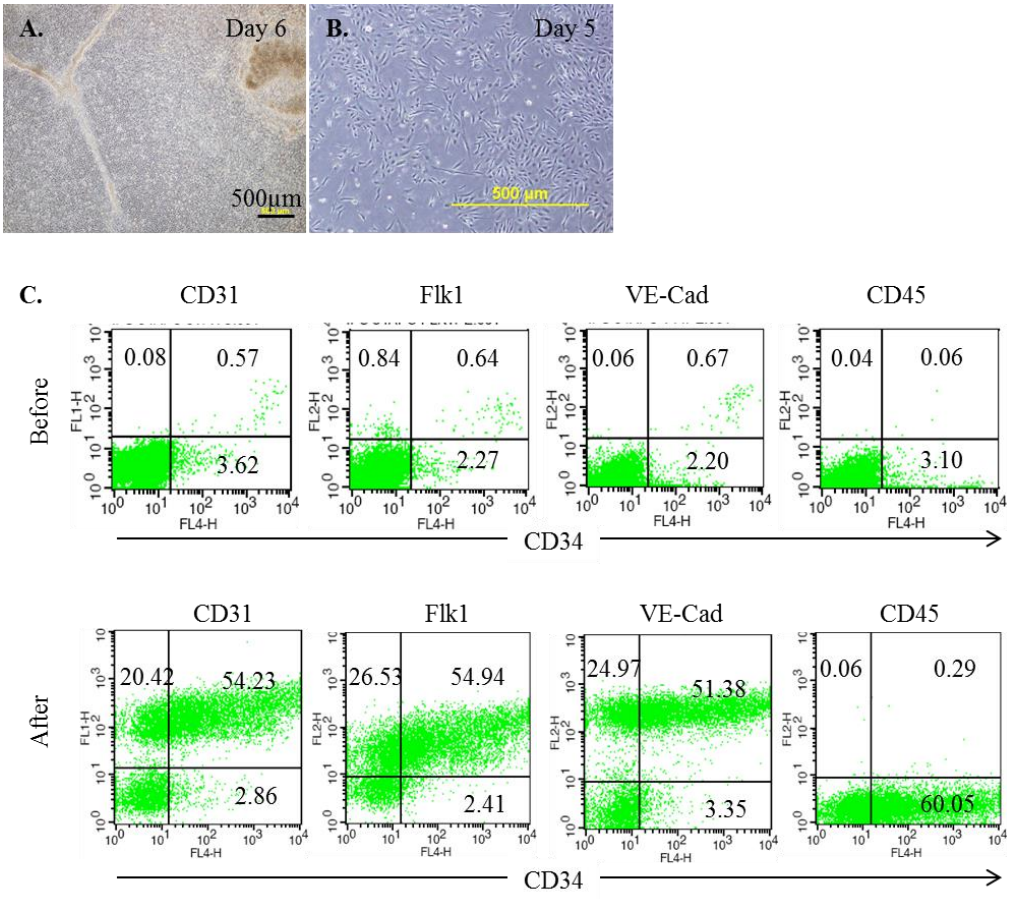

Figure 2.7. iPS cells-derived EPCs via 2-D differentiation method. A. Image showing iPS at day 6 of differentiation. **B.** Sorted $CD34^+$ cells plated on fibronectin coated plate. **C.** Flow cytometry of the cells before and after sorting via MACS of the different EPCs markers. Lower percentage of CD34 as well as other markers as compared to hESC-EPCs was observed before and after MACS.

2.3.1.4 Human iPS cell-derived EPCs via embryoid bodies formation

A protocol has been published to use well-established human ES cell lines to differentiate mesoderm cells in EBs into endothelial precursors[132]. We tested whether the protocol could be used to derive endothelial precursors from early-passage human iPS cells (around p10). EBs formed by human iPS cells cultured on low attachment dishes were plated onto a matrigel-coated culture dish and treated with BMP4 (day 0-7), Activin A (day 1-4), FGF2 (day 2 onwards), VEGF (day 4 onwards), and SB431542, a TGF-β inhibitor, (day 7

onwards) for 2 weeks (**Fig. 2.8A-B**). After the EB was replated, we observed the root-like structure again during the differentiation process (**Fig. 2.8B right**). From one 10-cm dish of EB (i.e from one well of a 6-well plate iPS cell culture), we could obtain approximately 1×10^6 $CD34^+$ cells with just one round of MACS (**Fig. 2.8C**).

The percentage of EPCs markers before sorting was highest using this method compared to other methods (**Fig. 2.8D**). Fluorescence-activated cell sorting (FACS) analysis revealed that the generated cells were a mixed population of cells containing ≥ 20% cells positive for CD34, a hematopoietic stem cell marker. The mixed population of cells co-expressed endothelial cell markers, including CD31 (17.60%), Flk1 (8.13%), and VE-cadherin (10.71%), but had a low expression level of the CD45 hematopoietic marker (1.44%).

After undergoing immunomagnetic separation to enrich the $CD34^+$ cells and promote cell expansion in an endothelial growth medium, flow cytometric analysis showed that ≥ 95% of cells at passage 2 were CD34-positive (**Fig. 2.8D**). A majority of the purified $CD34^+$ cells were also positive for CD31 (81.29%). While a majority of the purified $CD34^+$ cells were also positive for CD31 (81.29%), approximately 21% of the $CD34^+$ cells co-expressed Flk1, 48% expressed VE-cadherin, and only 8.98% of these cells were $CD45^+$. Since CD34 is expressed on both immature EPCs and mature circulating endothelial cells, we also examined the expression of CD133, a stem cell marker restricted to immature EPCs, on the sorted cells, and found that 30% of the cells were CD133-positive (**Fig. 2.8E**). As a negative control,

human fibroblasts used to generate iPS cells were tested and showed no CD133 expression (0.76%).

Furthermore, many of the iPS cell-derived cells were vWF-positive (**Fig. 2.9A**) and CD31-positive (**Fig. 2.9B**), as shown by immunostaining. Biological and functional characterization showed that the derived cells were able to incorporate the DiI-labelled acetylated LDL (**Fig. 2.9C**) and readily formed tubule-like structures upon seeding onto matrigel (**Fig. 2.9D**). Therefore, we use the term iPS-EPCs to refer to all endothelial lineage cells derived from iPS cells in the described method.

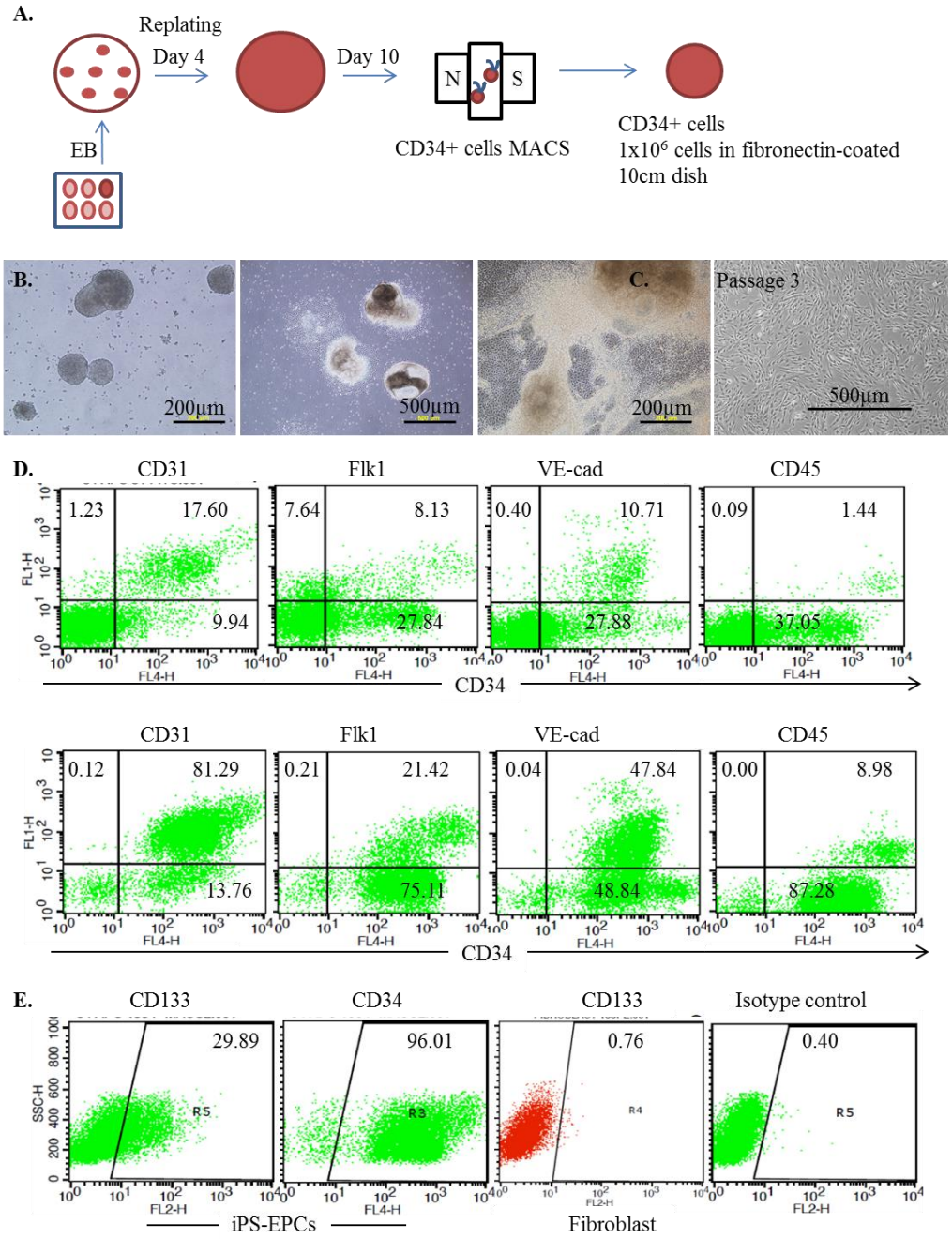

Figure 2.8. Generation of EPCs from human iPS cells via EB method. A. Generation of EPC from iPS. Confluent iPS colonies were scraped to generate EBs. After 4days, the EBs were replated onto matrigel-coated dish and cultured for 10 days. $CD34^+$ cells were then harvested and maintained on fibronectin-coated dish. **B.** Left to right: EB, 1 day after the EBs were replated, differentiation day 10. **C.** EPCs at passage 3 after MACS. **D.** Flow cytometry before and after the magnetic cell sorting to show expression of EPCs markers CD34, CD31, Flk1 and VE-cadherin, and less expression of hematopoietic marker CD45. **E.** Expression of CD34 and CD133 "stemness" markers on sorted for $CD34^+$ cells. Human fibroblast were used as negative control. Isotype controls were always set ≤1.

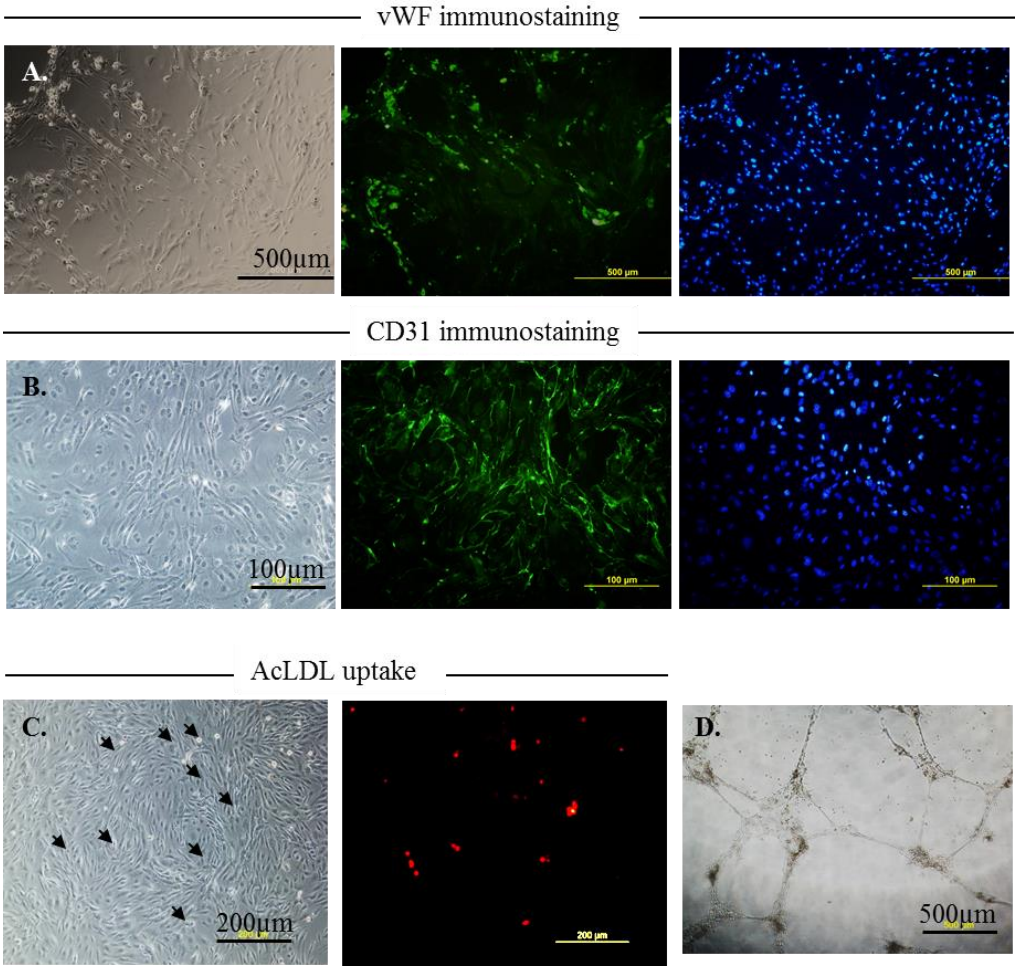

Figure 2.9. Characterization of iPS cells-derived EPCs. A. Expression of von Willebrand Factor as shown by immunostaining (left to right: phase contrast, GFP, Hoechst staining). **B.** Expression of CD31 as shown by immunostaining (left to right: phase contrast, GFP, Hoechst staining). **C.** iPS-EPCs could uptake AcLDL. Phase contrast (Left) and red fluorescence (Right) images of Ac-LDL taken up by the generated iPS-EPCs. Arrow shows DiI-Ac-LDL being taken up by the cells. **D.** iPS-EPCs could form tube-like formation upon seeded onto matrigel-coated dish.

2.3.2 Tumor tropism of iPS-EPCs

2.3.2.1 Homing of hPSC-EPCs to 4T1-luc orthotopic breast cancer model

To non-invasively examine the *in vivo* distribution of hPSCs-derived EPCs in mice over time following systemic injection, we employed IVIS dual color-imaging technology. This system detects and captures luminescent signals from 4T1-luc cells and fluorescent signals from DiR-labelled iPS-EPCs. Prior to animal experiments, labeling optimization of iPS-EPCs by DiR was performed. The cells can be efficiently stained with DiR at a concentration of 50 μg/ml for 30 min at 37^{o}C, a process which in having 95.93% of the cells positively and uniformly labeled as indicated by the sharp peak (**Fig. 2.10A**).

To examine the *in vivo* tumor tropism of the generated hPSCs-EPCs, we established two mouse breast cancer models in athymic Balb/c nude mice: an orthotopic breast cancer model generated by subcutaneous injection of luciferase-expressing mouse 4T1 breast cancer (4T1-luc) cells onto the mammary fat pad (**Fig. 2.10B**) and a breast cancer lung metastasis model generated by intravenous injection of 4T1-luc cells via the tail vein (**Fig. 2.10C**).

We first tested *in vivo* tumor tropism of iPS-EPCs in the orthotopic breast cancer model (**Fig. 2.11**). After labeling iPS-EPCs with the near-infrared fluorescent dye DiR, we injected the cells into the tumor-bearing mice through tail vein injections at day 7 post-tumor inoculation. The Xenogen IVIS Imaging System was employed for non-invasive dual-color *in vivo* imaging to longitudinally monitor the distribution of the labeled iPS-EPCs at days 0, 1, 3, 7, and 14 post-EPC injection in the same sets of animals. Whole-body

bioluminescence imaging showed that tumors grew quickly around the inoculated mammary fat pad during the 21-day observation period, and luciferase signals outside the primary tumor region were observed at day 21 post-tumor inoculation, indicating metastasis (**Fig. 2.11A**).

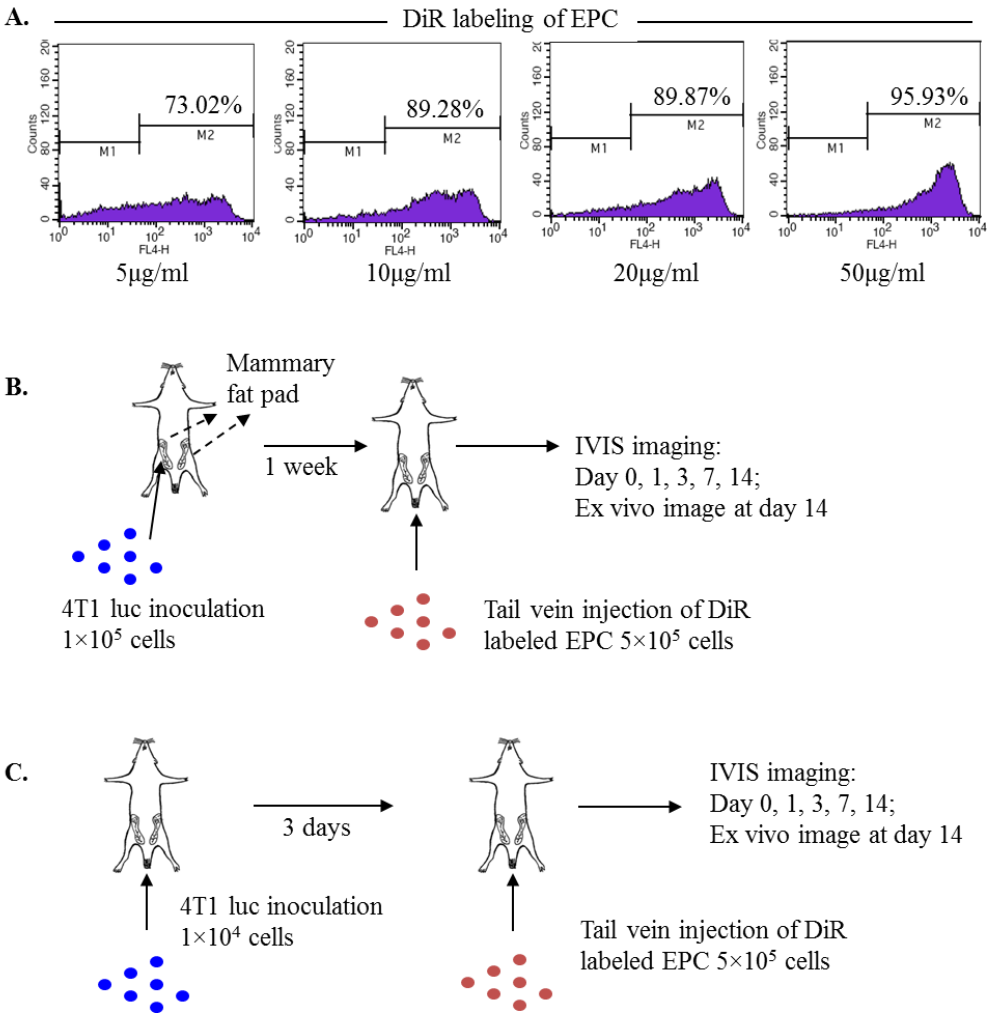

Figure 2.10. Dual *in vivo* imaging system. A. DiR labeling optimization of EPCs. EPCs can be efficiently labeled with DiR at concentration 50μg/ml for 30min at 37°C. **B.** Schematic illustration of the dual *in vivo* imaging system utilizing both 4T1luc and DiR-labeled EPC in mammary pad model. Breast cancer 4T1luc cells are inoculated into mammary fat pad of the mice. One week after the tumor inoculation, DiR-labeled EPCs are introduced into the mice via tail vein injection. IVIS imaging are carried out at day 1, 3, 7, and 14 post tail vein injection. **C.** Protocol for tumor tropism study in lung metastatic model. The 4T1luc cells are inoculated into the mice via tail vein injection. Three days after the tumor inoculation, DiR-labeled EPCs are introduced into the mice via tail vein injection. IVIS imaging are carried out at day 1, 3, 7, and 14 post tail vein injection.

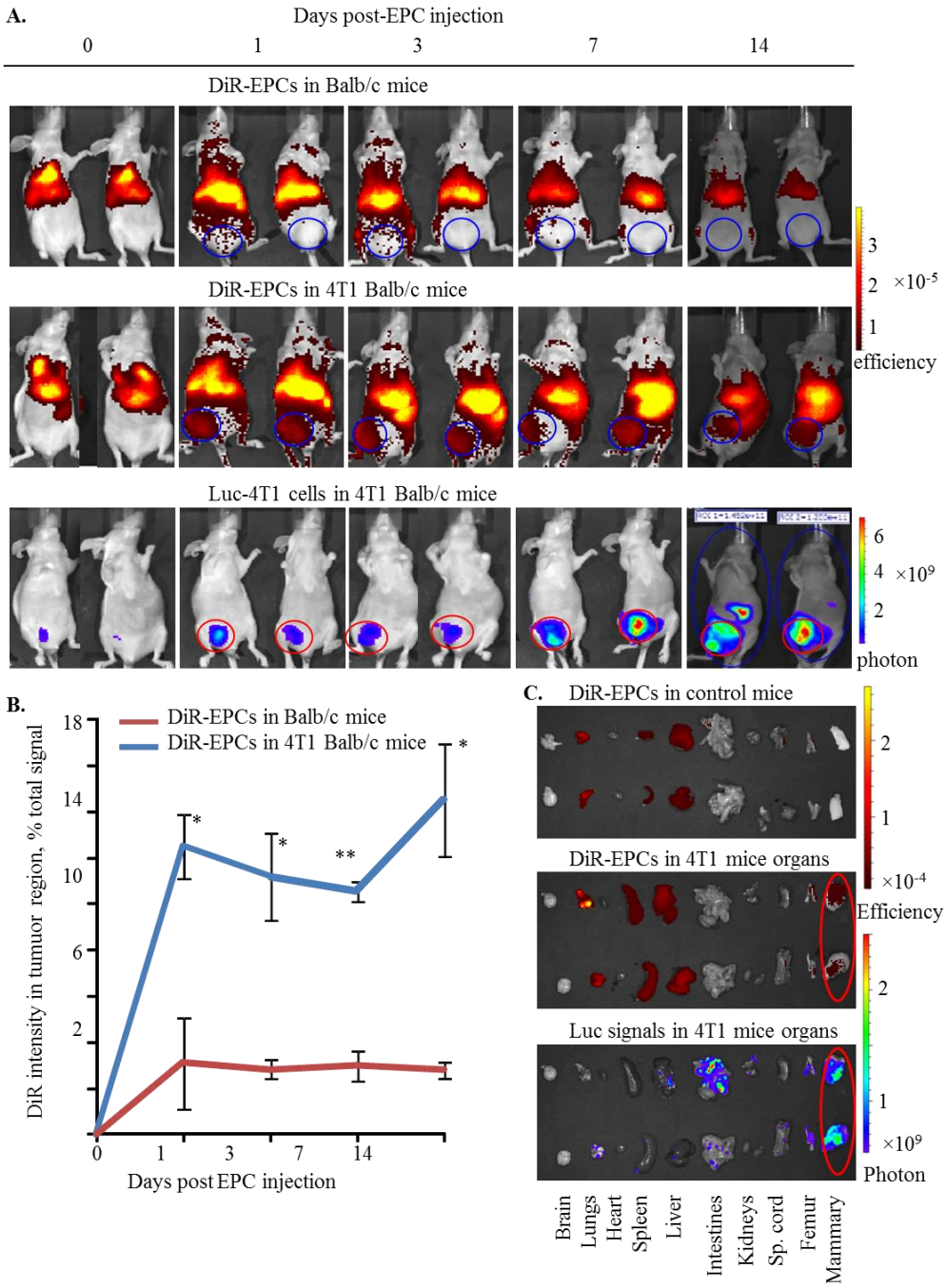

Figure 2.11. Tumor tropism of iPS cells-derived EPCs in the 4T1 orthotopic mouse model of breast cancer. A. Whole animal images of Balb/c nude mice of injected with DiR labeled – iPS-EPCs alone, and DiR-iPS-EPCs with 4T1luc breast cancer cells. EPCs can be seen migrating toward primary tumor site (mammary pad region) as early as day 1 post tail vein injection. After 14 days, more cells are migrating towards the tumor site. **B.** Percentage distribution of iPS-EPCs in the primary tumor region over the whole body. Overall average of 12% in the tumor-bearing mice as compared to 3% in animal without tumor over time. There values are statistically significant different as tested by one-way ANOVA (p=0.03, 0.026, 0.006,0.021 for day 1, 3, 7, and 14 respectively. **C.** *Ex vivo* image of the different organs: brain, lungs, heart, spleen, liver, intestines, kidneys, spinal cord, femur, mammary pad (left to right). Red circle indicates strong DiR signals in the mammary fat pad of tumor-bearing animals. No singles were detected in the same region in controls.

Whole-body DiR fluorescence imaging showed that tail vein-injected iPS-EPCs were initially distributed predominantly to the lung region. One day after tail vein injection, the size of the DiR signal-positive area in the thoracic region significantly increased. Meanwhile, we observed significantly increased DiR signals in the tumor inoculation site in tumor-bearing mice (**Fig. 2.11A**). The DiR signals in this region were significantly higher, compared with those in mice without tumors, and remained high for at least 14 days, although the overall DiR signal intensity reduced from day 3 onwards (**Fig. 2.11A**). On average, approximately 12% of the injected iPS-EPCs homed into the 4T1-luc tumor cell inoculated mammary pad region as calculated by the percentage of DiR signal in the region over the whole body signal (**Fig. 2.11B**).

At day 14, the mice were sacrificed and e*x vivo* images of different organs were taken (**Fig. 2.11C**). Here, we can scrutinize the metastases that have occurred in the mice, manifestations which could not be detected by whole-body imaging alone. The luc signals indicated that the 4T1 tumor cells metastasized to the lungs, spleen, liver, intestines, spinal cord and femur. There were overlaps of luminescent (luc) and fluorescent (DiR) signals in the primary tumor site, implying the homing property of iPS-EPCs (**Fig. 2.11C**).

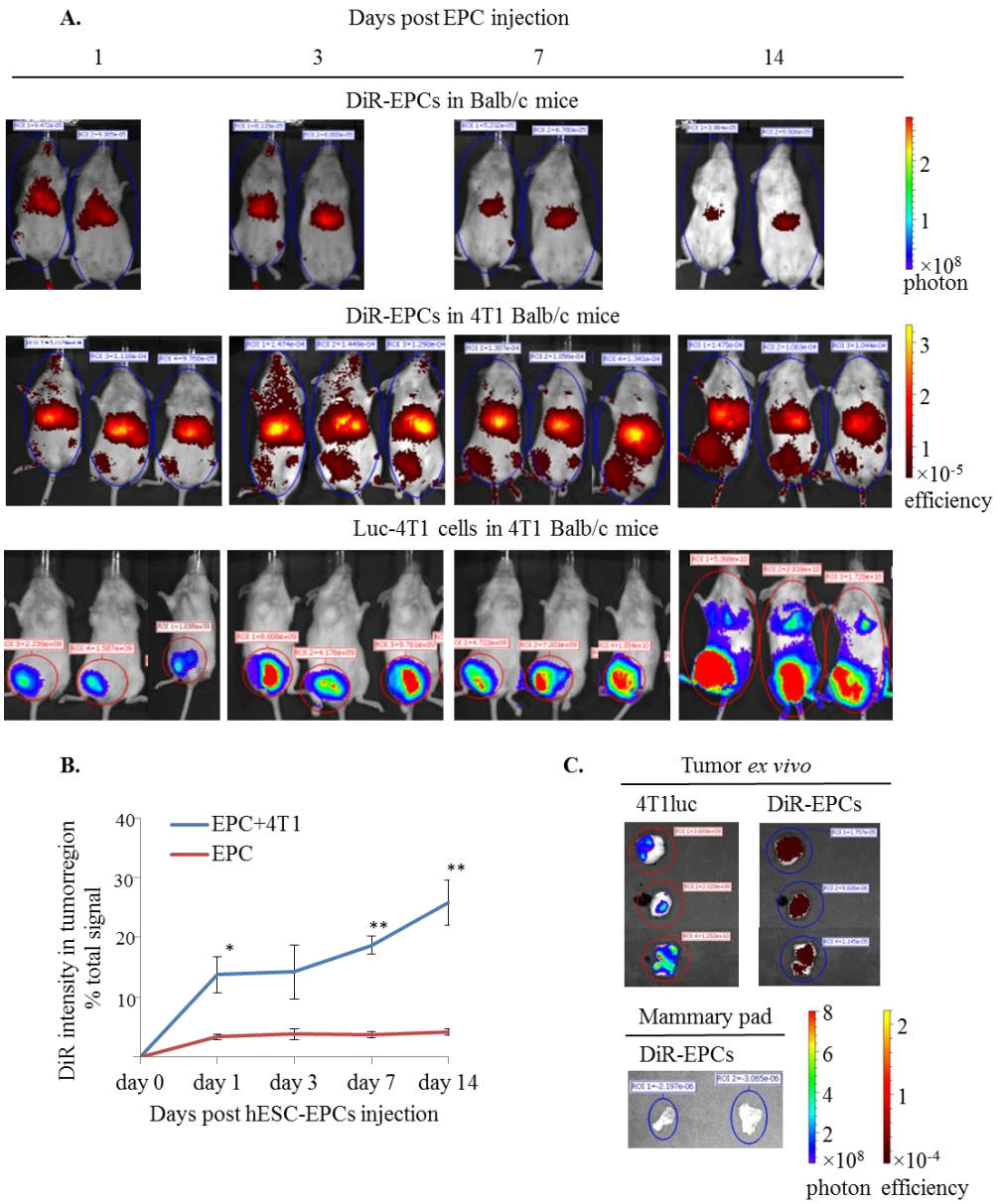

Figure 2.12. *In vivo* migration of hESC-EPCs toward 4T1 breast cancer cells in 4T1 orthotopic immunocompromised NSG mice. A. EPCs migrated toward primary tumor site as early as day 1 post tail vein injection. After 14 days, more cells are migrating towards the tumor site. **B.** Percentage distribution of iPS-EPCs in the primary tumor region over the whole body. Statistical tests showed significant difference in the values between the two groups (p=0.021, 0.0009, 0,005 for day 1, 7 and 14 respectively). **C.** *Ex vivo* image of the solid tumor mass shows overlap of luminescent luc and fluorescent DiR signals. This implies that EPCs have migrated to the tumor.

We also tested the *in vivo* distribution of hESC-derived EPCs in immune-compromised NSG mice bearing the 4T1-luc tumor in the mammary

pad. As early as day 1 post-intravenous injection, the DiR fluorescent signal can be seen around the mammary pad where the 4T1 tumor had been inoculated a week before (**Fig. 2.12A**). Most cells were trapped in the liver and lung area. Over time, more EPCs migrated to the 4T1 primary tumor site. More than 20% of cells migrated to the mammary pad region, based on the percentage of DiR signal in that region over the whole body signal at day 14 (**Fig. 2.12B**). The tumor *ex vivo* image reveals that there was an overlap of signals between the fluorescent DiR and luminescent luc, indicating that EPCs home to 4T1 tumor cells (**Fig. 2.12C**). Thus, we showed that both iPS cells and hESC derived EPCs have tumor homing properties.

2.3.2.2 Homing of iPS-EPCs to breast cancer lung metastasis model

Next, we tested *in vivo* tumor tropism of iPS-EPCs in the breast cancer lung metastasis model (**Fig. 2.13**). We injected the DiR-labeled iPS-EPCs into the tumor-bearing mice through tail vein injections at day 3 post-tumor inoculation. Whole-body bioluminescence imaging showed that tumor growth became detectable at day 10 post-tumor inoculation (day 7 post-EPC injection). By day 17 post-tumor inoculation, cancer cell dissemination to other organs was observed (**Fig. 2.13A**). Whole-body DiR fluorescence imaging showed that tail vein-injected iPS-EPCs were distributed predominantly to the lung region and decreased over time from day 1 to day 14 post-EPC injection (**Fig. 2.13A**). When compared with DiR signals in normal Balb/c mice that were injected with only the labeled iPS-EPCs without 4T1 tumor cell inoculation, it was found that DiR signals in the tumor-bearing mice were relatively stronger in

the lung region and a statistically significant difference between the two groups of mice was observed at day 14 (**Fig. 2.13B**).

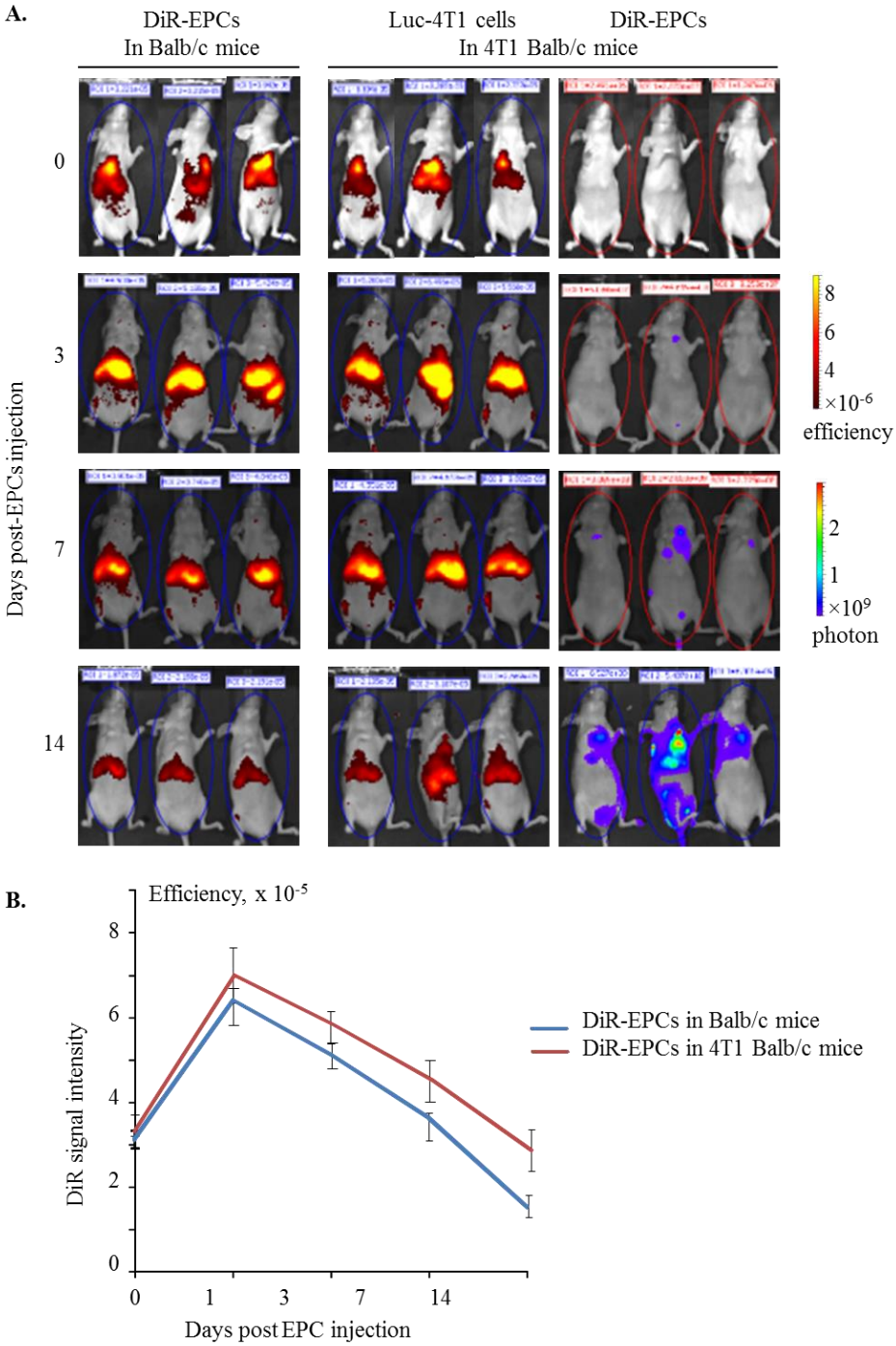

Figure 2.13. Tumor tropism of iPS cells-derived EPCs in the 4T1 breast cancer lung metastasis model. A. Whole body images showing the EPCs are trapped in the lungs regions, for both the control group and tumor bearing animal group. **B.** The DiR signal over time in both groups showed similar trend.

2.3.2.3 Tumor tropism of iPS-EPCs to 2M1 invasive glioma model

We also investigated the distribution of EPCs after intratumor injection into a 2M1 invasive glioma orthotopic tumor model (**Fig. 2.14A**). In the primary tumor site, we can see that the EPCs infiltrated the tumor mass, migrating towards the tumor vessels (**Fig. 2.14B-C**). More importantly, EPCs can be seen infiltrating successfully into the tumor blood vessels, as shown in the yellow circle (**Fig. 2.14D)**. Interestingly, EPCs can also be found in tumor satellites located in the lateral ventricle, away from the primary tumor site (**Fig. 2.15A-C**). This implies that EPCs can target secondary metastatic tumor sites.

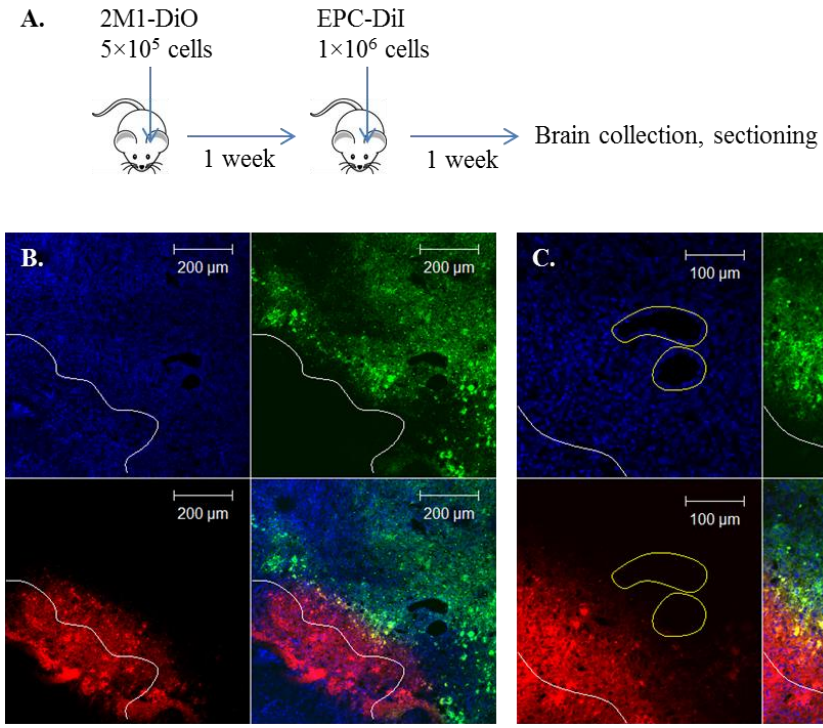

Figure 2.14. Biodistribution of EPCs in intracranial 2M1 glioma model at primary tumor mass. A. Protocol of the biodistribution experiment on mice glioma model. **B.** Primary DiO-labeled 2M1 tumor mass, infiltrated by DiI-labeled EPCs. White line: tumor border region. **C.** Magnified view of B, showing the tumor blood vessels. The EPCs infiltrate the tumor region, toward the tumor blood vessels. White line: tumor border region, yellow lines: the tumor blood vessels. **D.** EPCs incorporated into the tumor blood vessel (yellow line). White line: tumor border.

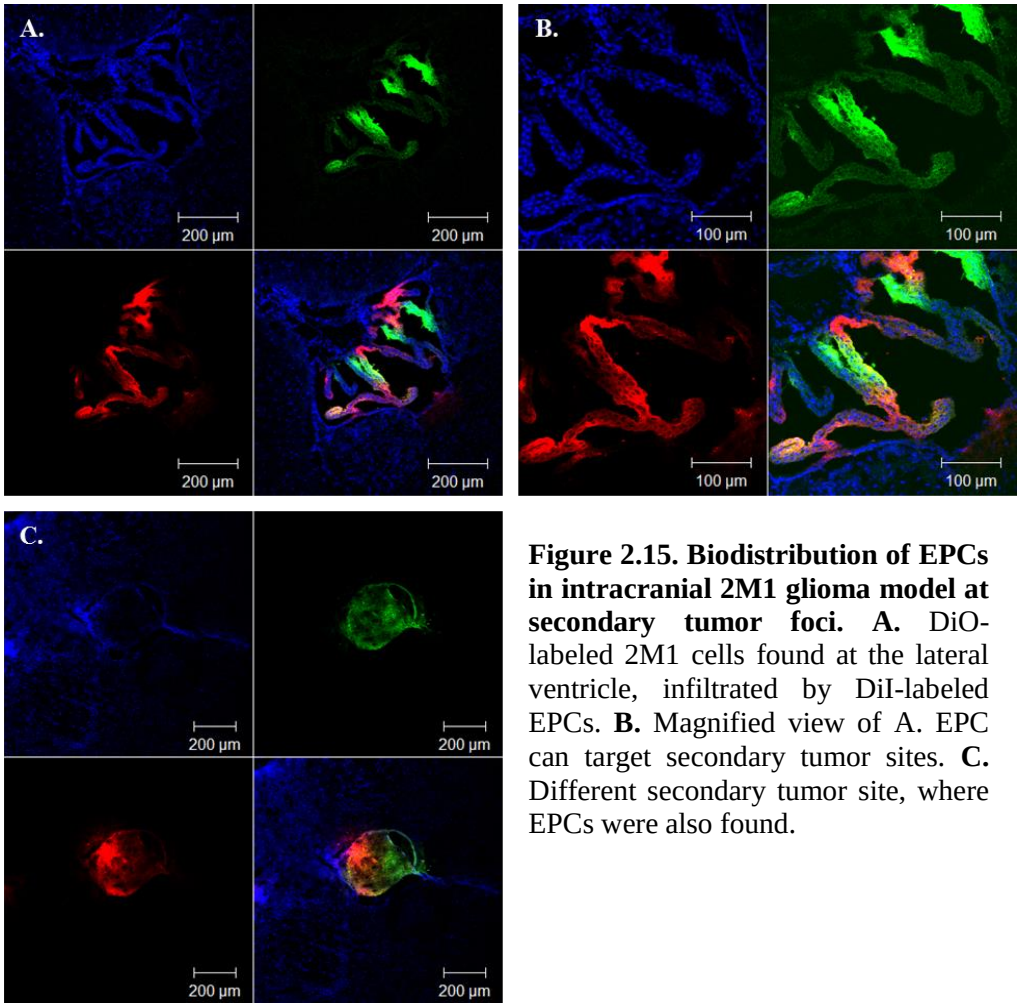

Figure 2.15. Biodistribution of EPCs in intracranial 2M1 glioma model at secondary tumor foci. A. DiO-labeled 2M1 cells found at the lateral ventricle, infiltrated by DiI-labeled EPCs. **B.** Magnified view of A. EPC can target secondary tumor sites. **C.** Different secondary tumor site, where EPCs were also found.

2.3.3 Effects of iPS-EPCs on tumor development and metastasis

The potential role of EPCs in promoting tumor growth is a concern when these cells are used as delivery vehicles for cancer therapy[138]. To investigate whether iPS-EPCs alone affect tumor progression and metastasis in the above orthotopic breast cancer model, we injected iPS-EPCs intratumorally at day 7 post-inoculation of 4T1-luc breast cancer cells (**Fig. 2.16A**). Intratumor injections of iPS cells, fibroblasts, and PBS were included as controls. Another well-established cellular delivery vehicle, iPS-NSCs, was also injected intratumorally for comparison (**Fig. 2.16A**). The tumor progression is similar throughout the different groups and comparable with the biodistribution

results (**Fig. 2.11**). The average tumor signals of the four groups were similar up to day 7 (**Fig. 2.16B**). Up to day 14, the tumor volume for the iPS-EPC group remained low compared to the rest of the groups. However, by day 21 the luc signal is comparable among all the groups. However, this can be due to the deaths of animals from the iPS group, which might explain the sudden drop in the luc signal at day 21 (**Fig. 2.16B**). The animals were sacrificed at day 21 and their organs were collected for *ex vivo* bioluminescence imaging (**Fig. 2.17A**). The 4T1-luc signal intensities in the examined organs were comparable in all groups (**Fig. 2.17B**). Although the tumor signal in the intestine was higher in the iPS-EPC group compared to the other groups, statistical analysis revealed that the differences were not significant.

Possible effects of iPS-EPCs on tumor development were further investigated in the breast cancer lung metastasis model. Taking advantage of the quick animal death in this model, we focused on the survival of tumor-bearing animals in this experiment. The mice were separated into five groups: PBS, iPS, human fibroblast, iPS-NSCs and iPS-EPCs. The different cells were injected intravenously via the tail vein 3 days after intravenous injection of 4T1-luc cells. Tumor growth was monitored by whole-body bioluminescent imaging of 4T1-luc cells. Whole body imaging of three mice from each group was shown as representatives (**Fig. 2.18A**). The bioluminescence intensities, indicative of tumor volume, demonstrated that there were no significant differences among the PBS group, iPS cell group, and iPS-EPC group, although a significantly higher level of 4T1-luc signal was observed in the HFF group at day 21 (**Fig. 2.18B**).

Mice started to die at day 17 in all groups. The median survival times were 26.2, 26.8, 25.6, and 27.6 days for the PBS, fibroblast, iPS cell and iPS-EPC groups respectively. There was no statistically significant difference among the four groups in survival rate (p = 0.946) (**Fig. 2.18C**). Our findings indicate that iPS-EPCs did not obviously promote tumor growth in the 2 tested tumor models.

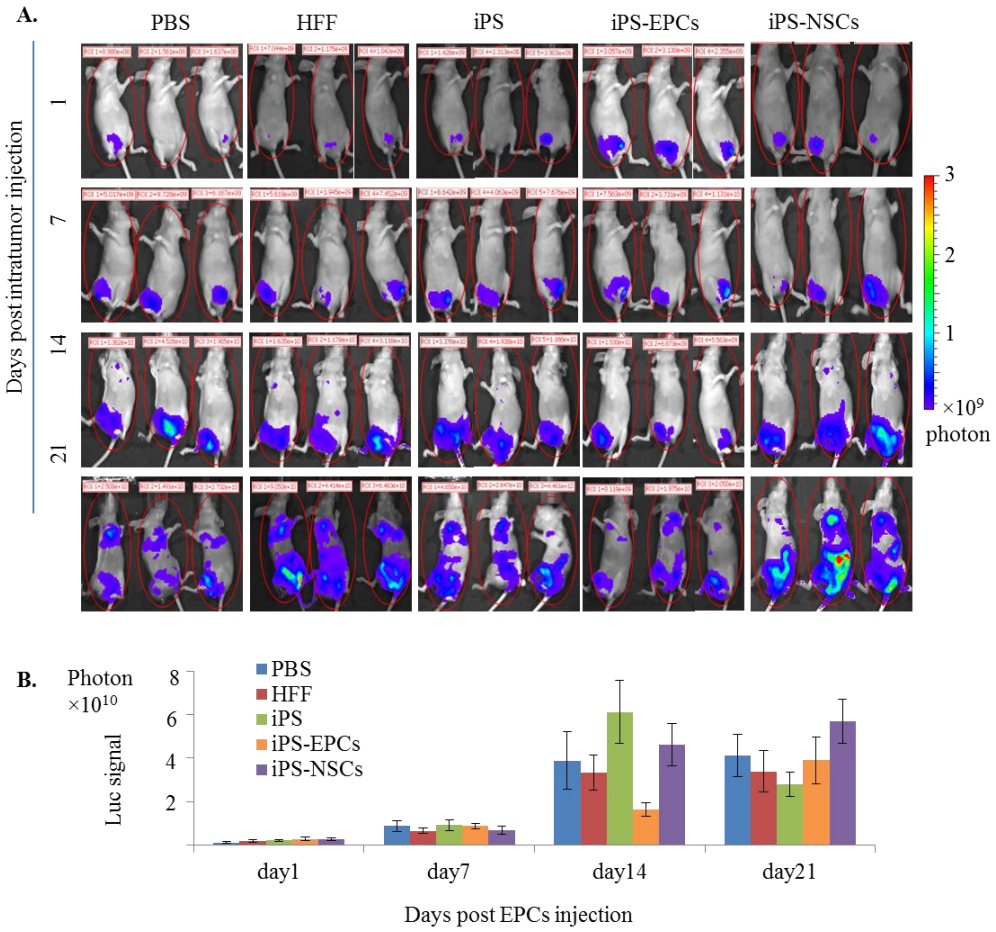

Figure 2.16. Effects of iPS-EPCs on 4T1 tumor development and metastasis in the 4T1 orthotopic mouse model of breast cancer. A. Whole body imagings of 3 representative animals from each groups: PBS, HFF, iPS and iPS-EPCs. Similar tumor progression as shown by the bioluminescent signals. Metastases can be detected at 2 weeks time point onwards. **B.** Tumor volume average from each groups. iPS-EPCs remained low.

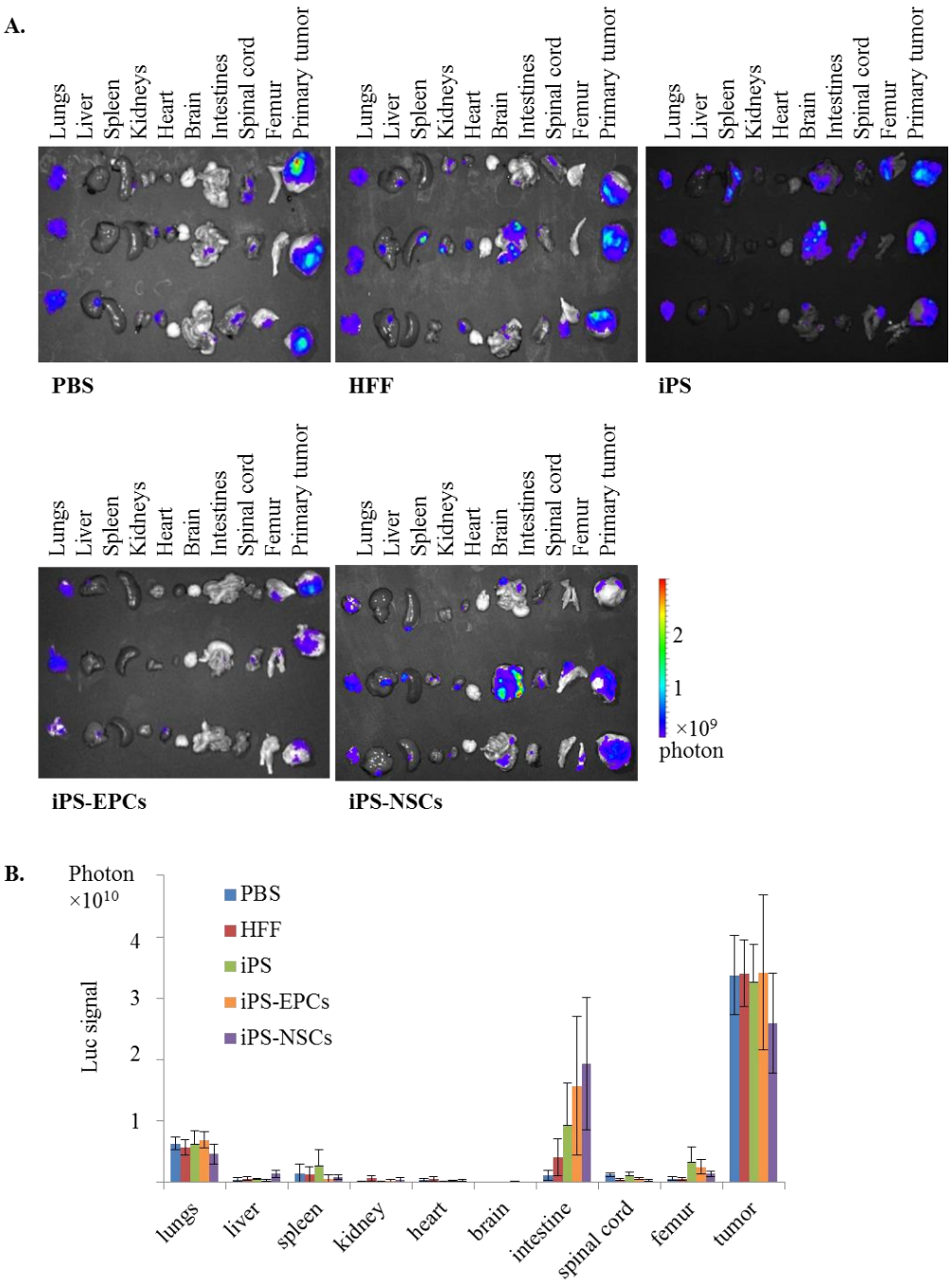

Figure 2.17. Effect of iPS-EPCs on tumor development and metastasis in 4T1 mammary pad model. A. Representative *ex vivo* images of different organs collected at day 21 post-intratumor injection: lungs, liver, spleen, kidneys, heart, brain, intestines, spinal cord, femur, primary tumor mass (from left to right). Images on iPS-EPCs group showed comparable metastatic progression as the other control groups. **B.** Luc signal of different organs. ANOVA statistics revealed that no statistically significant difference in the signal of the different organs among the groups.

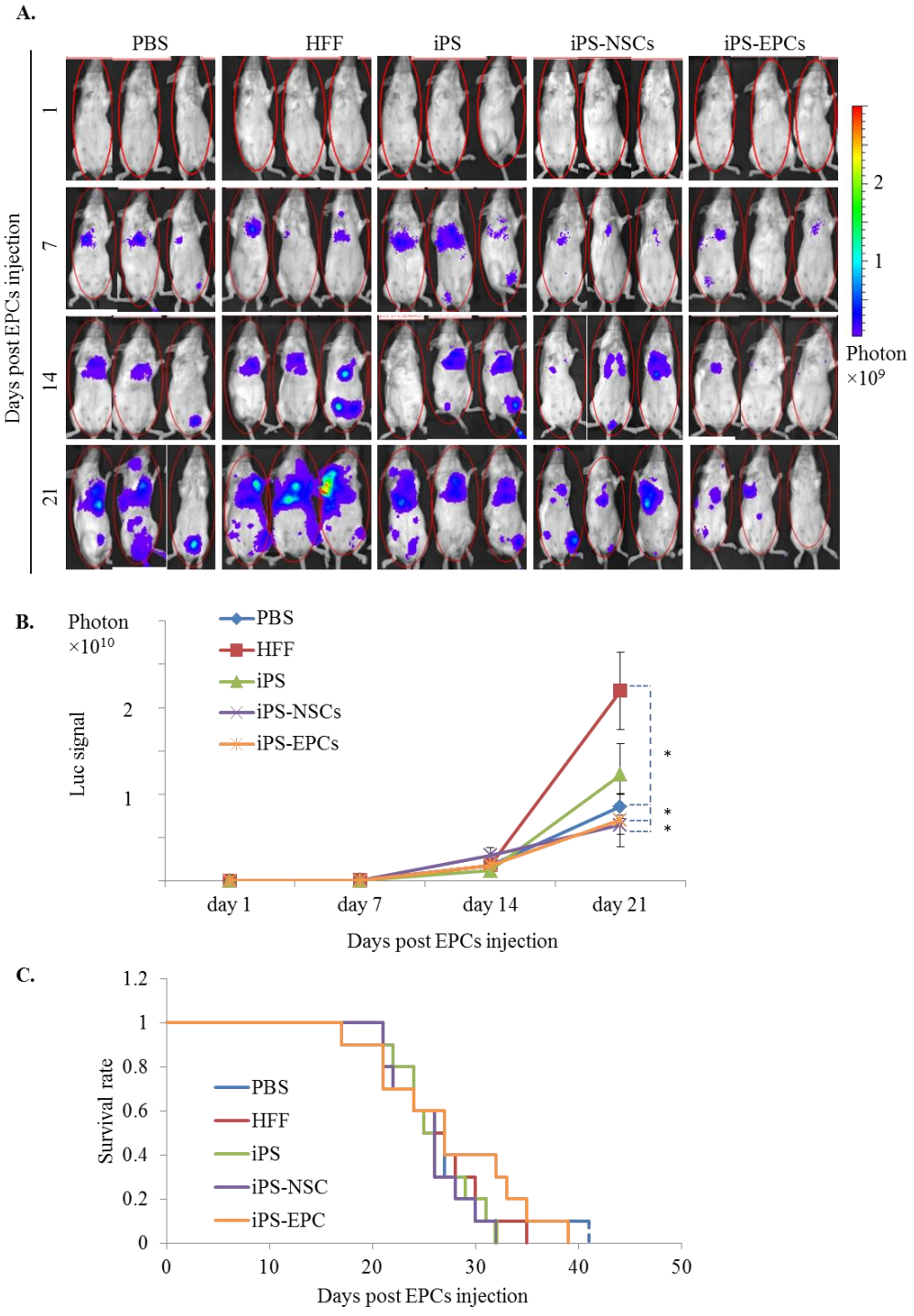

Figure 2.18. Effect of iPS-EPCs on 4T1luc tumor development in the 4T1 breast cancer lung metastasis model. A. Whole body imagings of 3 representative animals from each groups: PBS, human foreskin fibroblast (HFF), iPS and iPS-EPCs. Bioluminescent signal of 4T1luc show the tumor development over time after tail vein injection of different cells. At day 21, animals from iPS-EPCs group show less intense signal and less metastatic indication. **B.** Average tumor volume in each group represented by the bioluminescent luc signal. At day 21, there is a statistically significant difference in the luc signal among the groups (p=0.004). Value in HFF group is significantly different from PBS, iPS-NSCs and iPS-EPCs groups (p=0.00301, p=0.0007 and p=0.001 respectively). **C.** Survival curves of tumor-bearing mice. No statistically significant difference in the survival rates among the groups (p=0.946).

2.3.4 Genetic modification of EPCs

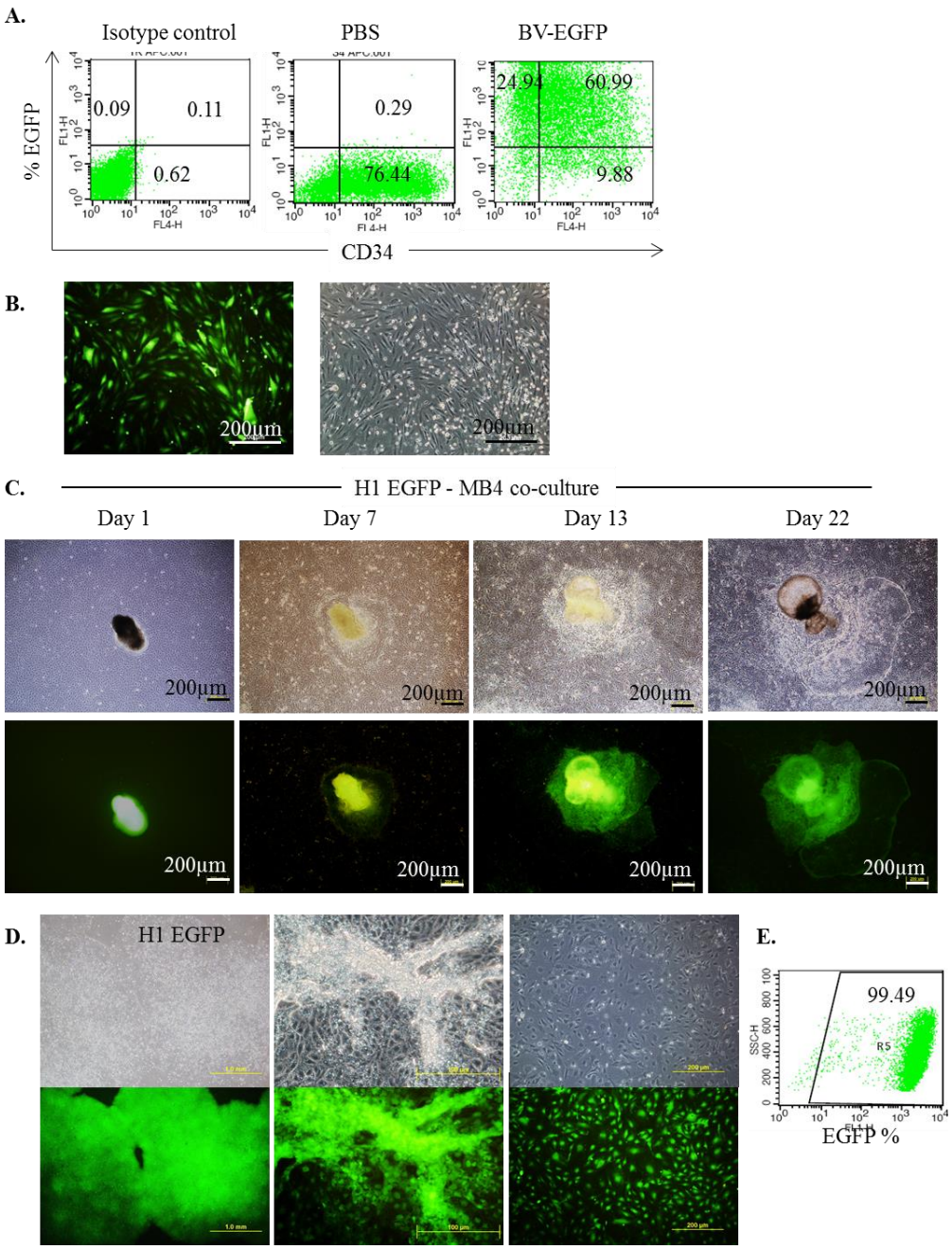

Figure 2.19. Genetic modifications of EPCs. A-B. Baculovirus transduction in EPCs (A.) Flow cytometry showing the percentage of EGFP in iPS-EPCs after transduction with baculoviral vector expressing EGFP. (B.) Cells expressing green eGFP after transduction with baculovirus (left) and the phase-contrast picture (right). **C.** H1-BV-RMCE-EGFP in M2-10B4 co-culture. H1 colonies maintained the EGFP expression throughout the differentiation process. **D-E.** H1-BV-RMCE-EGFP in 2D EPC differentiation. (D.) H1 colonies, $CD34^{+}$ cells after sorting and replating on fibronectin coated dish expressed EGFP as shown by the picture (E.) and flow cytometry of EGFP.

A high level of permissiveness to gene transfer is a vital requirement that allows the use of cellular vehicles for cancer gene therapy. Baculoviral vectors, which are derived from an insect virus *Autographa californica multiple nucleopolyhedrovirus,* emerge as a potentially safe class of gene delivery vectors due to their inability to replicate or cause toxicity in mammalian cells[125]. We showed that baculoviral vectors are capable of transducing iPS-EPCs. By using a baculoviral vector which expresses EGFP, we showed that 85.93% of the cells are EGFP positive, 60.99% of which are $CD34^+$ (**Fig. 2.19A**). The expression of EGFP in the cells were strong and bright (**Fig. 2.19B**).

Recently, our lab has successfully established a system to genetically modify hESCs specifically at *AAVS1* locus[139]. The system involves a two-step process combining homologous recombination with baculovirus-mediated (BV) Cre-RMCE (Cre recombinase-mediated cassette exchange). The generated master *loxP*-hESC line produced in the first step provides rich opportunities for readily introducing transgenes into *AAVS1* through efficient BV-Cre-RMCE. By using the two-step process combining homologous recombination with BV-Cre-RMCE, we can produce EGFP expressing EPCs from the *loxP*-hESC line (**Fig. 2.19C-D**). The stable EGFP-expressing H1 colonies could be differentiated into EPCs. In **Fig. 2.19C**, we see that the H1 colonies maintain their EGFP expression throughout the M2-10B4 co-culture period. The EGFP expressing H1 could also be differentiated via the 2-D differentiation method without any loss of EGFP expression (**Fig. 2.19D**). After sorting, all the $CD34^+$ cells expressed EGFP (**Fig. 2.19D**), and this was further confirmed by flow cytometric analysis (**Fig. 2.19E**).

2.3.5 EPCs therapeutic effects

2.3.5.1 iPS-EPC expressing CD40L impede tumor development in a breast cancer lung metastasis model

To assess the prospects of iPS-EPCs as the cellular delivery vehicle for therapeutic genes, we transduced the cells with baculovirus expressing CD40L gene, a member of the tumor necrosis factor (TNF) gene family[108]. Flow cytometric analysis indicated that up to 82.23% of iPS-EPCs could be transduced to express detectable levels of CD40L (**Fig. 2.20B**). The transduced cells were injected via the tail vein into athymic Balb/c nude mice bearing 4T1-luc breast cancer lung metastases. Tumor growth was monitored by whole-body bioluminescent imaging of 4T1-luc cells. **Figure 2.20A** shows representative 4T1 cell-bearing mice from different groups at 4 different time points. The bioluminescence intensities, indicative of tumor volume, demonstrate that the inhibitory effect of CD40L-expression iPS-EPCs on tumor growth was visible at day 14. Compared to the control groups, a statistically significant lower level of 4T1 cell-related luciferase signals was observed in the treated mice by day 21 post-tumor inoculation (**Fig. 2.20C**). Survival of the tumor-bearing mice in this group was significantly prolonged, and this was attributed to the effect of CD40L-expression of iPS-EPCs (**Fig. 2.20D**). On day 35, while all the mice in the three control groups had died, 60% of animals in the treated group were still alive (**Fig. 2.20E**). The median survival times were 25 to 29 days in the control groups, and 34 days in the treated group. The difference was statistically significant ($p = 0.004$ in Holm-Sidak test). There was no statistically significant difference among the control groups in median survival time ($p > 0.05$).

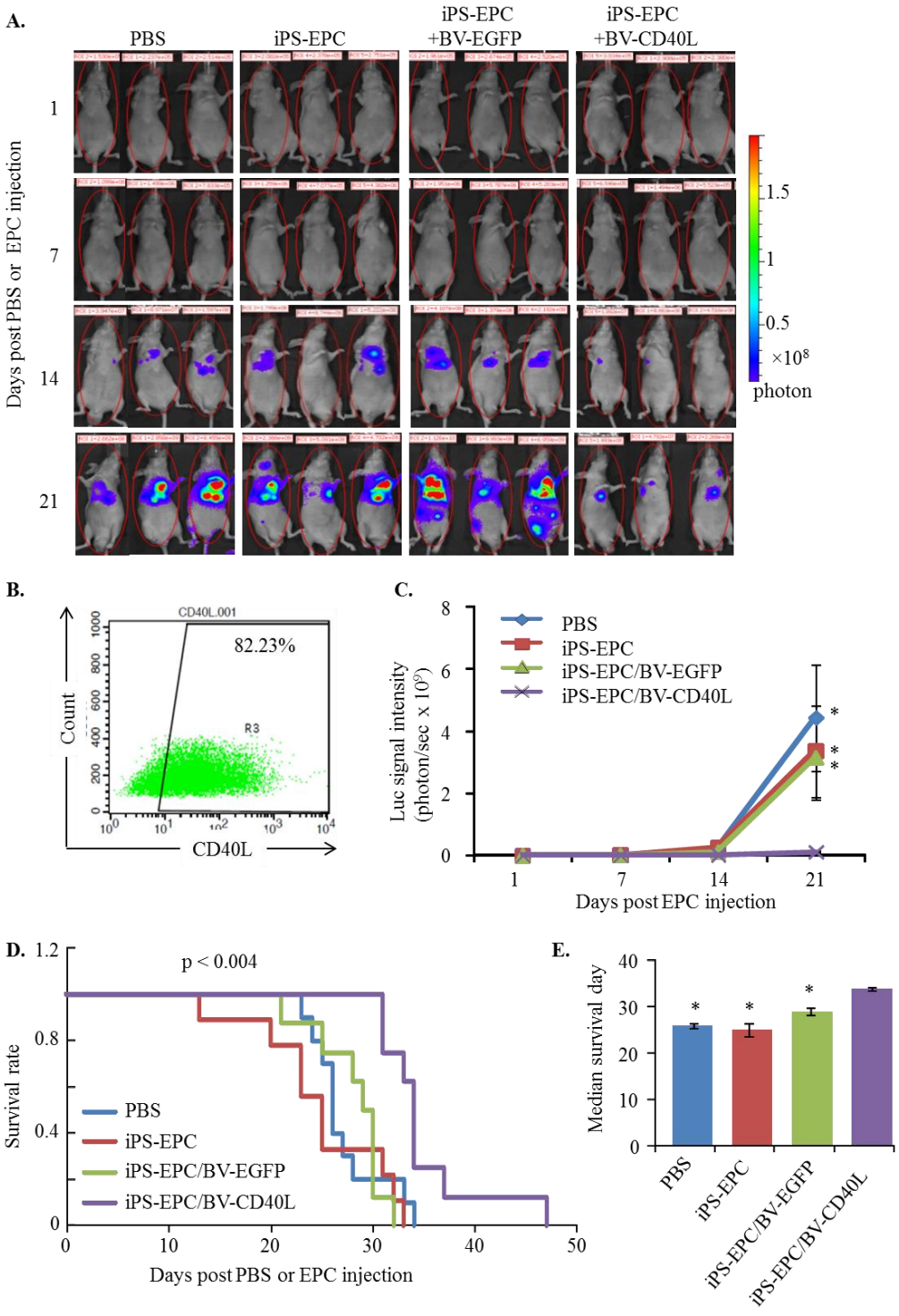
A.
PBS
iPS-EPC
iPS-EPC +BV-EGFP
iPS-EPC +BV-CD40L
Days post PBS or EPC injection
1
7
14
21
1.5
1
0.5
×10^8
photon
B.
CD40L_001
82.23%
R3
Count
CD40L
C.
PBS
iPS-EPC
iPS-EPC/BV-EGFP
iPS-EPC/BV-CD40L
Luc signal intensity (photon/sec x 10^6)
Days post EPC injection
D.
p < 0.004
Survival rate
PBS
iPS-EPC
iPS-EPC/BV-EGFP
iPS-EPC/BV-CD40L
Days post PBS or EPC injection
E.
Median survival day
PBS
iPS-EPC
iPS-EPC/BV-EGFP
iPS-EPC/BV-CD40L

Figure 2.20. Therapeutic effects of CD40L-expressing iPS-EPCs in the 4T1 breast cancer lung metastasis model. A. Bioluminescent images of tumor growth in representative animals from each group at days 1, 7, 14 and 21 after iPS-EPC injection. Tumor signal is weaker in animals belong to iPS-EPCs-CD40L. **B.** CD40L expression in iPS-EPCs after transduction with a baculoviral vector containing CD40L gene under the control of the CMV promoter. **C.** Quantitative analysis of bioluminescent signals. Up to week 2, the average tumor signal is comparable. At day 21, there is a significant difference in the tumor volume of iPS-EPCs-CD40L group against the other control groups ($P<0.001$). Bar: s.d. * $p < 0.05$ vs the group of mice injected with iPS-EPC/BV-CD40L by analysis of variance. **D.** Survival curves of 4T1 tumor-bearing mice. CD40L expression prolongs the life of 4T1 tumor-bearing mice.The Gehan-Breslow statistic for the survival curves is greater that would be expected by chance; there is a statistically significant difference between survival curves ($P = 0.004$). **E.** Graph showing the values of median survival times of animals from different groups. Statistical analysis by the log rank test reveals the significantly improved survival in the group of mice injected with iPS-EPC/BV-CD40L as compared with other groups.

2.3.5.2 iPS-EPCs expressing HSV-tk

We also tested the therapeutic effect of EPCs expressing the HSV-tk suicide gene. According to the images of the whole animal (**Fig. 2.21A**) and the average luc signal reading (**Fig. 2.21B**), the HSV-tk+GCV group has a lower tumor burden compared to the control groups (PBS, EPC alone, EPC-HSVtk without GCV) at day 14 and 21. However, when we ran the one way ANOVA tests, it was found that these differences are not statistically significant. Furthermore, the survival of the mice is only slightly prolonged and the survival curve (**Fig. 2.21C**) shows no significant differences among the groups according to the Gehan-Breslow test ($P=0.084$).

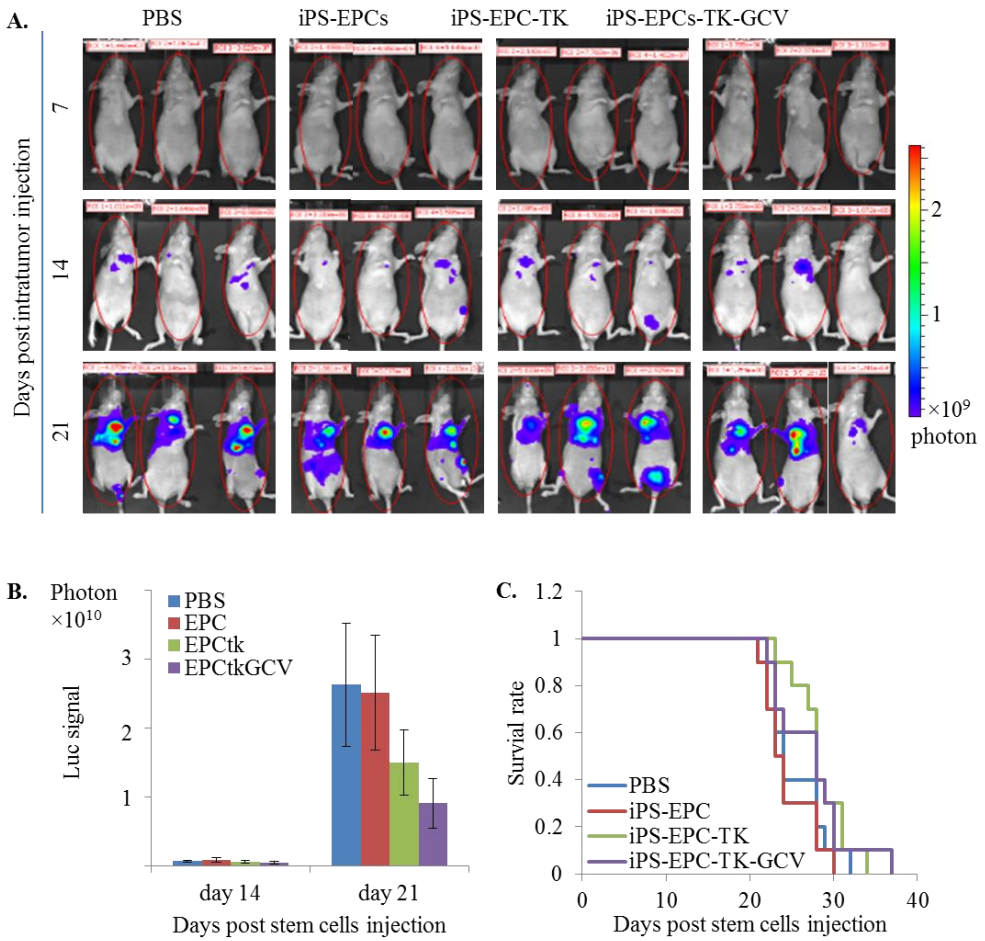

Figure 2.21. Therapeutic effect of iPS-EPCs expressing HSV-tk in 4T1luc lung metastatic Balbc/nude mice. A. Whole images of 3 representative animals from each group: PBS, iPS-EPCs, iPS-EPCs express empty baculoviral vector, and iPS-EPCs express baculoviral vector containing HSVtk gene. **B.** Tumor volume of the different groups of mice as shown by the luc signal. **C.** Survival curve of the animals. The Gehan-Breslow statistic for the survival curves is not great enough to exclude the possibility that the difference is due to random sampling variability; there is not a statistically significant difference (P = 0.084).

2.3.5.3 iPS-EPCs expressing Isthmin

Isthmin (ISM) is a 60kDa anti-angiogenesis protein that is secreted at high levels in the hindbrain-midbrain organizer in *Xenopus* embryos[126, 127]. We investigated the cancer therapeutic effect of this anti-angiogenic protein when it is expressed through EPCs. We constructed a baculoviral vector which

expresses mouse isthmin (BV-CMV-mISM-WPRE). The mouse isthmin plasmid was generously given by Prof Ge Ruowen's lab (Department of Biological Sciences, National University of Singapore).

BV-CMV-mISM-WPRE was tranduced into EPCs and its expression was confirmed through PCR (expected band size of 485 bp) (**Fig. 2.21A**). We then proceeded to test the anti-angiogenic activity of isthmin *in vitro* via matrigel tubulogenesis experiments (**Fig. 2.21B-F**). **Figure 2.21B** shows the results of matrigel tubulogenesis using EPCs which have been transduced with BV-CMV-EGFP-WPRE. We can see that the tubulogenesis was not affected, compared to the control set (**Fig. 2.21F**). Likewise, when we used the conditioned medium of EPCs transduced with EGFP, and ran the tubulogenesis experiment using freshly prepared EPCs, the tubulogenesis was not affected too (**Fig. 2.21C**). Unfortunately, when we tested the tubulogenesis of EPCs transduced with BV-CMV-mISM-WPRE (**Fig. 2.21D**) or fresh EPCs with a conditioned medium of EPCs transduced with isthmin (**Fig. 2.21E**), the tube-like formations were not affected as well.

Interestingly, when HUVEC is transduced with isthmin before matrigel tubulogenesis was performed, the same results were observed whereby the tubulogenesis was not affected. However, when the isthmin-conditioned medium was concentrated 100× and used for the matrigel tubulogenesis for fresh HUVECs, tubulogenesis failed to occur (data not shown, performed in Prof Ge Ruowen's lab, DBS, NUS). Thus, we proceeded to test whether isthmin-expressing EPCs have a therapeutic effect in 4T1-luc tumor bearing mice.

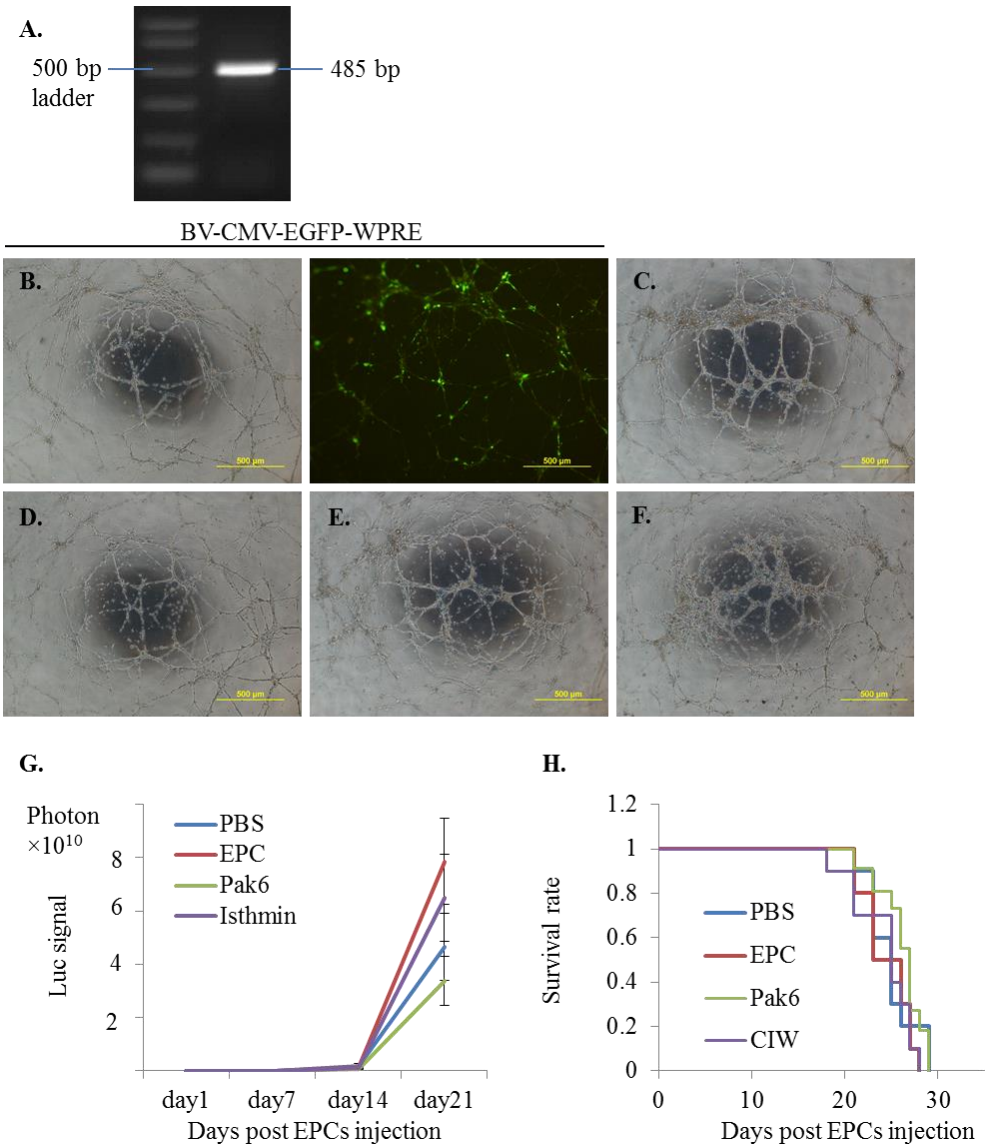

Figure 2.22. Therapeutic effects of EPCs encoding mIsthmin. A. *In vitro* expression of BV-CMV-mISM-WPRE in iPS-induced EPCs. **B.** matrigel tubulogenesis performed using EPCs transduced with BV-CMV-EGFP-WPRE in fresh EPC medium (left: phase contrast, right: EGFP expression). **C.** Negative control; Fresh EPCs in fresh EPC medium. **D.** matrigel tubulogenesis performed using EPCs transduced with BV-CMV-mISM-WPRE in fresh EPC medium. **E.** Matrigel tubulogenesis performed using fresh EPCs in BV-CMV-EGFP-WPRE transduced EPCs conditioned medium. **F.** Matrigel tubulogenesis performed using fresh EPCs in BV-CMV-mISM-WPRE transduced EPCs conditioned medium. **G.** Tumor volume of the different groups of mice as shown by the luc signal. One way ANOVA tests showed no significant difference among the groups. **H.** Survival curve of the animals. The Gehan-Breslow statistic for the survival curves is not great enough to exclude the possibility that the difference is due to random sampling variability; there is not a statistically significant difference P=0.401.

The 4T1-luc cells were injected intravenously to create lung metastatic model mice. Three days later, 5×10^5 iPS-EPCs transduced with BV-CMV-Isthmin-WPRE were injected intravenously into the tumor bearing mice. As controls, PBS, iPS-EPCs, and iPS-EPCs transduced with empty baculoviral vectors were injected into the mice. From both the average luc signal reading (**Fig. 2.21G**) and the survival rate of the animals (**Fig. 2.21H**), we were not able to observe any obvious therapeutic effect in the tumor-bearing mice.

2.4 Discussion

2.4.1 Derivation of EPCs

The hPSCs provide an unlimited source of cells for cell therapy. Moreover, hPSCs provide a method of studying basic human developmental biology without trespassing on ethical boundaries. During embryogenesis, the developmental progression of hematopoietic and endothelial lineages is closely associated. Thus, endothelial and hematopoietic progenitors share common markers such as CD34, CD31 and Flk1[79]. Hematopoietic cells were then distinguished from its endothelial counterpart by the expression of CD45, a common leukocyte antigen which is not expressed in endothelial cells[80, 130]. Our EPCs expressed CD34, CD31 and Flk1 but not the CD45 hematopoietic marker. After further culture in an EGM2 endothelial cell medium, these cells were positive for other characteristics associated with EC lineage markers such as VE-cadherin, von Willebrand Factor, uptake of Ac-LDL. In addition to this, the cells could form tubular structures when seeded onto matrigel[79, 83].

In our study, we initially utilized the mouse stromal cells, OP9 and M2-10B4, to produce EPCs from hESC and iPS cells. These cells have been

shown to support hematoendothelial differentiation of hESCs due to soluble/secreted factors that are important for hematoendothelial development[140]. Our generated EPCs via these co-culture methods were comparable to previous reports [141, 142]. However, the M2-10B4 co-culture process took a longer time to generate EPCs (13 days instead of 8 days for OP9 co-culture). Moreover, although Tian et al. showed that $CD45^+$ cells started to appear only in approximately 17-21 days of culture, we noticed that our produced EPCs expressed the CD45 marker earlier (we harvested at day 13-14). This CD45 expression is higher as compared to that of the OP9 co-culture derived EPCs. Furthermore, by observing the matrigel tubulogenesis results qualitatively, we noticed that tubulogenesis was more efficient for the cells that were produced via OP9 co-culture as compared to the M2-10B4 co-culture. Thus, we conclude from our studies that OP9 co-culture is more robust in producing EPCs than M2-10B4 co-culture.

The co-culture methods can recreate native stem cell niches, thus providing an inductive environment for the differentiation of hESCs. The ability to modify stromal cells to express various components that may promote or inhibit lineage-specific differentiation also provides a useful means to define specific niche factors that regulate human hematopoiesis[137, 140]. For example, M2-10B4 stromal cells expressing Wnt1 or Wnt could enhance EPC differentiation from hESCs[137]. However, avoidance of xenogeneic tissue, such as murine cells that are used for the maintenance of undifferentiated hPSCs or stromal cell lines that are commonly utilized to induce differentiation, is preferred in clinical settings[140].

Interestingly, in all the differentiation methods, we observed similar morphological changes during the differentiation process. The initial button-like structure of H1 or iPS grew into root-like structure be it in the stromal co-culture or stromal-independent culture. Previously, our lab has investigated the localization of $CD34^+$ cells in OP9 co-culture via live $CD34^+$ cell immunostaining of differentiated hESC colonies. We found that the main population of $CD34^+$ cells is located in the root-like structures that penetrate the OP9 portion of the co-culture. Thus, since we also observed similar structures in the other methods, we speculate further that these structures might mimic the hematopoietic niche in the bone marrow. However, further studies need to be done to prove this.

Our produced EPCs both from iPS cells and hESCs express markers in similar manners. However, in the 2-D differentiation method, we noted some differences in between the hESC and iPS cell-derived EPCs in terms of the purity of $CD34^+$ cells after sorting and the co-expressions of the EPCs markers. Such differences have also been reported previously[143, 144]. White and colleagues previously have shown that there are differences in the gene expression between ECs derived from hESC and iPS cells, notably genes related cell cycle and adhesion [92]. However, despite the gene expression heterogeneity, they concluded that ECs derived from both pluripotent cell types behave very similarly [92].

The yield and purity of EPCs derived using EB method was superior compared to the other methods. The differentiation medium was supplemented with BMP4, Activin A, bFGF, VEGF cytokines and TGF-β inhibitor

(SB431542). BMP4 has been shown to promote mesodermal lineage differentiation from hPSCs [88, 143]. Addition of VEGF and bFGF has been shown to enhance the expression of CD34 during the hematoendothelial differentiation [143]. Studies have shown that TGFβ pathway is important for hematopoietic development and that TGFβ inhibition maintains the proliferation and identity of endothelial cells *in vitro* [132, 140].

CD133 (AC133, prominin-1) is a transmembrane domain cell surface glycoprotein which serves as a marker of asymmetric division, lineage plasticity, tumor cell dormancy and inherent embryonic gene expression [80, 145]. CD133 have been repeatedly used as a marker for early endothelial lineage cells [81, 82, 146]. EB derived EPCs expressed CD133 stem cell marker indicating that they are still in early phase of endothelial differentiation. Moreover, these iPS cell-derived cells are positive for the above-mentioned endothelial progenitor markers and display other characteristics associated with EPCs, including VE-cadherin, von Willebrand Factor, uptake of AcLDL and formation of tubule structure upon seeding onto matrigel [79, 83].

In our study, the produced EPCs could maintain the markers and properties only for up to 5 passages. However, the self-renewing hPSCs possess unlimited proliferation capacity, thus can be used as a reliable source to generate vast amounts of human EPCs for cell therapeutics purpose. The use of human iPS cells especially garners attention since it can avoid the ethical concerns regarding its derivation, in contrast to the hESC counterpart.

iPS cells are a unique type of biological material that can be used to generate either autologous or allogeneic cells. If cells to be used are the

differentiated progeny of iPS cells reprogrammed from the patient's own cells, these cells are viewed as "autologous" cells. The likelihood of immune rejection towards them after transplantation will be significantly reduced. In the case that a human iPS bank consisting of various human leukocyte antigen (HLA) types is established, iPS cells selected from the cell bank can be used as an alternative to generate semi-allogeneic differentiated cells that share some of the HLA alleles with recipients. The third method of using iPS cells is to generate differentiated allogeneic cells suitable for applications that do not require the long-term survival of transplanted cells, such as when using stem cells as cellular vehicles for targeted cancer therapy. While long-term immunosuppressive treatment is required for many regenerative medicine applications of allogeneic stem/progenitor cells, it will not be necessary when iPS cell-derived cells are used as exogenous cellular vehicles for cancer treatment, since the application does not really require stem cell engraftment.

Using allogeneic cells derived from iPS cells as cellular vehicles for cancer therapy can be justified for several reasons. Firstly, it is possible to use genetic engineering to introduce a therapeutic gene into iPS cells, in order to generate a master cell line for cell therapeutic production. Secondly, the allogeneic cell approach allows large-scale mass production of cell therapeutics, a prerequisite for widespread application of cell therapy suitable for repeated patient treatments. Large-scale mass production will also increase cost-effectiveness by reducing labor costs and simplifying the logistics of cell culture operations. In addition, it becomes possible to prepare cryopreserved derived cells as commercial products in ready-to-go format. Thirdly, the allogeneic cell approach allows standardized manufacture, which should be

helpful in eliminating variability in the quality of cellular products, thus facilitating reliable comparative analysis of clinical outcomes.

Despite the advantages of iPS cells, more extensive studies need to be done to prove that the differentiated cells from iPS cells and hESCs are interchangeable. One concern about using iPS cells to derive downstream cells is the maintenance of genetic and epigenetic states of the iPS cells such as the methylation pattern. It has been shown that the reprogrammed stem cells carry an epigenetic memory of the original tissues which lingered even after the iPS cells had been differentiated into new tissues[147]. In addition to this, another important concern regarding the use of hPSCs derived cells is the ability of hPSCs to develop teratomas. This safety concern applies to iPSCs too, as they can also form teratomas[140].

2.4.2 Tumor tropism of iPS-EPCs

Our biodistribution experiments have clearly demonstrated the tumor tropism of the generated iPS-EPCs. However, our study also showed that majority of intravenously injected iPS-EPCs were trapped in the lungs in the orthotopic breast cancer model, possibly due to the narrow diameters of lung capillaries. After initial pulmonary trapping, many intravenously injected cells tended to be re-distributed from the lungs to the liver and spleen. Comparable results were shown by Wei et al., in which tail vein injections of mouse embryonic EPCs into C3H mice resulted in the injected cells being predominantly sequestered in the lung and spleen[85]. Our previous biodistribution studies using human neural stem cells (NSCs) also showed a similar cell distribution pattern[128]. This distribution pattern is useful for eliminating metastatic cancer

cells in the lungs, liver and spleen and has provided a rationale for us to test the therapeutic effects of intravenously injected iPS-EPCs in the breast cancer lung metastasis model in the current study. This cell distribution pattern, however, also emphasizes the importance of minimizing off-target transgene expression if the cell delivery aims to treat primary breast cancer.

In the invasive 2M1 glioma model, we showed that EPCs can be incorporated into the 2M1 tumor blood vessels. These results corroborate the study by Moore et al. which demonstrated systemically transplanted cord blood-derived EPCs *in vivo* tropism for intracranial gliomas[148]. Furthermore, EPCs were also found in tumor satellites away from the primary tumor site, suggesting that there is potential for cell delivery of gene therapy to metastatic sites.

2.4.3 Effect of iPS-EPCs in cancer growth and metastasis

Circulating bone-marrow-derived EPCs might follow the gradients of growth factors and cytokines that are released into circulation by tumors and contribute to tumor neovascularization, tumor growth, and metastasis[149]. However, this contribution remains controversial, since the existence of these EPCs during tumor progression vascularization has been established in certain models and disproved in others, depending on the tested tumor models and methodologies[150]. NSCs have also been exploited as cellular vehicles in many preclinical and clinical studies for targeted delivery of therapeutic genes for cancer therapies[39, 128, 151]. However, our group has demonstrated that hESC-derived NSCs suppress the maturation of DCs and impair the functional capacity of DCs to stimulate alloreactive T cells[152]. These immunosuppressive

effects exerted by stem cells will have a negative impact on cancer treatments when they are used as cellular gene therapy delivery vehicles. Thus, in this study, we also included iPS-NSCs alongside our iPS-EPCs to study the differences between different cellular vehicles.

We did not observe any obvious contributions of iPS-EPCs and iPS-NSCs to breast cancer growth and metastasis in both the primary and metastatic tumor models. Interestingly, in the lung metastatic cancer model, injection of fibroblasts alone resulted in an increased tumor volume at day 21, although there was no significant difference in animal survival by the end of the experiment. Carcinoma-associated fibroblasts (CAFs), the activated fibroblasts, are the primary type of host cells in tumor microenvironment. The origin of CAFs is not conclusively established and remains controversial[153]. Whether the systemically injected fibroblasts tested in the current study were recruited by the tumor and activated *in situ* to become CAFs is worth pursuing in future research.

2.4.4 Immunotherapy of EPCs using CD40L

To employ iPS-EPCs as donor cells to deliver the CD40L gene or other therapeutic genes for cancer therapy, it is essential that these cells can be genetically modified in a safe and effective way to carry therapeutic payloads of interest over the period of time crucial to the therapy. In the current study, we demonstrated for the first time that baculoviral vectors can be used for genetic modification of human EPCs to provide a window of transgene expression suitable for cancer therapy. Large cloning capacity, ease of virus production and low cytotoxicity to transduced cells are the obvious advantages

associated with the emergence of baculoviral vectors in the gene delivery field. Insect baculovirus also bypasses the risk of virus replication and potential viral infection in host cells, risks borne by conventionally-used animal viruses such as adenovirus, retrovirus and adeno-associated virus. The pre-existing host immune response against adenoviral vectors, a type of vectors commonly used for transient transgene expression, is another concern that restricts the use of these vectors[154, 155]. Unlike adenovirus, baculovirus is not targeted by pre-existing immunity in humans[156].

CD40L was used as a model therapeutic agent to test iPS-EPC-mediated gene delivery. CD40L, also called CD154, is a 33-kDa type II membrane protein belonging to the TNF gene family and is mainly expressed on activated $CD4^+$ T cells. It interacts with CD40 expressed on a wide range of antigen-presenting cells (APCs) including dendritic cells, macrophages, and B lymphocytes, as well as non-immune cells such as epithelial cells, endothelial cells and malignant cells[105]. CD40L-CD40 interaction induces activation in APCs in association with T cell receptor stimulation by MHC molecules on the APCs, ensuring the generation of antigen-specific cytotoxic T lymphocytes (CTLs). Increased antigen presentation by APCs can lead to increased cytokine production, expression of other co-stimulatory molecules, and induction of cytotoxicity. CD40L can also exert antitumor effects by inducing tumor cell apoptosis via autocrine/paracrine induction of death ligands such as TNFa, FasL, and TRAIL[105]. Local CD40L gene delivery to directly transduce tumor cells can mediate multiple antitumor effects, including the induction of T-cell responses, upregulation of TH1 cytokines and induction of apoptosis, which effectively inhibit tumor growth[108, 119, 157].

Our results showed that CD40L delivered by systemically injected iPS-EPCs could reduce the tumor burden and eventually prolong the survival of tumor-bearing animals. To test human EPCs, immunocompromised Balb/c nude mice were used to produce tumor models in the current study. This strain of mice lacks T cells, but still acquires B cells and innate immune cells such as NK cells and complement immune system. Thus, the upregulation of TH1 cytokines and the induction of apoptosis, but not induction of T-cell responses, might play more important roles in the observed antitumor action. Our approach is different from the strategy of direct transduction of tumor cells with the CD40L gene, as it uses baculoviral CD40L transduction of iPS-EPCs and the tumor tropism property of the cells to activate a local CD40L-CD40 interaction in tumors. This is most likely achieved through a bystander mechanism of intercellular transfer of the CD40L protein from donor iPS-EPCs to tumor cells. It has been established that CD40L protein transfer to tumor cells occurs in transduced fibroblasts, epithelial cells and bone marrow stromal cells[158].

We also studied the therapeutic effect of EPCs expressing HSV-tk using the same settings. However, we found that the effect is less pronounced compared to EPCs that express CD40L as the therapeutic gene. This may be due to the multiple antitumor mechanisms that CD40L has. Besides, homed EPCs might trigger tumor growth until the suicide gene system is activated as the suicide gene needs time to kill using the bystander effect. Furthermore, the suicide gene vehicle has an inherent disadvantage in that it destroys itself, limiting the amount of time it has in which to work[99]. Due to these reasons, it

is possible that the therapeutic effects exerted by HSVtk cannot overcome the fast growing tumor mass and metastasis.

We also investigated the therapeutic effect of a novel angiogenic inhibitor, Isthmin (ISM). This 60kD protein, which was first identified in the *Xenopus* brain, has been shown to inhibit endothelial cell (EC) capillary network formation on Matrigel and induce EC apoptosis[126, 127]. Although it has been shown that overexpression of ISM in mouse B16 melanoma resulted in inhibition of the tumor growth upon subcutaneous injection into the mice[126], our results showed that ISM could not inhibit the growth of pre-established tumour in mice when delivered systematically. One plausible reason is that a high concentration of ISM may be needed to exert the antiangiogenic effect. When overexpressed in the tumor, the tumor angiogenesis is inhibited from the start, thus making a more distinct impact on tumor growth. In a pre-established tumor, a higher concentration and more prolonged exposure of ISM may be required to exert the same effect. Moreover, studies have shown that only soluble ISM has antiangiogenic effects, whereas immobilized ISM loses its antiangiogenic function and instead promotes EC adhesion, survival and migration through avb5 integrin[127]. Further studies are needed to investigate whether the isthmin delivered by the EPCs are immobilized in the ECM of a tissue or soluble in circulation.

2.4.5 Challenges and future direction

In this study, while the term "iPS-EPC" was used for these iPS cell-derived cells, we do realize that the population could contain cells at different levels of differentiation along the endothelial lineage. A further purification step, e.g.

isolation of $CD133^+$ cells, can be added to remove relatively matured cells. For clinical applications, more robust and cost-effective cell expansion technologies will be required. In this aspect, expansion methods such as automated bioreactors and rotary culture machines hold promise for generating iPS cell derivatives in bulk[159].

An important concern regarding the use of therapeutic cells derived from iPS cells is the potential of the latter to form teratoma. Incomplete differentiation could bear a risk of teratoma development in mice or patients. Thus, an experiment to test teratoma formation in animal models after injection of iPS-EPCs can be performed to ensure the safety of this therapeutic mode.

One issue that needs to be resolved is the degree of the EPCs tumor tissue selectivity, to reduce potential toxicity due to off-target organ failures. Several strategies can be used to enhance the tumor tissue-specific transgene expression for cancer gene therapy. A popular method is the use of tumor environment-specific promoters including hypoxia response elements, a proendothelin-1 promoter, or a survivin promoter[93, 160-162]. Given that the vesicular stomatitis virus glycoprotein (VSV-G) can promote the formation of multinucleated syncytia to kill cells in a pH-dependent manner, we have generated a VSV-G mutant that efficiently promotes syncytium formation at the tumor extracellular pH but not at pH 7.4[163]. Using transduced NSCs derived from iPS cells to deliver the VSV-G mutant into mice with metastatic breast cancers in the lung through tail vein injections, we observed tumor-selective killing without obvious toxicity to normal non-targeted organs. We are also working

on the development of regulatory systems that regulate the transgene expression in the cellular vehicle in an inducible manner in response to tumor hypoxia.

The transient gene expression mediated by baculovirus of non-integrating nature has been noted to have limits to its efficacy in studies that require long-term transgene expression. One way to improve the survival rate of the animals is through multiple rounds of iPS-EPCs-CD40L injections. This way, the CD40L expression in the animal can be periodically boosted, which in turn will enhance the immune reaction against the tumor in the animals. Another way to overcome the limitation is by ensuring longer expression of the transgene in the iPS-EPCs. Our lab has developed several baculoviral transduction-based approaches using either recombinase-mediated cassette exchange (RMCE), zinc finger nuclease (ZFN) technology or transcription activator-like effector nuclease (TALEN) technology for site-specific integration, without random integration, of a transgene in human pluripotent cells [98, 139, 164, 165]. We are in the midst of establishing iPS cell lines to achieve stable expression of transgenes in the differentiated progeny of the iPS cells, including EPCs.

In conclusion, we have demonstrated the feasibility of generating EPCs from early-passage human iPS cells. We further showed the tumor tropism of the generated EPCs and the effectiveness of using intravenously injected EPCs to deliver CD40L to inhibit metastatic breast cancer growth in the lung, possibly through an intercellular transfer mechanism. The potential of this approach is not limited to metastatic breast cancer therapy but can likely be extended to

treat primary lung cancer and many other types of pulmonary metastases. In this chapter we demonstrated that an immune-modulatory gene, CD40L, could result in cancer therapeutic effects after being delivered via EPCs. In the next chapter, we explored another targeted approach in immunotherapy.

CHAPTER III: TARGETED CANCER THERAPY USING CYTOTOXIC T LYMPHOCYTES ACTIVATED BY DENDRITIC CELLS PULSED WITH CANCER STEM CELL-LIKE CELLS

3.1 Introduction

3.1.1 Cancer stem cells

Cancer stem cells (CSCs) are a small population of cells in the tumor that possesses the ability to self-renew and drive the tumorigenesis[166, 167]. Studies have shown that CSCs express similar gene expression as normal embryonic stem cells, including STAT3, Oct3/4 and nanog, which explains their similar properties in self-renewal and differentiation properties[166, 168]. However, isolation and further observations have been hampered by the small number of cells since CSCs are a minority population just like normal stem cells. Efficient methods to enrich this cell population would alleviate this problem significantly. The non-adherent, 3-D tumor spheres culture method and reprogramming approach have been shown to enrich CSCs *in vitro*[169, 170].

Taking advantage of sphere culture, surface markers analyses, functional studies *in vitro* (spheres formation and *in vitro* differentiation assays) and *in vivo* tumor initiation models, the existence of CSCs has been demonstrated in several cancers including breast, ovarian and prostate cancers, melanomas, gliomas, head and neck squamous carcinoma and many more[166, 167, 171]. The tumor-initiating cells were first isolated from a breast cancer by Al-Hajj et al. and identified as $CD44^{+}$/CD24-/low population[167, 172]. Other well-studied cell surface markers for CSCs include CD133, epithelial cell adhesion molecule (epCAM), THY1, and ATP-binding cassette B5 (ABCB5)[166].

The four factors (Oct4, Sox2, Klf4 and Nanog) in Takahashi/Yamanaka reprogramming iPS cocktails are oncogenes by

definition, and their over-expression has been associated with cancers[173-175]. Thus, many researchers have turned their focus to the use of reprogramming approach to enrich CSCs by introducing at least one of these factors[170, 175]. Hypoxic conditions have also been utilized to reprogram glioblastoma cells into CSC-like cells[176]. The acquired stem cell phenotypes have been shown to be more tumorigenic and resistant to chemotherapeutic drugs[170, 176]. Thus, these cells are very promising novel targets for tumor therapy.

3.1.2 Objective

DC-based vaccines have been perceived as a powerful immunotherapy approach against cancer. This is because DCs hold a very important place in the stimulation of immune responses, especially CTLs, powerful immune killer cells to eradicate cancer cells. Depending on the antigens loaded onto and presented by the DCs, T cells will target populations of cells that express them. Thus, the choice of target antigen is crucial. Conventional chemotherapy and radiation therapy, which target rapidly growing tumor cells, are incapable of destroying the CSCs[166, 167, 170]. The quiescent state of CSCs, efficient mechanisms of DNA repair, intrinsic expression of anti-apoptotic mechanisms and expression of efflux transporters are some strategies to build this resistance[166, 167]. The survival of CSCs explains the tumor recurrence in patients. Therefore, CSCs emerge as a promising therapeutic target for anticancer therapies.

Our lab has successfully developed several baculoviral transduction-based approaches using zinc finger nuclease (ZFN) technology for site-specific integration, without random integration, of reprogramming factor

genes to facilitate the generation of human pluripotent cells[177]. Zinc Finger Nucleases (ZFNs) technology facilitates site-specific integration of the transgene encoding the four reprogramming factors at adeno-associated virus type 2 target region (AAVS1 locus) on chromosome 19. This site is known as a 'safe-harbor' human genomic site for exogenous DNA insertion[98, 139]. Using the same method, we have also successfully reprogrammed various cancer cell lines such as glioma and colorectal cancer (CRC) into CSC-like cell states. Our lab showed that CRC-CSC-like possess higher propensities to form tumorspheres in vitro as compared to wild-type CRC. Moreover they express significantly higher CSC markers such as CD133 and CD24 (data not shown, performed by lab members).

The conceptual flow of the project can be seen in **Figure 3.1**. Whole tumor lysates were produced from the CRC and glioma CSC-like cells. We then used these whole lysate antigens to pulse PBMC-derived DCs. We believed that the four reprogramming factors are also included in the lysate and we hypothesized that these antigens can be presented by DCs to the T cells and subsequently results in the activation of CTL which can target the CSCs population.

The key factors in this project were the viability of the DCs used and the proper assessment of the T cells activation. In the first part of our study, we focused on producing a sufficient quantity of highly functional DCs from PBMCs. We relied on flow cytometry which has been widely used to characterize the PBMC-derived DCs.

In the second part, T naïve cells isolation and characterization were carried out. In this project, naïve T cells were isolated and memory T cells were depleted. This is because memory T cells have been shown to have lower activation threshold, thus can result in non-specific expansion[178]. Flow cytometry to characterize the co-stimulatory as well as inhibitory markers of T cells will be tested.

In the last section, the level of CTL activity in terms of functionality and specificity will be examined. A functional assessment of T cells in terms of the production of cytokines such as IFNγ will be performed. The ELISPOT assay is a highly sensitive antibody-capture-based method for enumerating specific T cells that can secrete cytokines. Thus, this technique will be adopted in this project. We aimed to test whether IFNγ production by the T cells was specific to the target cells that expressed the CSC-like antigens. Ultimately, we postulated that a CSC-specific T cell response from DC vaccination using CSC-like antigens can be generated.

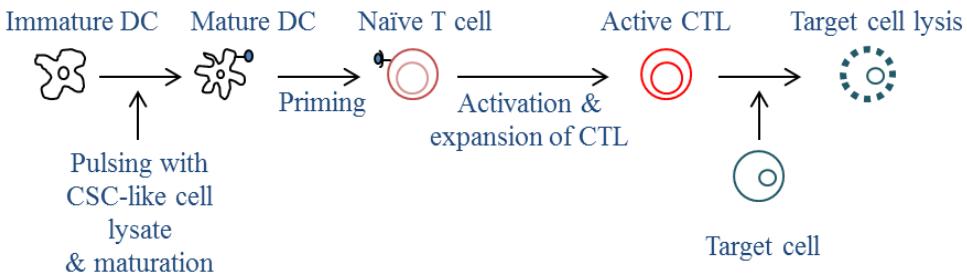

Figure 3.1. Antigen presentation and CTL activation. CSC-like antigens presentation by the DCs leads to CTL activation and eventually targeting of cells expressing the antigens.

3.2 Material and methods

3.2.1 DCs and naïve T cells derivation from PBMC

DCs and naïve T cells were derived from human peripheral blood mononuclear cells (PBMCs), both HLA-A2 positive and negative (AllCells, Stemcell Technologies Inc) based on previous studies [178]. To generate DCs, 1×10^8 human PBMCs were seeded onto a T-175 cm^2 flask and incubated for 3 h at 37°C in Cellgro® DC medium (CellGenix, GmbH, Freiburg, Germany) supplemented with 5% human AB serum and 1×P/S. After 3 h, 20 ml of DC differentiation medium (Cellgro DC medium + 5% human serum + 1×P/S + 50 ng/ml GM-CSF + 100 ng/ml IL4) was added to the attached cells. Half of the medium was changed 2 days later. As most of the cells have detached at this point, the medium change was performed as follows: take out 10 ml medium, spin down 300 g for 5 min, re-suspend with 10 ml fresh medium and put the re-suspended cells back to the flask. On day 4, the immature DCs were collected for DC pulsing and maturation or for DC characterization by flow cytometry. Meanwhile, the non-attached cells were collected and cultured separately in Cellgro medium as above with additional supplementation of IL7 (5 ng/ml). Prior to T cell priming, selection of $CD8^+CD45RO^-CD57^-$ naïve T cell population from the PBMC was carried out via MACS using CD8, CD45RO and CD57 microbead kit (Miltenyi Biotec). All the cytokines were purchased from Peprotech or Miltenyi Biotec.

3.2.2 Tumor lysate preparation

To prepare for the tumor lysate, wild type and 4F-BV-ZFN reprogrammed glioma and colorectal cancer cells were used. Tumor cells were harvested and

re-suspended at 1×10^6 cells/ml in PBS. The cells were then subjected to six cycles of freeze-thaw treatment (freezing with liquid nitrogen for 20 min and thawing 5 min at 37^{o}C water bath) to produce the whole tumor lysate.

3.2.3 DCs pulsing with tumor lysate and maturation

The dendritic cells were harvested and separated into different groups: DC pulsed with 4F-BV-ZFN-tumor, DCs pulsed with WT tumor and unpulsed DCs. The DCs were then mixed with the whole tumor lysates with a cell ratio of 1:1 according to the groupings. After a 16 h incubation, 60 EU/ml of LPS (*Escherichia coli*; Sigma) and 2000 IU/ml of IFNγ were added into the culture to stimulate DC maturation for a further 16 h at 37°C, 5% CO2.

3.2.4 CTL stimulation and expansion

The naïve T cells were then primed with the pulsed and matured DCs at 1:4 DC: T cell ratio. Prior to the priming, the DCs were subjected to mitomycin C treatment in order to inhibit cell proliferation including the contaminants NK cells and monocytes. The cell mixtures were cultured and expanded in a Cellgro medium supplemented with 5% human serum, 1×P/S, IL21 (30 ng/ml), IL7 (5 ng/ml) and IL15 (5 ng/ml) for 10 – 11 days.

3.2.5 Flow cytometry

For DCs characterization, flow cytometric analyses were performed using the antibodies: CD11c, CD86, DC-SIGN, CD80, CD40, CD83 and HLA-DR (BD Biosciences). For T cell characterization flow cytometric analyses were performed using these antibodies: CD8, CD4, CD62L, CCR7, CD27, CD28,

CD45RO, CD45RA, CD57, CD25, CD127, HLA-ABC and HLA-A2 (BD Biosciences).

3.2.6 ELISPOT

To detect the cytokine (IFNγ) production by the stimulated CTL, we performed ELISPOT assay (MabTech AB, Sweden). As target cells, T2 cells or 0.05% glutaraldehyde-fixed DCs were used when the PBMCs were HLA-A2 positive or HLA-A2 negative respectively. The pulsed or unpulsed DCs were fixed with 0.05% glutaraldehyde for 30 seconds. The T2 cells were incubated with 3 µg/ml Oct4 or EGFP peptide at room temperature for 3 h.

The T responder cells were then co-cultured with fixed DCs or T2 target cells at responder: target = 10: 1 in Cellgro medium using 96-well U-bottom plates. After 24 h of incubation, the cells were then transferred to the antibody-coated microtiter plates. The antigen-specific T cells were detected by the sequential addition of biotinylated mouse anti-human IFNγ (2 h at room temperature), five washes with DPBS, alkaline phosphatase-conjugated streptavidin (1 h at room temperature), five further washes with DPBS, and substrates for streptavidin. Spots were then developed and stopped after 10 min by washing vigorously with tap water. The spots corresponding to the IFNγ producing cells were then scanned and analyzed using an automatic plate reader CTL – Biospot® S6 UV analyzer (Cellular Technology Limited, Ohio, USA).

3.2.7 Statistical analyses

All data are represented as mean ±SD. The statistical significance of differences was determined by one-way ANOVA followed by the Holm-Sidak method for pairwise multiple comparison tests. A p value of <0.05 was considered to be statistically significant.

3.3 Results

3.3.1 DCs derivation and characterization

The production of sufficient and functional DCs is crucial in DC-based cancer immunotherapy. In this study, DCs were derived from PBMCs, with **Figure 3.2A** showing the schematic diagram of the protocol. The PBMCs were seeded and incubated for 3 h. The attached cells were the monocytes which will be differentiated to DCs whereas the floating cells were collected for T naïve cell sorting. To differentiate DCs from PBMCs, IL4 and GM-CSF were added to the differentiation medium. Thereafter, the attached monocyte-DCs become floating or loosely attached DCs (**Fig. 3.2B, C**). Furthermore, we observed morphological changes in the cells over time. In the beginning, most of the cells are spherical. However, at day 4, most of the cells are irregular-shaped with dendritic arms starting to develop (**Fig. 3.2C**). We can produce up to 8×10^6 DCs from 1×10^8 PBMCs.

Our lab has established the CSC-like cells by reprogramming cancer cells such as colorectal cancer (CRC) and U87 glioma cells by using the baculoviral vector expressing four reprogramming factors (Oct4, Sox2, Klf4 and C-Myc), zinc finger and EGFP (4F-ZF-EGFP). The increased expression of the four factors has been analysed using RT-PCR, real time PCR and

western blot (data not shown). These reprogrammed cancer cells were used to make the cell lysates. CRC and U87 wild type cells were used as controls, as well as PBS as unpulsed control. After pulsing with the lysates, the cells were subjected to IFNγ and LPS in order to induce the DC maturation. Interestingly, after pulsing followed by maturation, most of the DCs became tightly attached cells (**Fig. 3.2D**).

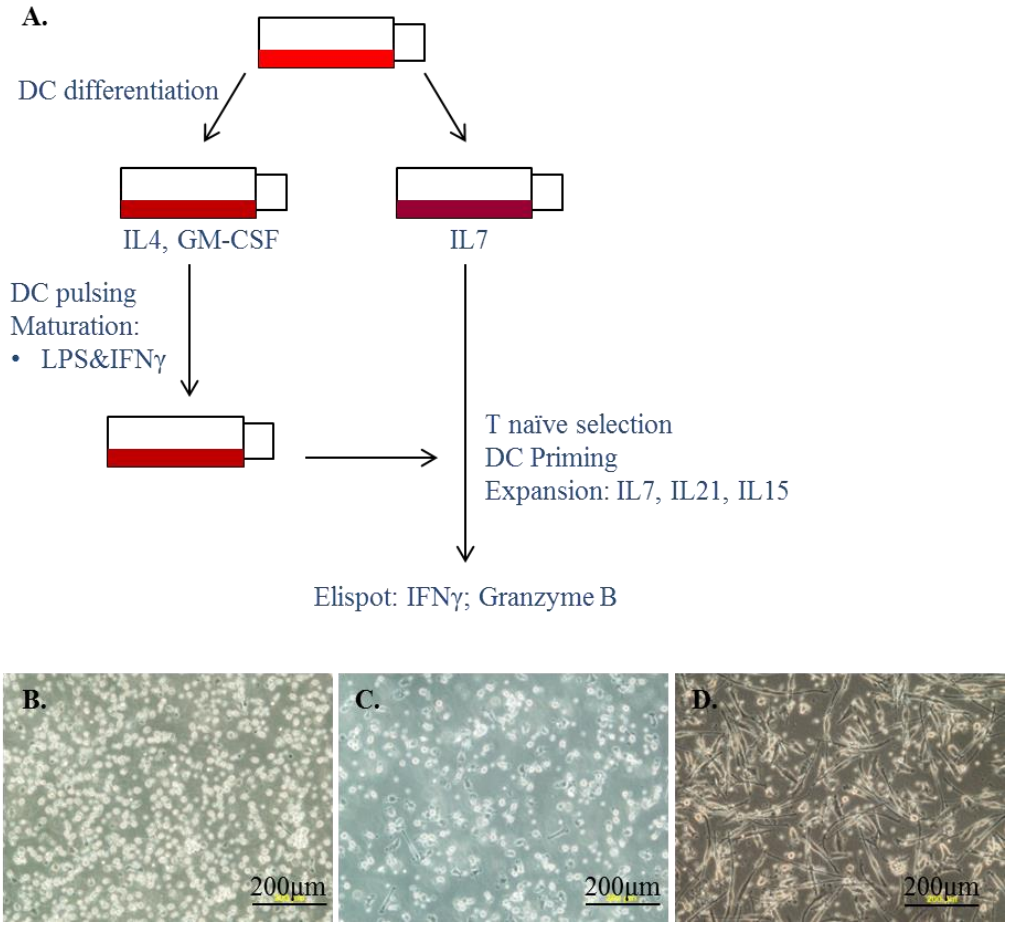

Figure 3.2. Dendritic Cells and T cells derivation from PBMC. A. DCs differentiation and naïve T cells selection from human PBMC. **B.** Differentiated DCs at day 1. **C.** DC differentiation at day 4. **D.** DC after pulsing and maturation.

Evaluation of immunological surface markers is a common yet important method to evaluate the identity and functionality of the DCs. At first, we performed flow cytometry of the whole population of PBMCs to examine the profile of the cells available (**Fig. 3.3**). We could see that all the cells were positive for CD45 marker which is the leukocyte common antigen (99.95%). High expressions of lymphocytes markers were found. The cells were positive for cytotoxic and helper T cells markers, CD8 (34.98%) and CD4 (50.35%) respectively. They were also positive for other lymphocytes markers CD3 (80.31%) and CD7 (73.24%). HSC marker CD34 was negative (0.2%) but 75.34% of the cells were positive for CD31 marker. Furthermore, a small but distinct population of the PBMC expressed NK cell markers: CD16 (4.52%), CD94 (3.02%) and CD56 (0.67%).

We then evaluated the expression of DC markers in the immature and mature DCs (**Fig. 3.4**). The immature DCs were positive for DC markers such as CD11c, CD86 and DC-SIGN with expression of more than 90%. However, the expression of CD40 was dimmed (48.97%) and no expression of CD83 was detected (0.96%). Upon maturation, the expression of CD83 and CD40 increased considerably, from 0.96% to 98.76% and from 48.97% to 99.30% respectively. Furthermore, the expressions of the other DC markers were maintained at high levels. In addition to this, the DCs were positive for MHC I and II (HLA-ABC & HLA-DR), with the percentage expression of 99.93% and 98.12% respectively.

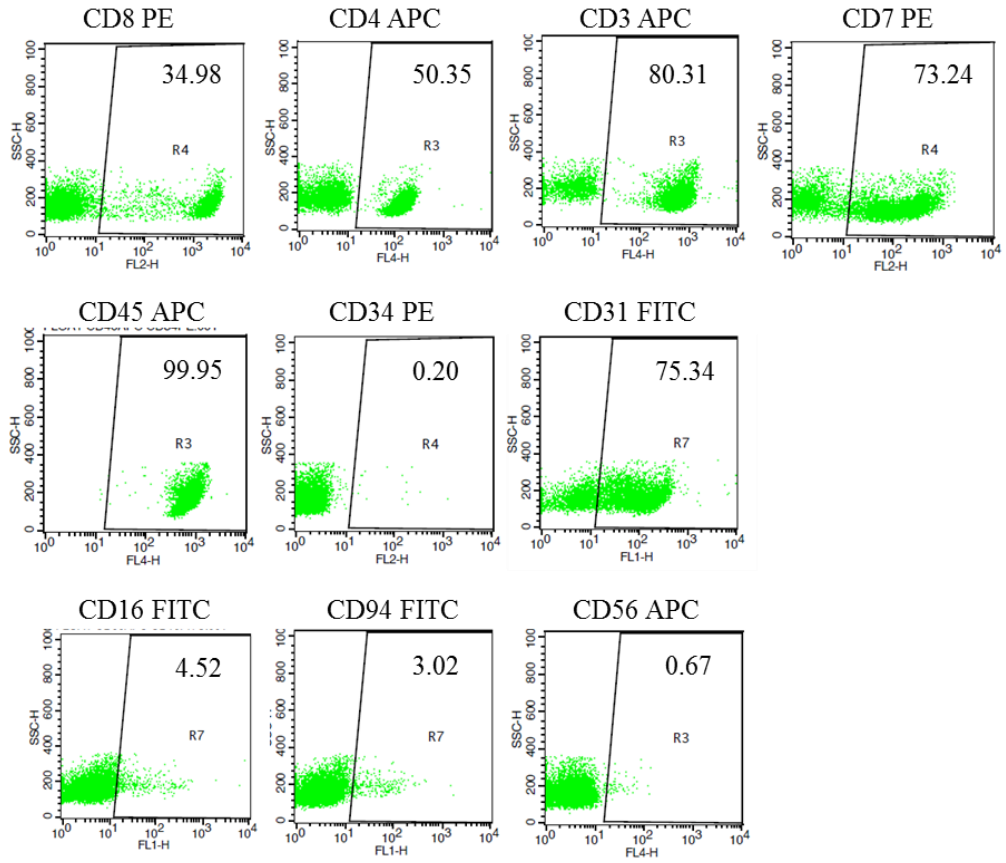

Figure 3.3. Characterization of PBMCs by flow cytometry. The cells are positive for cytotoxic and helper T cells markers, CD8 (34.98%) and CD4 (50.35%) respectively. They are also positive for other lymphocytes markers CD3 (80.31%) and CD7 (73.24%). All the cells are positive for leukocyte common antigen, CD45. The cells are negative for HSC marker CD34 (0.2%) but 75.34% positive for CD31 marker. Small population of the PBMC expressed NK cell markers: CD16 (4.52%), CD94 (3.02%) and CD56 (0.67%).

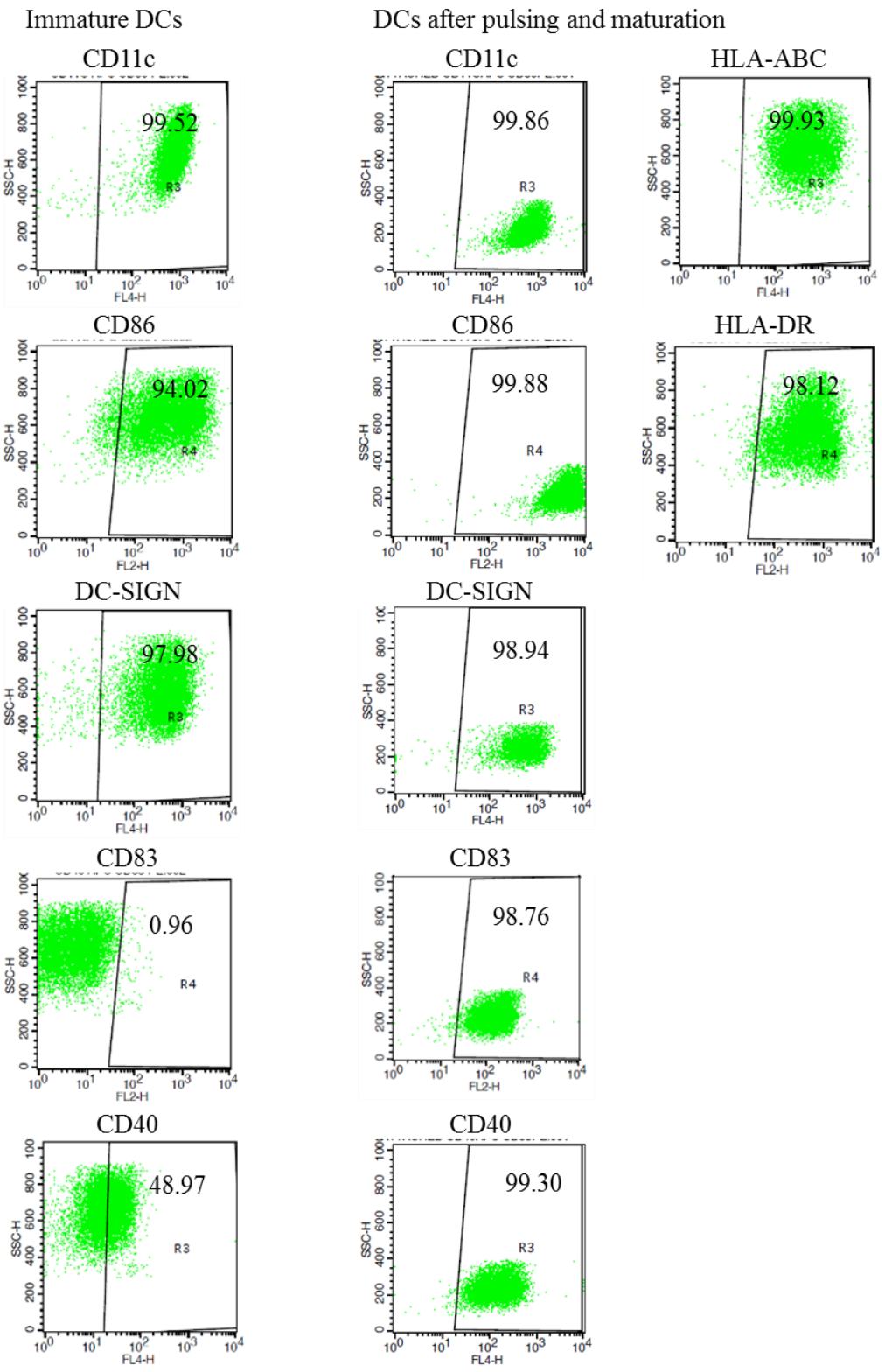

Figure 3.4. Characterization of DCs by flow cytometry before and after pulsing and maturation. The DCs are positive for MHC I and II (HLA-ABC & HLA-DR). The DCs are also positive for DC markers such as CD11c, CD86, DC-SIGN with expression of more than 90%. Upon maturation, the expression of CD83 and CD40 increased considerably, from 0.96% to 98.76% and from 48.97% to 99.30% respectively.

3.3.2 Naïve T cells selection and characterization

We investigated whether tumor antigen-specific CTL can be mounted from the naïve T cells. Thus, we selected the naïve T cells from the PBMC derived lymphocytes repertoire by using MACS (**Fig. 3.2A**). First we selected the $CD8^+$ T cells from the whole floating PBMC-lymphocytes, followed by depletion of $CD45RO^+CD57^+$ memory T cells. From the flow cytometry results, we observed that the proportion of $CD8^+$ cells out of the whole PBMC-lymphocytes was approximately 30% on average (28.3% as shown in **Figure 3.5A**). After cell sorting, the purity of the $CD8^+$ cells reached 98.2%. We tested the memory T cell markers and the results showed that 28.57% of the cells expressed CD45RO (**Fig. 3.5A**). The CD57 memory T marker expression was lower than that of CD45RO, 9.37% (**Fig. 3.5A**). However, after depletion of memory T cells by magnetic sorting, expression of these markers was not detected (**Fig 3.5A**). On average, we obtained 1×10^7 naïve T cells from 1×10^8 PBMCs. We also checked the expressions of T cell co-stimulatory molecules such as CD62L, CCR7, CD27 and CD28 before and after priming with the DCs (**Fig. 3.5B**). All markers were expressed before and after DC activation.

Tregs inhibit the CTL activation and antitumor effect. Thus, we checked the expression of Treg markers in the sorted naïve T cells population. Treg cell population is normally identified as $CD4^+CD25^+CD127^-$ cells. From **Figure 3.5C**, we observed that our sorted T cells were negative for Treg markers as the expression of CD4 marker was very low (0.87%). Moreover,

the CD25 marker albeit expressed at 9.66%, showed a dimmed expression. In addition, almost all of the cells (97.56%) were positive for CD127.

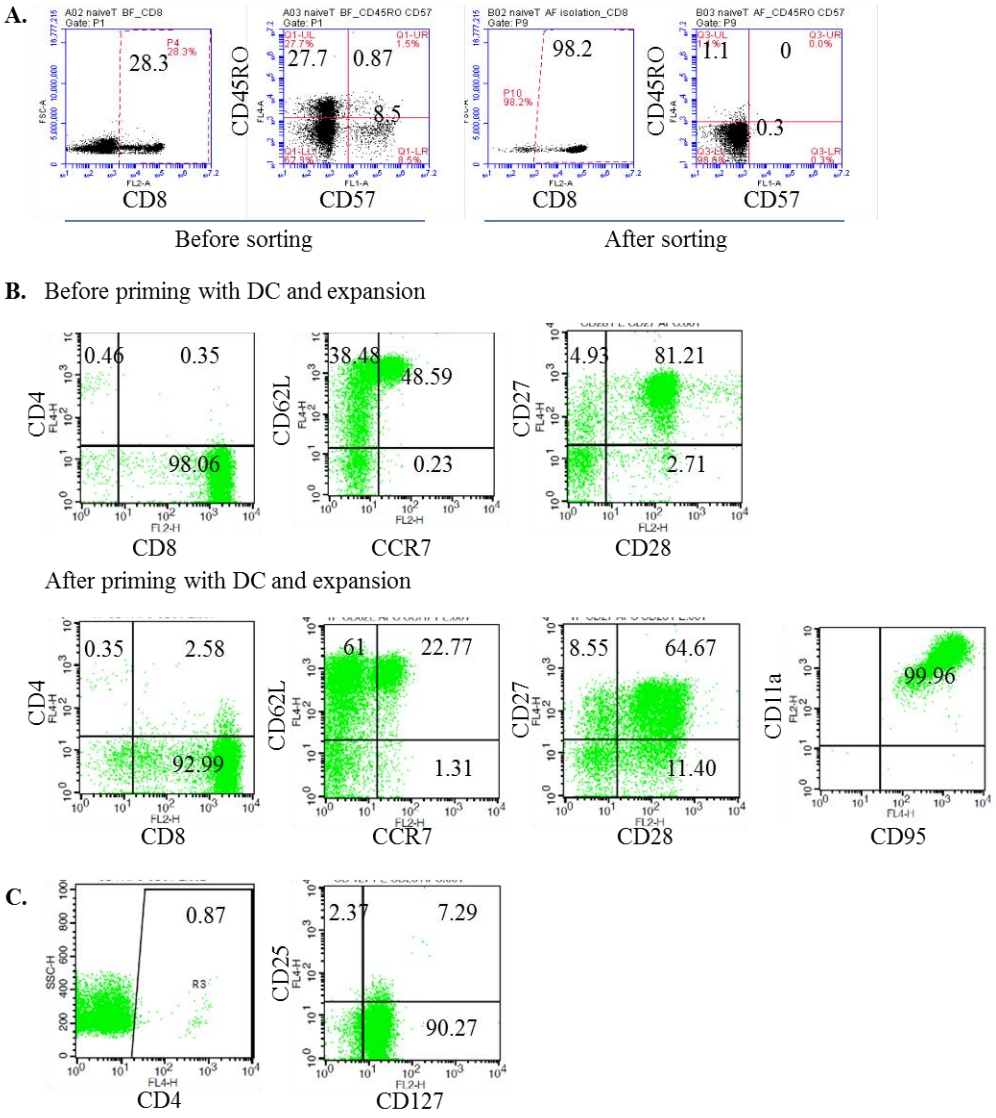

Figure 3.5. Characterization of CTL by flow cytometry before and after priming with DCs. A. Naïve T cells characterization before and after sorting. CD8 expression before sorting was 28.3% and after sorting, the purity of $CD8^+$ cells was 98.2%. The expression of memory T cells markers was 28.57 and 9.37% for CD45RO and CD57 respectively. After depletion of memory T cells, the memory T cells markers expression were very low (1.1%). **B.** Expression of costimulatory molecules before and after DC priming as shown by flow cytometry. **C.** Flow cytometry for Treg markers: CD4 (0.87%), CD25 (9.66%) and CD127 (97.56%).

3.3.3 IFNγ production of CTL activated by CSC-like-CRC-pulsed DC

After the activation and expansion period, the T cells were mixed with the target cells and their IFNγ production was evaluated. **Figure 3.6** shows the cytokine production by CTL activated by CSC-like CRC lysate-pulsed DCs. The groupings of the cells are shown in **Table 3.1**. T2 cells were used as the target cells as the PBMCs were HLA-A2 positive. These cells were pulsed with Oct4, EGFP peptides or PBS as control. T2 target cells alone without the addition of effector T cells were used as a negative control, as these T2 cells should not produce IFNγ. As a background control, spontaneous production of IFNγ from naïve T cells alone was measured. On the other hand, the cytokine productions from naïve T cells which have been activated by CD3 antibody were used as positive control.

As expected, T2 cells alone did not release any IFNγ, but the T cells alone spontaneously released IFNγ at low levels with an average of 61.67 T cells/ 50,000 cells. More T cells produced IFNγ after activation by CD3 antibody, 96.5 T cells/50,000 cells. Production of IFNγ is the highest in CTLs which have been primed with DCs pulsed with 4F-ZF-EGFP CRC cells mixed with T2 target cells pulsed with Oct4 or EGFP. The ANOVA and the Holm-Sidak pairwise comparison tests showed that the differences between these two groups are not significant. However, when either of this group was compared to the rest of the groups, then the differences are very significant. Furthermore, statistical tests comparing the WT-T, UP-T, T alone and 3.11-T-T2 groups showed no significant differences.

Table 3.1. Grouping of ELISPOT for T cells after activation by DCs pulsed with CRC stem cell-like cells.

Effector cells (Primed T cells) 50,000 cells	Target cells (Pulsed or unpulsed T2 cells) 5000 cells Effector:Target = 10:1		
	Oct4 T2	GFP T2	T2 alone
3.11DC-T	3.11-T +Oct4-1 T2	3.11-T +GFP T2	3.11-T + T2
WTDC-T	WT-T + Oct4-1 T2	WT-T + GFP T2	WT-T + T2
UpDC-T	Up-T + Oct4-1 T2	Up-T + GFP T2	Up-T +T2
T alone	T+ Oct4-1 T2	T + GFP T2	T + T2
	T only (background)		
	T + CD3 (positive)		
			T2 only (negative)

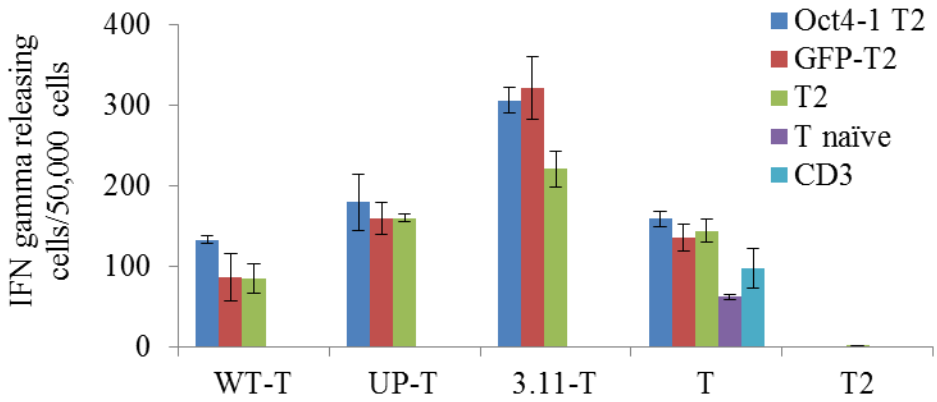

Figure 3.6. Production of IFNγ by CTL after activation by DCs pulsed with reprogrammed CRC cell lysate. Production of IFNγ is the highest in T cells which have been primed with DC pulsed with 4F-ZF-EGFP CRC cells mixed with T2 target cells pulsed with Oct4 or EGFP (Anova P value =<0.001).

3.3.4 IFNγ production of CTL activated by CSC-like-glioma-pulsed DC

We have also established CSC-like glioma cells by transducing U87 glioma cells with 4F-EGFP-ZF baculovirus. We then utilized this CSC-like glioma to produce a cell lysate that contains all the tumor antigens including the proteins of the four factors. Subsequently, this lysate was used to pulse the DCs which

in turn were used to prime the autologous naïve T cells. We then examined the production of IFNγ by these activated CTLs upon mixing with target cells. As the PBMCs from which the DCs and T cells were derived from are HLA-A2 negative, peptide pulsed T2 cells were not used as the target cells. Instead, dendritic cells pulsed with the CSC-like U87 lysate and subsequently fixed by glutaraldehyde were used as target cells. The groupings of the cells were shown in Table 3.2.

As shown in **Figure 3.7**, IFNγ production was the highest in the T cells group that had been pulsed with DCs and mixed with the glutaraldehyde-fixed pulsed-DC. The ANOVA and Holm-Sidak tests showed a significant difference between this group and the rest of the groups. On the other hand, when comparing the other groups, no statistically significant differences were observed.

Table 3.2. Grouping of ELISPOT for T cells after activation by DCs pulsed with U87 glioma stem cell like cells.

Effector cells (Primed T cells) 100,000 cells Effector:Target = 10:1	Target cells (Pulsed or unpulsed DCs fixed with glutaraldehyde) 10,000 cells	
	Fixed-pulsed DC	Fixed-unpulsed DC
PulsedDC-T	TpDC +pDC	TpDC +upDC
UnpulsedDC-T	TupDC + pDC	TupDC + upDC
T alone	T + pDC	T + upDC

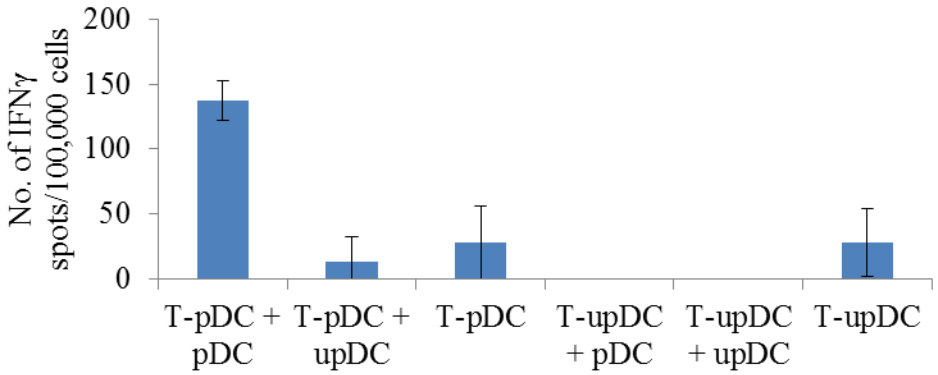

Figure 3.7. Production of IFNγ by CTL after activation by DCs pulsed with reprogrammed glioma cell lysate. Production of IFNγ is the highest in T cells which have been primed with DC pulsed with 4F-ZF-EGFP U87 glioma cell lysate mixed with fixed-DC target cells pulsed with the lysate; ANOVA P = <0.001.

3.4 Discussion

3.4.1 DC differentiation and characterization

Dendritic cells are the center of innate and adaptive immune axes. Numerous studies have been done to investigate their derivation, differentiation and functions in immunology and immunotherapies. Human DCs can be differentiated from various cellular sources, such as $CD34^+$ progenitor cells from bone marrow, cord blood and pluripotent stem cells, or from circulating monocytes from PBMC, and using various protocols and cytokine cocktails to skew the differentiation towards DCs[178-181]. The most widely used DCs for clinical trials are monocytes-derived DCs from PBMC in the presence of GM-CSF and IL4[179].

In this study, we adopted a method from the study by Wolfl et al.[178] to generate both DCs and naïve T cells from PBMCs. The profiles of the whole PBMC we used are similar to previous data using freshly isolated human PBMCs except that lower NK cell markers were detected[182, 183]. These

differences can be due to batch-to-batch variations of the PBMCs used. Likewise, the derived DCs are comparable to previous reports which used GM-CSF and IL4 supplements[179, 184-186]. Lysate pulsing represents a maturation inducer for the DCs. Moreover, this maturation process was further supported by LPS and IFNγ supplementations. Other maturation conditions have been described by others, such as the use of TNFα. However, the combination of LPS and IFNγ has been shown to stimulate IL12 production by the DCs, which is necessary for skewing towards a Th1 activation and augmenting CTL responses[6, 178, 179]. Indeed, upon pulsing with lysate, there was upregulation in CD83 and CD40 DC maturation markers expression, comparable to previous studies[179, 185, 186].The upregulation of these co-stimulatory molecules is necessary to enhance the capacity for antigen presentation and T cell stimulation, which most probably occurred at the cost of antigen uptake capacity[4]. Moreover, the DCs were positive for MHC I which is crucial for antigen presentation process. In addition to this, morphological changes were also detected. The mature DCs developed long arms of dendrites as opposed to small irregular shaped appendages on the immature ones. These long dendritic processes have been known to increase the chance of T capture and interaction[34].

Thus, using this protocol and based on the surface markers detection, we have generated sufficient numbers of functional DCs. These lysate-pulsed-DCs were used to prime the naïve T cells. Aside from detection of surface markers, DCs can be characterized by their phagocytic capability (immature state) as well as their capacity to produce cytokines (mature state) such as IL12, IL6. These are areas that we can explore further.

3.4.2 Activated CTLs display appropriate co-stimulatory molecules and antigen-specific targeting

Naïve T cells are T cells that have not come across antigen activation. Once stimulated, these cells will differentiate into CTLs and memory T cells although the exact process of differentiation has not been elucidated yet[21]. The memory T cells are responsible for generating responses if the same antigen is detected again. When this happens, the duration of the immune response mounted is shorter as memory T cells have a lower activation threshold[178]. This is the reason why these cells need to be depleted. Similar to what was reported by Wolfl et al., non-specific T activation shown by higher variations amongst the elispot wells were detected when no memory T cell depletion was performed.

The flow cytometry results of our isolated naïve T cells were comparable with results by Wolfl et al[178]. We observed that the naïve T cells could not survive past 10 days without stimulation by DCs. Interestingly, the survival of the cells improved greatly when no sorting was carried out. With this in mind, we performed sorting just prior to DC pulsing to minimize the T cell deaths. This implies that $CD4^+$ cells support the survival of the $CD8^+$ naïve T cells. This may have great implications for adoptive T cell therapy. While it is very tempting to select only $CD8^+$ T cells, exclusion of other subtypes of T cells may lead to deleterious effects for the T cells.

As mentioned in Chapter I, antigen recognition alone is not sufficient for T cell activation. Interactions of co-stimulatory molecules on the T cell surface are critical for T cell survival and functions. Our flow results show that

our T cells maintained the expressions of the necessary co-stimulatory molecules comparable to previous findings[178, 183]. CD28, as mentioned, is needed to activate the CTLs via amplification of the signals from TCR. Moreover, CD28 stimulation also maintains T cell telomeric length which may improve their survival[21]. CD27, on the other hand, has been shown to support antigen specific expansion of naïve T cells and to complement CD28 activity[187, 188]. In addition, CD11c and CD96 play a role in the homeostasis of T cells[189, 190].

Monitoring chemokine receptor expression provides information regarding the status of T cells. After maturation, there seemed to be a downregulation of CCR7 expression, but not CD62L. Although this result is not indicated in Wolfl's study, Dumortier et al. demonstrated the downregulation of both CCR7 and CD62L expression on T cells after LPS-matured DCs priming. Both CD62L and CCR7 are lymph node homing receptors[6, 178, 191, 192]. By downregulating these markers, the T cells possess migratory capacity towards the target site[192-194]. As to why the downregulation was only detected in CCR7 but not CD62L in our case, the reason is unclear and requires more investigations.

While $CD8^+$ cells represent the CTLs which are involved in the tumor killing, the $CD4^+$ T lineages are more complex. They comprise of T helpers (Th1 and Th2) which are important in assisting antibodies production by B cell and T cells proliferation through cytokine signaling. However, a different subpopulation of $CD4^+$ named Tregs has been known to attenuate immune response. Thus, it is important to exclude this subpopulation of cells from the

activated CTLs. Treg cells make up 5-10% of naïve $CD4^+$ T cells in the periphery[36]. By the end of the expansion phase, the expression of Treg markers on the T cell population was low; hence we expected little inhibition in CTL activity.

The main cytolytic components from CTL are granzyme B and IFNγ. We have shown that the production of IFNγ is the highest on the target cells that express the antigen (T2 pulsed with Oct4 or lysate-pulsed-DCs fixed with glutaraldehyde). Therefore, based on the flow cytometric analyses and the ELISPOT results of the activated CTLs, we have demonstrated that the DCs pulsed with CSC-like cells antigens can stimulate specific CTL responses. Although these results are still at a preliminary stage, the potential of CTLs targeting CSC population could already be perceived.

3.5 Future Direction

As this is an ongoing project, there are several future works which need to be tackled. We are in the midst of testing the antigen-specificity targeting of CTLs by investigating granzyme B production of the cells. Moreover, we will also assess the CTLs killing effect using the CSC-like cells as well as primary tumor cells as the target cells, to verify this concept under more practical conditions in a preclinical experimental setting. In addition to this, we are eager to evaluate the CSC-like targeting using DC-based vaccine approach in other cancer lines which have been reprogrammed in our lab (for example, melanoma).

The limitation in the number of monocytes that can be obtained from PBMCs and the variability of DC-differentiation potential from different

patients/donors lead to a demand for a better source of DCs for vaccination purposes. An alternative approach to this is the use of human iPS cells as an unlimited source to generate human DCs of consistent quality[195, 196]. As already discussed in the previous chapter, the use of iPS cells has many advantages, including ease of genetic engineering and the feasibility of large-scale mass production of cell therapeutics. An especially fascinating direction is the possibility of generating human iPS banks with various human HLA types. This way, donor iPS cells selected from the cell bank can be matched with the HLA alleles of the recipients and used to produce semi-allogeneic differentiated DC vaccines.

We have demonstrated that the combination of baculoviral vector and zinc finger nucleases technologies can be used to introduce stably site-specific integration of transgene[164, 165, 177]. Thus, using this method, we can overexpress tumor antigenic genes or DC activation/co-stimulatory molecules into the iPS cells, then differentiate the iPS into the DCs. The DCs expressing the antigens could then be used to activate CTLs responses. Our lab has also shown that hESCs stably modified with CD1d (a glycolipid MHC-related molecule[197]) gene may serve as a convenient, unlimited and competent DC source for iNKT cell activation, a unique subpopulation of lymphocytes which has the ability to lyse iNKT cell-sensitive tumor cells [180, 198, 199]. However, the safety of viral vectors has always been one significant problem of DNA-based DCs vaccines. By using site-specific integration into the AAVS1 site, the 'safe-harbor' human genomic site for exogenous DNA insertion, this problem can be circumvented.

Another interesting approach will be the use of iPS cells to generate activated T cells, thus bypassing the requirement of DCs stimulation. As mentioned above, genetic modification of T cells through tumor antigen-specific TCR gene transfer or development of chimeric antigen receptor (CAR) T cells for adoptive therapy purpose also represents encouraging modalities in immunotherapy. One possibility is to generate genetically modified iPS cells which can be used as a master cell line to produce a sufficient amount of active CTLs for cancer therapy.

To summarize, the DCs that have been loaded with CSC-like tumor lysate were able to activate CTLs. Subsequently the activated CTLs could specifically target the cells expressing the CSC-related antigens, which are the reprogramming factors used to enrich the CSC population. We believe that our approach in targeting CSCs via immunotherapy would be profoundly valuable in clinics. If it is used in combination with other therapies that target the bulk of tumor mass, such as surgical resection, chemotherapy or radiotherapy, then the complete eradication of tumors is a possibility within reach.

CHAPTER IV: CONCLUSION

In the preceding chapters, we have described the intricate mechanisms of our in-built immune system for fighting against cancerous cells. Elaborate interplays among innate and adaptive immune effectors are necessary to recognize and eventually eradicate the tumor cells. The innate immune system is fast in responding against cancer, with the killing effect mainly performed by NK cells. The other components of innate effectors, the APCs (dendritic cells and macrophages) are responsible for relaying the 'danger signal' to the adaptive arms of the immune system. The main killer of the tumor cells is the CTL. However, their survival and activities depend on the other adaptive immune cell populations, the helper T cells. The helper T cells produce cytokines and activate B cells to produce antibodies against tumor cells. When all the parts are functional, tumor eradication will ensue.

Unfortunately, in cancer patients, the tumor cells have evolved to evade the immune system, or worse, to impair the immune mechanisms. This is the reason why cancer immunotherapy holds great potential in the clinics, by providing repair of or a new source of missing immune effectors. In the subsequent chapters, we adopted two approaches of immunotherapies: the stem cell- and DC- based therapies.

In chapter 2, we experimented with cancer immune gene therapy by utilizing the CD40L gene delivered using iPS-EPCs to treat lung metastatic mice cancer model. We have shown that human pluripotent stem cells, hESC and iPS cells could serve as unlimited sources for the production of EPCs. We further showed the tumor tropism of the generated hPSCs-EPCs in different animal models: 4T1 mammary pad and lung metastatic models as well as

intracranial glioma model. Moreover, our findings add more value to baculovirus as a means to genetically modify mammalian cells effectively because we showed the efficient genetic modification of hPSCs-EPCs.

Most importantly, we demonstrated the capability of EPCs to be an excellent cellular vehicle for cancer gene therapy. The intravenously injected EPCs can deliver CD40L to inhibit metastatic breast cancer growth in the lung and prolong the survival of tumor-bearing mice, possibly through an intercellular transfer mechanism. Interestingly, compared to other therapeutic genes (HSV-tk and isthmin), CD40L has a more effective therapeutic effect against the fast growing 4T1 metastatic breast cancer cells in an immunodeficient mice model, which may be due to the multiple antitumor effects possessed by CD40L. These effects include upregulation of TH1 cytokines, NK cell activation, antibodies production and apoptosis. The exact mechanism of each effect is beyond this scope of study and will require further investigations to be unraveled. The inherent tumor tropism of EPCs combined with the immuno-modulation capacities of CD40L provide synergistic antitumor effects which are not only limited to metastatic breast cancer therapy but can potentially be extended to treat primary lung cancer and many other types of pulmonary metastases.

In Chapter 3, we adopted the DC-based vaccine to target cancer stem cell populations. As most of the available cancer treatments have been shown to spare CSCs population, these cells are capable of reestablishing tumor mass, resulting in the tumor recurrence in patients. Our lab has established reprogrammed human glioma and colorectal cancer CSC-like cells by utilizing

the baculovirus zinc-finger technology. We used whole cell tumor lysate generated via free-thaw-cycles of these enriched CSCs as a source of tumor associated antigens.

The crucial factor in this project is to produce sufficient viable and fully functional DCs which can present the tumor associated antigens into the T cells. We showed that we could obtain sufficient functional DCs which expressed MHC I and co-stimulatory markers such as CD86, CD83 and CD40 which are important for the antigen presentation process. Upon pulsing with the CSC-like cell lysate, these DCs were capable of stimulating naïve T cells into CTLs. The stimulated CTLs were capable of producing IFNγ cytokine. Moreover, the highest cytokine production is observed in target cells that expressed the tumor associated antigens. Thus, in this study we have developed a DC-based immunotherapy approach which targets the CSC-like cell population. This CSC-targeting DC-based vaccine approach is not limited only to glioma and CRC, which makes it more promising for clinical applications. We believe that in combination with other therapies that target the bulk of tumor mass, such as surgical resection, chemotherapy or radiotherapy, it is possible to achieve tumor eradication.

Overall, our work has emphasized the importance of immunotherapy in the field of cancer research. By stimulating the patient's own immune system, be it by delivering therapeutic agents using stem cells or vaccination via tumor antigen-loaded dendritic cells, tumor development can be abrogated. We believe that our concepts and findings are of substantial translational potency.

Furthermore, we expect this work to spur further studies pertaining to the development of efficacious cancer treatments.

CHAPTER V: BIBLIOGRAPHY

1. Marr LA, Gilham DE, Campbell JD, et al. Immunology in the clinic review series; focus on cancer: double trouble for tumours: bi-functional and redirected T cells as effective cancer immunotherapies. Clinical and experimental immunology. 2012;167:216-225.
2. Zanoni I, Granucci F. Regulation of antigen uptake, migration, and lifespan of dendritic cell by Toll-like receptors. Journal of molecular medicine. 2010;88:873-880.
3. Granucci F, Zanoni I, Ricciardi-Castagnoli P. Central role of dendritic cells in the regulation and deregulation of immune responses. Cellular and molecular life sciences : CMLS. 2008;65:1683-1697.
4. Mellman I, Steinman RM. Dendritic cells: specialized and regulated antigen processing machines. Cell. 2001;106:255-258.
5. McDonnell AM, Robinson BW, Currie AJ. Tumor antigen cross-presentation and the dendritic cell: where it all begins? Clinical & developmental immunology. 2010;2010:539519.
6. Banchereau J, Palucka AK. Dendritic cells as therapeutic vaccines against cancer. Nat Rev Immunol. 2005;5:296-306.
7. Petersdorf EW. Genetics of graft-versus-host disease: the major histocompatibility complex. Blood reviews. 2013;27:1-12.
8. Trowsdale J. Genomic structure and function in the MHC. Trends in genetics : TIG. 1993;9:117-122.
9. Wei MQ, Metharom P, Ellem KA, et al. Search for "weapons of mass destruction" for cancer -- immuno/ gene therapy comes of age. Cell Mol Immunol. 2005;2:351-357.
10. Bhargava A, Mishra D, Banerjee S, et al. Dendritic cell engineering for tumor immunotherapy: from biology to clinical translation. Immunotherapy. 2012;4:703-718.
11. Alatrash G, Jakher H, Stafford PD, et al. Cancer immunotherapies, their safety and toxicity. Expert opinion on drug safety. 2013.
12. Hagn M, Sontheimer K, Dahlke K, et al. Human B cells differentiate into granzyme B-secreting cytotoxic B lymphocytes upon incomplete T-cell help. Immunology and cell biology. 2012;90:457-467.
13. Walzer T, Dalod M, Robbins SH, et al. Natural-killer cells and dendritic cells: "l'union fait la force". Blood. 2005;106:2252-2258.
14. Waldhauer I, Steinle A. NK cells and cancer immunosurveillance. Oncogene. 2008;27:5932-5943.
15. Castriconi R, Daga A, Dondero A, et al. NK cells recognize and kill human glioblastoma cells with stem cell-like properties. Journal of immunology. 2009;182:3530-3539.
16. Pellegatta S, Eoli M, Frigerio S, et al. The natural killer cell response and tumor debulking are associated with prolonged survival in recurrent glioblastoma patients receiving dendritic cells loaded with autologous tumor lysates. Oncoimmunology. 2013;2:e23401.
17. Vivier E, Tomasello E, Baratin M, et al. Functions of natural killer cells. Nat Immunol. 2008;9:503-510.
18. Fehniger TA, Cooper MA, Nuovo GJ, et al. CD56bright natural killer cells are present in human lymph nodes and are activated by T cell-derived IL-2: a potential new link between adaptive and innate immunity. Blood. 2003;101:3052-3057.

19. Alli RS, Khar A. Interleukin-12 secreted by mature dendritic cells mediates activation of NK cell function. FEBS letters. 2004;559:71-76.
20. Gill S, Kalos M. T cell-based gene therapy of cancer. Transl Res. 2013;161:365-379.
21. June CH. Principles of adoptive T cell cancer therapy. J Clin Invest. 2007;117:1204-1212.
22. Bonilla FA, Oettgen HC. Adaptive immunity. The Journal of allergy and clinical immunology. 2010;125:S33-40.
23. Prlic M, Williams MA, Bevan MJ. Requirements for CD8 T-cell priming, memory generation and maintenance. Current opinion in immunology. 2007;19:315-319.
24. Blattman JN, Greenberg PD. Cancer immunotherapy: a treatment for the masses. Science. 2004;305:200-205.
25. Williams MA, Bevan MJ. Effector and memory CTL differentiation. Annu Rev Immunol. 2007;25:171-192.
26. Pavoni E, Monteriu G, Santapaola D, et al. Tumor-infiltrating B lymphocytes as an efficient source of highly specific immunoglobulins recognizing tumor cells. BMC Biotechnol. 2007;7:70.
27. Topalian SL, Weiner GJ, Pardoll DM. Cancer immunotherapy comes of age. Journal of clinical oncology : official journal of the American Society of Clinical Oncology. 2011;29:4828-4836.
28. Rabinovich GA, Gabrilovich D, Sotomayor EM. Immunosuppressive strategies that are mediated by tumor cells. Annu Rev Immunol. 2007;25:267-296.
29. Eisele G, Wischhusen J, Mittelbronn M, et al. TGF-beta and metalloproteinases differentially suppress NKG2D ligand surface expression on malignant glioma cells. Brain : a journal of neurology. 2006;129:2416-2425.
30. Onishi H, Morisaki T, Baba E, et al. Dysfunctional and short-lived subsets in monocyte-derived dendritic cells from patients with advanced cancer. Clinical immunology. 2002;105:286-295.
31. Satthaporn S, Robins A, Vassanasiri W, et al. Dendritic cells are dysfunctional in patients with operable breast cancer. Cancer Immunol Immunother. 2004;53:510-518.
32. Alshamsan A. Induction of tolerogenic dendritic cells by IL-6-secreting CT26 colon carcinoma. Immunopharmacology and immunotoxicology. 2012;34:465-469.
33. Ma Y, Shurin GV, Peiyuan Z, et al. Dendritic cells in the cancer microenvironment. Journal of Cancer. 2013;4:36-44.
34. Mellman I, Coukos G, Dranoff G. Cancer immunotherapy comes of age. Nature. 2011;480:480-489.
35. de Visser KE, Eichten A, Coussens LM. Paradoxical roles of the immune system during cancer development. Nat Rev Cancer. 2006;6:24-37.
36. Nizar S, Copier J, Meyer B, et al. T-regulatory cell modulation: the future of cancer immunotherapy? Br J Cancer. 2009;100:1697-1703.
37. Finn OJ. Immuno-oncology: understanding the function and dysfunction of the immune system in cancer. Annals of oncology : official journal of the European Society for Medical Oncology / ESMO. 2012;23 Suppl 8:viii6-9.

38. Cihova M, Altanerova V, Altaner C. Stem cell based cancer gene therapy. Mol Pharm. 2011;8:1480-1487.
39. Kim SU. Neural stem cell-based gene therapy for brain tumors. Stem Cell Rev. 2011;7:130-140.
40. Lee EX, Lam DH, Wu C, et al. Glioma gene therapy using induced pluripotent stem cell derived neural stem cells. Molecular pharmaceutics. 2011;8:1515-1524.
41. Zhao Y, Wang S. Human NT2 neural precursor-derived tumor-infiltrating cells as delivery vehicles for treatment of glioblastoma. Hum Gene Ther. 2010;21:683-694.
42. Narumi K, Udagawa T, Kondoh A, et al. In vivo delivery of interferon-alpha gene enhances tumor immunity and suppresses immunotolerance in reconstituted lymphopenic hosts. Gene Ther. 2012;19:34-48.
43. Rosenberg SA. Progress in human tumour immunology and immunotherapy. Nature. 2001;411:380-384.
44. Elzaouk L, Moelling K, Pavlovic J. Anti-tumor activity of mesenchymal stem cells producing IL-12 in a mouse melanoma model. Experimental dermatology. 2006;15:865-874.
45. Benedetti S, Pirola B, Pollo B, et al. Gene therapy of experimental brain tumors using neural progenitor cells. Nat Med. 2000;6:447-450.
46. Ehtesham M, Kabos P, Kabosova A, et al. The use of interleukin 12-secreting neural stem cells for the treatment of intracranial glioma. Cancer Res. 2002;62:5657-5663.
47. Dickson PV, Hamner JB, Burger RA, et al. Intravascular administration of tumor tropic neural progenitor cells permits targeted delivery of interferon-beta and restricts tumor growth in a murine model of disseminated neuroblastoma. Journal of pediatric surgery. 2007;42:48-53.
48. Jelovac D, Emens LA. HER2-directed therapy for metastatic breast cancer. Oncology (Williston Park). 2013;27:166-175.
49. Frank RT, Najbauer J, Aboody KS. Concise review: stem cells as an emerging platform for antibody therapy of cancer. Stem cells. 2010;28:2084-2087.
50. Frank RT, Edmiston M, Kendall SE, et al. Neural stem cells as a novel platform for tumor-specific delivery of therapeutic antibodies. PLoS One. 2009;4:e8314.
51. Zhou Y, Bosch ML, Salgaller ML. Current methods for loading dendritic cells with tumor antigen for the induction of antitumor immunity. Journal of immunotherapy. 2002;25:289-303.
52. Wei J, Gao W, Wu J, et al. Dendritic cells expressing a combined PADRE/MUC4-derived polyepitope DNA vaccine induce multiple cytotoxic T-cell responses. Cancer biotherapy & radiopharmaceuticals. 2008;23:121-128.
53. Yamanaka R, Zullo SA, Tanaka R, et al. Enhancement of antitumor immune response in glioma models in mice by genetically modified dendritic cells pulsed with Semliki forest virus-mediated complementary DNA. J Neurosurg. 2001;94:474-481.
54. Steitz J, Tormo D, Schweichel D, et al. Comparison of recombinant adenovirus and synthetic peptide for DC-based melanoma vaccination. Cancer Gene Ther. 2006;13:318-325.

55. Sadanaga N, Nagashima H, Mashino K, et al. Dendritic cell vaccination with MAGE peptide is a novel therapeutic approach for gastrointestinal carcinomas. Clin Cancer Res. 2001;7:2277-2284.
56. Yamaguchi S, Tatsumi T, Takehara T, et al. Immunotherapy of murine colon cancer using receptor tyrosine kinase EphA2-derived peptide-pulsed dendritic cell vaccines. Cancer. 2007;110:1469-1477.
57. Koski GK, Koldovsky U, Xu S, et al. A novel dendritic cell-based immunization approach for the induction of durable Th1-polarized anti-HER-2/neu responses in women with early breast cancer. Journal of immunotherapy. 2012;35:54-65.
58. Gholamin M, Moaven O, Farshchian M, et al. Induction of cytotoxic T lymphocytes primed with tumor RNA-loaded dendritic cells in esophageal squamous cell carcinoma: preliminary step for DC vaccine design. BMC Cancer. 2010;10:261.
59. Kim BR, Yang EK, Kim DY, et al. Generation of anti-tumour immune response using dendritic cells pulsed with carbonic anhydrase IX-Acinetobacter baumannii outer membrane protein A fusion proteins against renal cell carcinoma. Clinical and experimental immunology. 2012;167:73-83.
60. Lasky JL, 3rd, Panosyan EH, Plant A, et al. Autologous tumor lysate-pulsed dendritic cell immunotherapy for pediatric patients with newly diagnosed or recurrent high-grade gliomas. Anticancer Res. 2013;33:2047-2056.
61. Hwang EC, Lim MS, Im CM, et al. Generation of potent cytotoxic T lymphocytes against castration-resistant prostate cancer cells by dendritic cells loaded with dying allogeneic prostate cancer cells. Scandinavian journal of immunology. 2013;77:117-124.
62. Hong S, Li H, Qian J, et al. Optimizing dendritic cell vaccine for immunotherapy in multiple myeloma: tumour lysates are more potent tumour antigens than idiotype protein to promote anti-tumour immunity. Clinical and experimental immunology. 2012;170:167-177.
63. Barth RJ, Jr., Fisher DA, Wallace PK, et al. A randomized trial of ex vivo CD40L activation of a dendritic cell vaccine in colorectal cancer patients: tumor-specific immune responses are associated with improved survival. Clin Cancer Res. 2010;16:5548-5556.
64. Xu Q, Liu G, Yuan X, et al. Antigen-specific T-cell response from dendritic cell vaccination using cancer stem-like cell-associated antigens. Stem cells. 2009;27:1734-1740.
65. Grupp SA, Kalos M, Barrett D, et al. Chimeric antigen receptor-modified T cells for acute lymphoid leukemia. N Engl J Med. 2013;368:1509-1518.
66. Fox BA, Schendel DJ, Butterfield LH, et al. Defining the critical hurdles in cancer immunotherapy. Journal of translational medicine. 2011;9:214.
67. Hahn KA, Bravo L, Adams WH, et al. Naturally occurring tumors in dogs as comparative models for cancer therapy research. In vivo. 1994;8:133-143.
68. Khanna C, Hunter K. Modeling metastasis in vivo. Carcinogenesis. 2005;26:513-523.

69. Khanna C, Vail DM. Targeting the lung: preclinical and comparative evaluation of anticancer aerosols in dogs with naturally occurring cancers. Current cancer drug targets. 2003;3:265-273.
70. Vail DM, MacEwen EG. Spontaneously occurring tumors of companion animals as models for human cancer. Cancer investigation. 2000;18:781-792.
71. Copier J, Dalgleish AG, Britten CM, et al. Improving the efficacy of cancer immunotherapy. European journal of cancer. 2009;45:1424-1431.
72. Bandura DR, Baranov VI, Ornatsky OI, et al. Mass cytometry: technique for real time single cell multitarget immunoassay based on inductively coupled plasma time-of-flight mass spectrometry. Analytical chemistry. 2009;81:6813-6822.
73. Chang S, Kohrt H, Maecker HT. Monitoring the immune competence of cancer patients to predict outcome. Cancer immunology, immunotherapy : CII. 2014.
74. Ornatsky O, Bandura D, Baranov V, et al. Highly multiparametric analysis by mass cytometry. Journal of immunological methods. 2010;361:1-20.
75. Tanner SD, Baranov VI, Ornatsky OI, et al. An introduction to mass cytometry: fundamentals and applications. Cancer immunology, immunotherapy : CII. 2013;62:955-965.
76. Finn OJ. Cancer immunology. The New England journal of medicine. 2008;358:2704-2715.
77. Zitvogel L, Apetoh L, Ghiringhelli F, et al. Immunological aspects of cancer chemotherapy. Nature reviews. Immunology. 2008;8:59-73.
78. McDermott DF, Atkins MB. PD-1 as a potential target in cancer therapy. Cancer medicine. 2013;2:662-673.
79. Zhang H-r, Chen F-l, Xu C-p, et al. Incorporation of endothelial progenitor cells into the neovasculature of malignant glioma xenograft. Journal of neuro-oncology. 2009;93:165-174.
80. Yoder MC. Human endothelial progenitor cells. Cold Spring Harbor perspectives in medicine. 2012;2:a006692.
81. Peichev M, Naiyer AJ, Pereira D, et al. Expression of VEGFR-2 and AC133 by circulating human CD34(+) cells identifies a population of functional endothelial precursors. Blood. 2000;95:952-958.
82. Gehling UM. Hemangioblasts and their progeny. Methods in enzymology. 2006;419:179-193.
83. Debatin KM, Wei J, Beltinger C. Endothelial progenitor cells for cancer gene therapy. Gene therapy. 2008;15:780-786.
84. De P, Venneri MA, Naldini L. In vivo targeting of tumor endothelial cells by systemic delivery of lentiviral vectors. Human gene therapy. 2003;14:1193-1206.
85. Wei J, Blum S, Unger M, et al. Embryonic endothelial progenitor cells armed with a suicide gene target hypoxic lung metastases after intravenous delivery. Cancer Cell. 2004;5:477-488.
86. Arap W, Pasqualini R. Engineered embryonic endothelial progenitor cells as therapeutic Trojan horses. Cancer cell. 2004;5:406-408.

87. Park SJ, Moon SH, Lee HJ, et al. A comparison of human cord blood- and embryonic stem cell-derived endothelial progenitor cells in the treatment of chronic wounds. Biomaterials. 2013;34:995-1003.
88. Menendez P, Bueno C, Wang L. Human embryonic stem cells: A journey beyond cell replacement therapies. Cytotherapy. 2006;8:530-541.
89. Slukvin, II. Deciphering the hierarchy of angiohematopoietic progenitors from human pluripotent stem cells. Cell cycle. 2013;12:720-727.
90. Murry CE, Keller G. Differentiation of embryonic stem cells to clinically relevant populations: lessons from embryonic development. Cell. 2008;132:661-680.
91. Li Z, Han Z, Wu JC. Transplantation of human embryonic stem cell-derived endothelial cells for vascular diseases. J Cell Biochem. 2009;106:194-199.
92. White MP, Rufaihah AJ, Liu L, et al. Limited gene expression variation in human embryonic stem cell and induced pluripotent stem cell-derived endothelial cells. Stem cells. 2013;31:92-103.
93. Dudek AZ. Endothelial lineage cell as a vehicle for systemic delivery of cancer gene therapy. Translational research : the journal of laboratory and clinical medicine. 2010;156:136-146.
94. Su W, Wang L, Zhou M, et al. Human Embryonic Stem Cell-Derived Endothelial Cells as Cellular Delivery Vehicles for Treatment of Metastatic Breast Cancer. Cell transplantation. 2012.
95. Narsinh KH, Plews J, Wu JC. Comparison of human induced pluripotent and embryonic stem cells: fraternal or identical twins? Mol Ther. 2011;19:635-638.
96. Nishikawa S, Goldstein RA, Nierras CR. The promise of human induced pluripotent stem cells for research and therapy. Nature reviews. Molecular cell biology. 2008;9:725-729.
97. Patel M, Yang S. Advances in reprogramming somatic cells to induced pluripotent stem cells. Stem Cell Rev. 2010;6:367-380.
98. Simara P, Motl JA, Kaufman DS. Pluripotent stem cells and gene therapy. Transl Res. 2013;161:284-292.
99. Wei J, Blum S, Unger M, et al. Embryonic endothelial progenitor cells armed with a suicide gene target hypoxic lung metastases after intravenous delivery. Cancer cell. 2004;5:477-488.
100. Keung EZ, Nelson PJ, Conrad C. Concise review: genetically engineered stem cell therapy targeting angiogenesis and tumor stroma in gastrointestinal malignancy. Stem cells. 2013;31:227-235.
101. Liu LL, Smith MJ, Sun BS, et al. Combined IFN-gamma-endostatin gene therapy and radiotherapy attenuates primary breast tumor growth and lung metastases via enhanced CTL and NK cell activation and attenuated tumor angiogenesis in a murine model. Annals of surgical oncology. 2009;16:1403-1411.
102. Mizukami Y, Sasajima J, Ashida T, et al. Abnormal tumor vasculatures and bone marrow-derived pro-angiogenic cells in cancer. Int J Hematol. 2012;95:125-130.

103. Ojeifo JO, Lee HR, Rezza P, et al. Endothelial cell-based systemic gene therapy of metastatic melanoma. Cancer gene therapy. 2001;8:636-648.
104. Hamanishi J, Mandai M, Matsumura N, et al. Activated local immunity by CC chemokine ligand 19-transduced embryonic endothelial progenitor cells suppresses metastasis of murine ovarian cancer. Stem cells. 2010;28:164-173.
105. Loskog A, Tötterman TH. CD40L - a multipotent molecule for tumor therapy. Endocrine, metabolic & immune disorders drug targets. 2007;7:23-28.
106. Ullenhag G, Loskog AS. AdCD40L--crossing the valley of death? International reviews of immunology. 2012;31:289-298.
107. Kuwashima N, Kageyama S, Eto Y, et al. CD40 ligand immunotherapy in cancer: an efficient approach. Leukemia & lymphoma. 2001;42:1367-1377.
108. Gomes EM, Rodrigues MS, Phadke AP, et al. Antitumor activity of an oncolytic adenoviral-CD40 ligand (CD154) transgene construct in human breast cancer cells. Clin Cancer Res. 2009;15:1317-1325.
109. Gurdon JB. The developmental capacity of nuclei taken from intestinal epithelium cells of feeding tadpoles. Journal of embryology and experimental morphology. 1962;10:622-640.
110. Lensch MW, Mummery CL. From Stealing Fire to Cellular Reprogramming: A Scientific History Leading to the 2012 Nobel Prize. Stem cell reports. 2013;1:5-17.
111. Do JT, Scholer HR. Nuclei of embryonic stem cells reprogram somatic cells. Stem cells. 2004;22:941-949.
112. Stadtfeld M, Hochedlinger K. Induced pluripotency: history, mechanisms, and applications. Genes & development. 2010;24:2239-2263.
113. Cao S, Loh K, Pei Y, et al. Overcoming barriers to the clinical utilization of iPSCs: reprogramming efficiency, safety and quality. Protein & cell. 2012;3:834-845.
114. Ma T, Xie M, Laurent T, et al. Progress in the reprogramming of somatic cells. Circulation research. 2013;112:562-574.
115. Gunaseeli I, Doss MX, Antzelevitch C, et al. Induced pluripotent stem cells as a model for accelerated patient- and disease-specific drug discovery. Current medicinal chemistry. 2010;17:759-766.
116. Walia B, Satija N, Tripathi RP, et al. Induced pluripotent stem cells: fundamentals and applications of the reprogramming process and its ramifications on regenerative medicine. Stem cell reviews. 2012;8:100-115.
117. Robbins RD, Prasain N, Maier BF, et al. Inducible pluripotent stem cells: not quite ready for prime time? Current opinion in organ transplantation. 2010;15:61-67.
118. Taylor CJ, Bolton EM, Bradley JA. Immunological considerations for embryonic and induced pluripotent stem cell banking. Philosophical transactions of the Royal Society of London. Series B, Biological sciences. 2011;366:2312-2322.

119. Diaconu I, Cerullo V, Hirvinen MLM, et al. Immune response is an important aspect of the antitumor effect produced by a CD40L-encoding oncolytic adenovirus. Cancer research. 2012;72:2327-2338.
120. Vonderheide RH, Glennie MJ. Agonistic CD40 Antibodies and Cancer Therapy. Clin Cancer Res. 2013;19:1035-1043.
121. Elzey BD, Ratliff TL, Sowa JM, et al. Platelet CD40L at the interface of adaptive immunity. Thrombosis research. 2011;127:180-183.
122. Karnoub AE, Dash AB, Vo AP, et al. Mesenchymal stem cells within tumour stroma promote breast cancer metastasis. Nature. 2007;449:557-563.
123. Galderisi U, Giordano A, Paggi MG. The bad and the good of mesenchymal stem cells in cancer: Boosters of tumor growth and vehicles for targeted delivery of anticancer agents. World journal of stem cells. 2010;2:5-12.
124. Klopp AH, Gupta A, Spaeth E, et al. Concise review: Dissecting a discrepancy in the literature: do mesenchymal stem cells support or suppress tumor growth? Stem cells (Dayton, Ohio). 2011;29:11-19.
125. Wang S, Balasundaram G. Potential cancer gene therapy by baculoviral transduction. Current gene therapy. 2010;10:214-225.
126. Xiang W, Ke Z, Zhang Y, et al. Isthmin is a novel secreted angiogenesis inhibitor that inhibits tumour growth in mice. Journal of cellular and molecular medicine. 2011;15:359-374.
127. Zhang Y, Chen M, Venugopal S, et al. Isthmin exerts pro-survival and death-promoting effect on endothelial cells through alphavbeta5 integrin depending on its physical state. Cell death & disease. 2011;2:e153.
128. Yang J, Lam DH, Goh SS, et al. Tumor Tropism of Intravenously Injected Human Induced Pluripotent Stem Cell-Derived Neural Stem Cells and Their Gene Therapy Application in a Metastatic Breast Cancer Model. Stem cells (Dayton, Ohio). 2012:10.
129. van der Zijpp YJT, Poot AA, Feijen J. ICAM-1 and VCAM-1 expression by endothelial cells grown on fibronectin-coated TCPS and PS. Journal of biomedical materials research. Part A. 2003;65:51-59.
130. Wang ZZ, Au P, Chen T, et al. Endothelial cells derived from human embryonic stem cells form durable blood vessels in vivo. Nature biotechnology. 2007;25:317-318.
131. Ng ES, Davis R, Stanley EG, et al. A protocol describing the use of a recombinant protein-based, animal product-free medium (APEL) for human embryonic stem cell differentiation as spin embryoid bodies. Nature protocols. 2008;3:768-776.
132. James D, Nam HS, Seandel M, et al. Expansion and maintenance of human embryonic stem cell-derived endothelial cells by TGFbeta inhibition is Id1 dependent. Nat Biotechnol. 2010;28:161-166.
133. Choudhury Y, Tay FC, Lam DH, et al. Attenuated adenosine-to-inosine editing of microRNA-376a* promotes invasiveness of glioblastoma cells. The Journal of clinical investigation. 2012;122:4059-4076.
134. Lin J, Teo S, Lam DH, et al. MicroRNA-10b pleiotropically regulates invasion, angiogenicity and apoptosis of tumor cells resembling

mesenchymal subtype of glioblastoma multiforme. Cell Death Dis. 2012;3:e398.
135. Vodyanik MA, Slukvin II. Hematoendothelial differentiation of human embryonic stem cells. Current protocols in cell biology / editorial board, Juan S. Bonifacino ... [et al.]. 2007;Chapter 23:Unit 23.26.
136. Woll PS, Morris JK, Painschab MS, et al. Wnt signaling promotes hematoendothelial cell development from human embryonic stem cells. Blood. 2008;111:122-131.
137. Hill KL, Obrtlikova P, Alvarez DF, et al. Human embryonic stem cell-derived vascular progenitor cells capable of endothelial and smooth muscle cell function. Exp Hematol. 2010;38:246-257 e241.
138. Resch T, Pircher A, Kahler CM, et al. Endothelial progenitor cells: current issues on characterization and challenging clinical applications. Stem Cell Rev. 2012;8:926-939.
139. Ramachandra CJA, Shahbazi M, Kwang TWX, et al. Efficient recombinase-mediated cassette exchange at the AAVS1 locus in human embryonic stem cells using baculoviral vectors. Nucleic acids research. 2011.
140. Kaufman DS. Toward clinical therapies using hematopoietic cells derived from human pluripotent stem cells. Blood. 2009;114:3513-3523.
141. Vodyanik MA, Bork JA, Thomson JA, et al. Human embryonic stem cell-derived CD34+ cells: efficient production in the coculture with OP9 stromal cells and analysis of lymphohematopoietic potential. Blood. 2005;105:617-626.
142. Tian X, Hexum MK, Penchev VR, et al. Bioluminescent imaging demonstrates that transplanted human embryonic stem cell-derived CD34(+) cells preferentially develop into endothelial cells. Stem cells (Dayton, Ohio). 2009;27:2675-2685.
143. Park S-W, Jun Koh Y, Jeon J, et al. Efficient differentiation of human pluripotent stem cells into functional CD34+ progenitor cells by combined modulation of the MEK/ERK and BMP4 signaling pathways. Blood. 2010;116:5762-5772.
144. Niwa A, Umeda K, Chang H, et al. Orderly hematopoietic development of induced pluripotent stem cells via Flk-1(+) hemoangiogenic progenitors. Journal of cellular physiology. 2009;221:367-377.
145. Yu X, Lin Y, Yan X, et al. CD133, Stem Cells, and Cancer Stem Cells: Myth or Reality? Current colorectal cancer reports. 2011;7:253-259.
146. Gehling UM, Ergun S, Schumacher U, et al. In vitro differentiation of endothelial cells from AC133-positive progenitor cells. Blood. 2000;95:3106-3112.
147. Dolgin E. Flaw in induced-stem-cell model. Nature. 2011;470:13.
148. Moore XL, Lu J, Sun L, et al. Endothelial progenitor cells' "homing" specificity to brain tumors. Gene therapy. 2004;11:811-818.
149. Mancuso P, Calleri A, Bertolini F. Circulating endothelial cells and circulating endothelial progenitors. Recent results in cancer research. Fortschritte der Krebsforschung. Progres dans les recherches sur le cancer. 2012;195:163-170.

150. Patenaude A, Parker J, Karsan A. Involvement of endothelial progenitor cells in tumor vascularization. Microvasc Res. 2010;79:217-223.
151. Zhao Y, Lam DH, Yang J, et al. Targeted suicide gene therapy for glioma using human embryonic stem cell-derived neural stem cells genetically modified by baculoviral vectors. Gene therapy. 2012;19:189-200.
152. Shahbazi M, Kwang TW, Purwanti YI, et al. Inhibitory effects of neural stem cells derived from human embryonic stem cells on differentiation and function of monocyte-derived dendritic cells. J Neurol Sci. 2013;330:85-93.
153. Haviv I, Polyak K, Qiu W, et al. Origin of carcinoma associated fibroblasts. Cell cycle. 2009;8:589-595.
154. Bessis N, GarciaCozar FJ, Boissier MC. Immune responses to gene therapy vectors: influence on vector function and effector mechanisms. Gene Ther. 2004;11 Suppl 1:S10-17.
155. Jooss K, Chirmule N. Immunity to adenovirus and adeno-associated viral vectors: implications for gene therapy. Gene Ther. 2003;10:955-963.
156. Ong ST, Li F, Du J, et al. Hybrid cytomegalovirus enhancer-h1 promoter-based plasmid and baculovirus vectors mediate effective RNA interference. Hum Gene Ther. 2005;16:1404-1412.
157. Fernandes MS, Gomes EM, Butcher LD, et al. Growth inhibition of human multiple myeloma cells by an oncolytic adenovirus carrying the CD40 ligand transgene. Clin Cancer Res. 2009;15:4847-4856.
158. Biagi E, Yvon E, Dotti G, et al. Bystander transfer of functional human CD40 ligand from gene-modified fibroblasts to B-chronic lymphocytic leukemia cells. Hum Gene Ther. 2003;14:545-559.
159. Fong C-Y, Gauthaman K, Bongso A. Teratomas from pluripotent stem cells: A clinical hurdle. Journal of cellular biochemistry. 2010;111:769-781.
160. Modlich U, Pugh CW, Bicknell R. Increasing endothelial cell specific expression by the use of heterologous hypoxic and cytokine-inducible enhancers. Gene therapy. 2000;7:896-902.
161. Varda-Bloom N, Shaish A, Gonen A, et al. Tissue-specific gene therapy directed to tumor angiogenesis. Gene therapy. 2001;8:819-827.
162. Yang L, Cao Z, Li F, et al. Tumor-specific gene expression using the survivin promoter is further increased by hypoxia. Gene therapy. 2004;11:1215-1223.
163. Zhu D, Lam DH, Purwanti YI, et al. Systemic Delivery of Fusogenic Membrane Glycoprotein-expressing Neural Stem Cells to Selectively Kill Tumor Cells. Mol Ther. 2013.
164. Tay FC, Tan WK, Goh SL, et al. Targeted transgene insertion into the AAVS1 locus driven by baculoviral vector-mediated zinc finger nuclease expression in human-induced pluripotent stem cells. The journal of gene medicine. 2013;15:384-395.
165. Zhu H, Lau CH, Goh SL, et al. Baculoviral transduction facilitates TALEN-mediated targeted transgene integration and Cre/LoxP cassette exchange in human-induced pluripotent stem cells. Nucleic acids research. 2013;41:e180.

166. Lobo NA, Shimono Y, Qian D, et al. The biology of cancer stem cells. Annu Rev Cell Dev Biol. 2007;23:675-699.
167. Ailles LE, Weissman IL. Cancer stem cells in solid tumors. Current opinion in biotechnology. 2007;18:460-466.
168. Ben-Porath I, Thomson MW, Carey VJ, et al. An embryonic stem cell-like gene expression signature in poorly differentiated aggressive human tumors. Nature genetics. 2008;40:499-507.
169. Wei B, Han XY, Qi CL, et al. Coaction of spheroid-derived stem-like cells and endothelial progenitor cells promotes development of colon cancer. PLoS One. 2012;7:e39069.
170. Kumar SM, Liu S, Lu H, et al. Acquired cancer stem cell phenotypes through Oct4-mediated dedifferentiation. Oncogene. 2012;31:4898-4911.
171. Prince ME, Sivanandan R, Kaczorowski A, et al. Identification of a subpopulation of cells with cancer stem cell properties in head and neck squamous cell carcinoma. Proc Natl Acad Sci U S A. 2007;104:973-978.
172. Al-Hajj M, Wicha MS, Benito-Hernandez A, et al. Prospective identification of tumorigenic breast cancer cells. Proc Natl Acad Sci U S A. 2003;100:3983-3988.
173. Liu SV. iPS cells: a more critical review. Stem Cells Dev. 2008;17:391-397.
174. Leng Z, Tao K, Xia Q, et al. Kruppel-like factor 4 acts as an oncogene in colon cancer stem cell-enriched spheroid cells. PLoS One. 2013;8:e56082.
175. Palla AR, Piazzolla D, Abad M, et al. Reprogramming activity of NANOGP8, a NANOG family member widely expressed in cancer. Oncogene. 2013.
176. Heddleston JM, Li Z, McLendon RE, et al. The hypoxic microenvironment maintains glioblastoma stem cells and promotes reprogramming towards a cancer stem cell phenotype. Cell cycle. 2009;8:3274-3284.
177. Phang RZ, Tay FC, Goh SL, et al. Zinc finger nuclease-expressing baculoviral vectors mediate targeted genome integration of reprogramming factor genes to facilitate the generation of human induced pluripotent stem cells. Stem cells translational medicine. 2013;2:935-945.
178. Wolfl M, Merker K, Morbach H, et al. Primed tumor-reactive multifunctional CD62L+ human CD8+ T cells for immunotherapy. Cancer Immunol Immunother. 2011;60:173-186.
179. Chiang CL, Hagemann AR, Leskowitz R, et al. Day-4 myeloid dendritic cells pulsed with whole tumor lysate are highly immunogenic and elicit potent anti-tumor responses. PLoS One. 2011;6:e28732.
180. Zeng J, Shahbazi M, Wu C, et al. Enhancing Immunostimulatory Function of Human Embryonic Stem Cell-Derived Dendritic Cells by CD1d Overexpression. Journal of immunology (Baltimore, Md: 1950). 2012.
181. Tseng S-Y, Nishimoto KP, Silk KM, et al. Generation of immunogenic dendritic cells from human embryonic stem cells without serum and feeder cells. Regenerative medicine. 2009;4:513-526.

182. Segain JP, Rolli-Derkinderen M, Gervois N, et al. Urotensin II is a new chemotactic factor for UT receptor-expressing monocytes. Journal of immunology. 2007;179:901-909.
183. Distler E, Bloetz A, Albrecht J, et al. Alloreactive and leukemia-reactive T cells are preferentially derived from naive precursors in healthy donors: implications for immunotherapy with memory T cells. Haematologica. 2011;96:1024-1032.
184. Morse MA, Zhou LJ, Tedder TF, et al. Generation of dendritic cells in vitro from peripheral blood mononuclear cells with granulocyte-macrophage-colony-stimulating factor, interleukin-4, and tumor necrosis factor-alpha for use in cancer immunotherapy. Annals of surgery. 1997;226:6-16.
185. Mahdian R, Kokhaei P, Najar HM, et al. Dendritic cells, pulsed with lysate of allogeneic tumor cells, are capable of stimulating MHC-restricted antigen-specific antitumor T cells. Medical oncology. 2006;23:273-282.
186. Ho WY, Nguyen HN, Wolfl M, et al. In vitro methods for generating CD8+ T-cell clones for immunotherapy from the naive repertoire. Journal of immunological methods. 2006;310:40-52.
187. Hendriks J, Xiao Y, Borst J. CD27 promotes survival of activated T cells and complements CD28 in generation and establishment of the effector T cell pool. J Exp Med. 2003;198:1369-1380.
188. Hendriks J, Gravestein LA, Tesselaar K, et al. CD27 is required for generation and long-term maintenance of T cell immunity. Nat Immunol. 2000;1:433-440.
189. Vinay DS, Kwon BS. CD11c+CD8+ T cells: two-faced adaptive immune regulators. Cellular immunology. 2010;264:18-22.
190. Paulsen M, Janssen O. Pro- and anti-apoptotic CD95 signaling in T cells. Cell communication and signaling : CCS. 2011;9:7.
191. Campbell JJ, Murphy KE, Kunkel EJ, et al. CCR7 expression and memory T cell diversity in humans. Journal of immunology. 2001;166:877-884.
192. Dumortier H, van Mierlo GJ, Egan D, et al. Antigen presentation by an immature myeloid dendritic cell line does not cause CTL deletion in vivo, but generates CD8+ central memory-like T cells that can be rescued for full effector function. Journal of immunology. 2005;175:855-863.
193. Egawa H, Ozawa K, Takada Y, et al. Coupled regulation of interleukin-12 receptor beta-1 of CD8+ central memory and CCR7-negative memory T cells in an early alloimmunity in liver transplant recipients. Clinical and experimental immunology. 2010;160:420-430.
194. Yang S, Liu F, Wang QJ, et al. The shedding of CD62L (L-selectin) regulates the acquisition of lytic activity in human tumor reactive T lymphocytes. PLoS One. 2011;6:e22560.
195. Senju S, Haruta M, Matsumura K, et al. Generation of dendritic cells and macrophages from human induced pluripotent stem cells aiming at cell therapy. Gene Ther. 2011;18:874-883.
196. Senju S, Hirata S, Motomura Y, et al. Pluripotent stem cells as source of dendritic cells for immune therapy. Int J Hematol. 2010;91:392-400.

197. Joyce S. CD1d and natural T cells: how their properties jump-start the immune system. Cellular and molecular life sciences : CMLS. 2001;58:442-469.
198. Corgnac S, Perret R, Derre L, et al. CD1d-antibody fusion proteins target iNKT cells to the tumor and trigger long-term therapeutic responses. Cancer Immunol Immunother. 2013;62:747-760.
199. Zeng J, Wang S. Human dendritic cells derived from embryonic stem cells stably modified with CD1d efficiently stimulate antitumor invariant natural killer T cell response. Stem cells translational medicine. 2014;3:69-80.

APPENDICES

Suppl. Table 1. Overview of iPS-EPCs derivation methods.

	Co-culture		2-D culture	Embryoid bodies formation
	OP9	M210B4		
Duration	8 days	13 days	10 days	14 days
Medium	α-MEM + 10% FBS + 100uM MTG	RPMI-1640 + 15% FBS + 1mM NEAA + 0.1mM β-mercaptoethanol	IMDM + 15% FBS + 450µM MTG + 2mM L-glutamine + 0.1mM NEAA	APEL™ + 20ng/ml BMP4 (day 0-7) + 10ng/ml Activin A (day 1-4) + 8ng/ml FGF2 (day 2 onwards) + 25ng/ml VEGF (day 4 onwards) +10 µM SB431542 (day 7 onwards)
Starting point	3 wells of 6-well-plate of confluent iPS cells	3 wells of 6-well-plate of confluent iPS cells	10cm2 dish of confluent iPS cells	1 wells of 6-well-plate of confluent iPS cells
Endpoint (average)	$1x10^6$ EPCs	$1x10^6$ EPCs	$1x10^6$ EPCs	$1x10^6$ EPCs

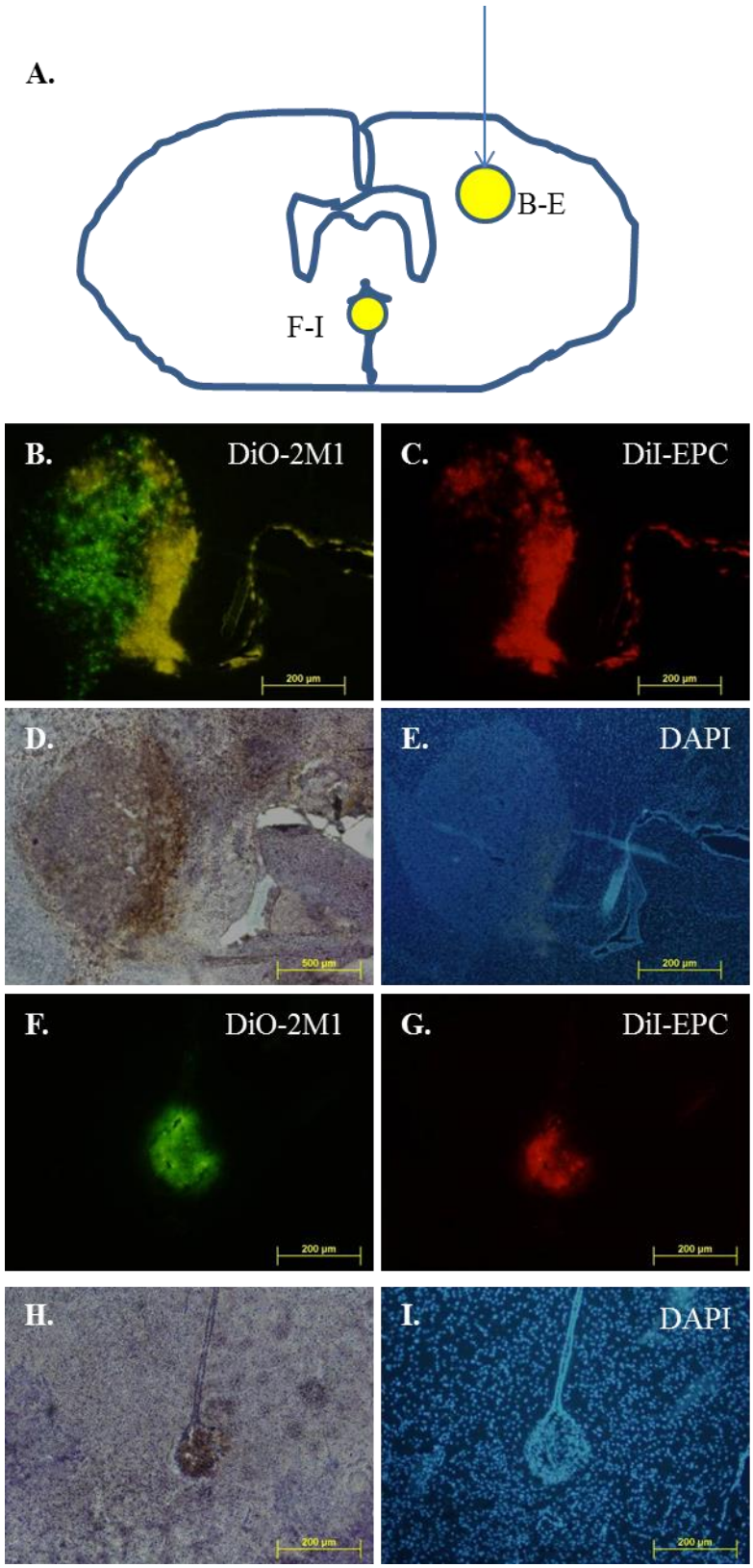

Supplementary figure 1. iPS-EPCs tumor tropism to 2M1 glioma intracranial model. A. Schematic diagram of injection and location of the cells. Injection was performed 2mm right of bregma point. **B-E.** Primary DiO-labeled 2M1 tumor mass infiltrated by DiI-labeled EPCs. **F-I.** iPS-EPCs can be observed at 2M1 secondary tumor site.